

INFORMATION TO USERS

This manuscript has been reproduced from the microfilm master. UMI films the text directly from the original or copy submitted. Thus, some thesis and dissertation copies are in typewriter face, while others may be from any type of computer printer.

The quality of this reproduction is dependent upon the quality of the copy submitted. Broken or indistinct print, colored or poor quality illustrations and photographs, print bleedthrough, substandard margins, and improper alignment can adversely affect reproduction.

In the unlikely event that the author did not send UMI a complete manuscript and there are missing pages, these will be noted. Also, if unauthorized copyright material had to be removed, a note will indicate the deletion.

Oversize materials (e.g., maps, drawings, charts) are reproduced by sectioning the original, beginning at the upper left-hand corner and continuing from left to right in equal sections with small overlaps.

Photographs included in the original manuscript have been reproduced xerographically in this copy. Higher quality 6" x 9" black and white photographic prints are available for any photographs or illustrations appearing in this copy for an additional charge. Contact UMI directly to order.

**ProQuest Information and Learning
300 North Zeeb Road, Ann Arbor, MI 48106-1346 USA
800-521-0600**

UMI[®]

University of Alberta

**The *Escherichia coli* YnfEFGHI Operon:
A Dimethyl Sulfoxide Reductase (DmsABC) Parologue**

By

Shannon Patricia Lubitz

A thesis submitted to the Faculty of Graduate Studies and Research in
partial fulfillment of the requirements for the degree of Master of Science

Department of Medical Microbiology and Immunology

Edmonton, Alberta
Spring 2002



**National Library
of Canada**

**Acquisitions and
Bibliographic Services**

**395 Wellington Street
Ottawa ON K1A 0N4
Canada**

**Bibliothèque nationale
du Canada**

**Acquisitions et
services bibliographiques**

**395, rue Wellington
Ottawa ON K1A 0N4
Canada**

Your file Votre référence

Our file Notre référence

The author has granted a non-exclusive licence allowing the National Library of Canada to reproduce, loan, distribute or sell copies of this thesis in microform, paper or electronic formats.

The author retains ownership of the copyright in this thesis. Neither the thesis nor substantial extracts from it may be printed or otherwise reproduced without the author's permission.

L'auteur a accordé une licence non exclusive permettant à la Bibliothèque nationale du Canada de reproduire, prêter, distribuer ou vendre des copies de cette thèse sous la forme de microfiche/film, de reproduction sur papier ou sur format électronique.

L'auteur conserve la propriété du droit d'auteur qui protège cette thèse. Ni la thèse ni des extraits substantiels de celle-ci ne doivent être imprimés ou autrement reproduits sans son autorisation.

0-612-69733-9

Canada

**University of Alberta
Library Release Form**

Name of Author: Shannon Patricia Lubitz

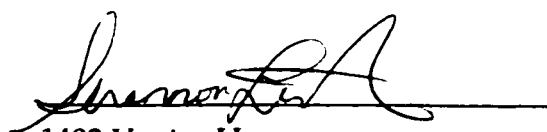
Title of Thesis: The *Escherichia coli* YnfEFGHI Operon: A Dimethyl Sulfoxide Reductase (DmsABC) Parologue

Degree: Master of Science

Year this Degree Granted: 2002

Permission is hereby granted to the University of Alberta Library to reproduce single copies of this thesis and to lend or sell such copies for private, scholarly or scientific research purposes only.

The author reserves all other publication and other rights in association with the copyright in the thesis, and except as herein before provided, neither the thesis nor any substantial portion thereof may be printed or otherwise reproduced in any material form whatever without the author's prior written permission.




1403 Vanier House
Michener Park
Edmonton, Alberta
T6H 4N1

Date: April 11, 2002

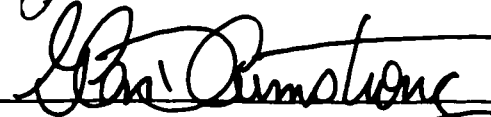
University of Alberta

Faculty of Graduate Studies and Research

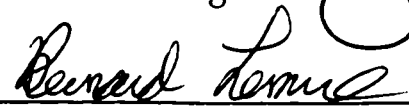
The undersigned certify that they have read, and recommend to the Faculty of Graduate Studies and Research for acceptance, a thesis entitled *The Escherichia coli YnfEFGHI Operon: A Dimethyl Sulfoxide Reductase (DmsABC) Parologue*, submitted by Shannon Patricia Lubitz in partial fulfillment of the requirements for the degree of Master of Science.



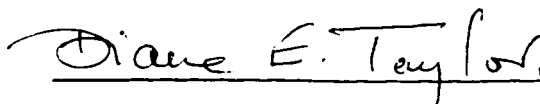
Dr. Joel Weiner




Dr. Glen Armstrong



Dr. Bernard Lemire



Dr. Diane Taylor



Dr. Tracy Raivio

Date: April 11/02

Abstract

The *ynfEFGHI* operon is a paralogue of the well-characterized *Escherichia coli* *dmsABC* operon. YnfEFG could be expressed from a *tac* or *dms* promoter vector. YnfEFGH were membrane-localized but both protein expression and complementation of growth of a *dms* deletion on dimethyl sulfoxide were poor. We used chimeric enzymes to study the function and interchangeability of the subunits. Exchange of the membrane anchor DmsC by YnfH (DmsAB-YnfH) resulted in membrane localization, anaerobic growth on dimethyl sulfoxide and binding of 2-*n*-hepty-4-hydroxyquinoline-N-oxide indicating that YnfH was a competent anchor. YnfG replaced DmsB as the electron transfer subunit and assembled the 4 [4Fe-4S] clusters. When YnfF replaced DmsA, expression of the complex was poor and only YnfFG-DmsC and YnfFGH demonstrated glycerol-DMSO growth and enzymatic activity. Hydroxypyridine N-oxide was the best acceptor. When YnfE replaced DmsA, either alone, or in combination with YnfF, no complementation or activity was observed.

Acknowledgments

I would first like to thank my supervisor, Joel Weiner, for his guidance and teaching. He's given me the tools and the confidence I need to pursue my goal of a career in drug research. His enthusiasm was contagious and his infinite patience and suggestions were very appreciated!

I would also like to acknowledge all of my co-workers, especially Glen Zhang and Gillian Shaw for their technical advice and assistance, Dr. Richard Rothery for performing the EPR experiment found in Chapter 2 and his many suggestions throughout my studies, and Dr. Paulina Geiger and Dr. Steve Brokx for critical reading of the results chapter. You all made my research and time in the lab very enjoyable and rewarding!

I would also like to express my gratitude to my supervisory committee, Drs. Glen Armstrong, Bernie Lemire and Diane Taylor. Thank you all for your help and wonderful recommendations over the years!

My husband Troy, who has supported and encouraged me throughout my graduate studies, also deserves a huge thank you! I'll never be able to thank him enough for being here with me which required moving across the country! He inspired me to follow my dreams of pursuing a graduate degree, and was wonderfully caring and understanding throughout the ups and downs of grad school.

I am very appreciative to the Alberta Heritage Foundation for Medical Research, and to the Departments of Medical Microbiology and Immunology, and Biochemistry for their financial support.

Table of Contents

Chapter 1: Introduction	1
1.1. Introduction	1
1.2. Respiration	2
1.3. Regulation	2
1.3.1. ArcAB.....	3
1.3.2. FNR.....	5
1.3.3. NAR.....	6
1.4. Prosthetic Groups.....	7
1.4.1. Molybdenum Cofactor.....	7
1.4.2. Hemes.....	10
1.4.3. Iron-Sulfur Centres	10
1.4.4. Flavins	12
1.5. Dehydrogenases	12
1.5.1. NADH Dehydrogenase	12
1.5.2. Formate Dehydrogenase.....	13
1.5.3. Glycerol-3-Phosphate Dehydrogenase.....	14
1.5.4. Hydrogenase.....	15
1.5.5. Pyruvate Dehydrogenase	16
1.5.6. Succinate Dehydrogenase.....	17
1.6. Quinones.....	17
1.7. Oxidases	18
1.7.1. Cytochrome <i>bd</i> Oxidase.....	18

1.7.2. Cytochrome <i>bo</i> ₃ Oxidase	19
1.8. Reductases.....	20
1.8.1. Fumarate Reductase.....	20
1.8.2. Nitrate Reductase	24
1.8.3. Nitrite Reductase.....	27
1.8.4. TMAO Reductase	28
1.8.5. Biotin Sulfoxide Reductase	29
1.8.6. Methionine Sulfoxide Reductase	29
1.8.7. DMSO Reductase	30
1.8.7.1. Introduction	30
1.8.7.2. <i>Rhodobacter</i> DMSO Reductase	31
1.8.7.3. <i>Escherichia coli</i> DMSO Reductase	37
1.9. Translocation	44
1.9.1. Membrane Targeting and Translocation System (MTT).....	44
1.9.2. YnfI	44
1.10. Thesis Introduction and Objectives	45
Chapter 2: Investigation of Expression, Localization and Function of the YnfEFGH Operon	48
2.1. Introduction	48
2.2. Material and Methods.....	50
2.2.1 Materials	50
2.2.2 Cloning Strategy.....	50
2.2.3. Aerobic Growth.....	56
2.2.4. Anaerobic Growth.....	56

2.2.5. Preparation of Membranes and Soluble Fractions	56
2.2.6. Polyacrylamide Gel Electrophoresis and Immunoblotting of Ynf Proteins	57
2.2.7. Protein Determination	57
2.2.8. Benzyl Viologen Enzyme Assays.....	57
2.2.9. Lapachol Enzyme Assays	58
2.2.10. Fluorescence Analysis of Molybdopterin Cofactor	58
2.2.11. 2- <i>n</i> -hepty-4-hydroxyquinoline-N-oxide (HOQNO) Fluorescence Binding.....	58
2.2.12. EPR Spectroscopy	59
2.3. Results	60
2.3.1. A paralogue of the <i>dmsABC</i> operon in <i>E. coli</i>	60
2.3.2. Detection of the products of the <i>ynf</i> Open Reading Frames.....	61
2.3.3. Localization of YnfEFGH.....	65
2.3.4. Growth Complementation in DSS301	68
2.3.5. Expression and Localization of the Chimeric Enzymes.....	71
2.2.6. HOQNO Binding	74
2.3.7. Enzymatic Assays.....	76
2.3.8. Substrate Specificity of YnfF	78
2.3.9. Form A Fluorescence	80
2.3.10. Electron Paramagnetic Resonance of the Fe-S Clusters	82
2.4. Discussion	84
References	88
Appendix: Inclusion Body Reduction	111

List of Tables

Table 2.1 Bacterial strains and plasmids used in this study	52
Table 2.2 PCR primers used to amplify <i>ynf</i> and <i>dms</i> genes	53
Table 2.3 Enzymatic activity of selected chimeric plasmids.....	77
Table 2.4 Benzyl viologen enzyme assays of membrane fractions.....	79

List of Figures

Figure 1.1 Signal transduction by the Arc system.....	4
Figure 1.2 Molybdenum cofactor biosynthesis.....	9
Figure 1.3 Structures of iron-sulfur clusters	11
Figure 1.4 Crystal structure of DMSO reductase from <i>Rhodobacter sphaeroides</i> .	35
Figure 1.5 Mechanism of DMSO reduction	36
Figure 1.6 Proposed topology of <i>Escherichia coli</i> DMSO Reductase.....	43
Figure 2.1 Restriction map of cassette plasmids.....	55
Figure 2.2 Western blot of <i>E. coli</i> TG1 whole cells expressing the <i>ynf</i> operon ...	64
Figure 2.3 Expression of YnfFGH in <i>E. coli</i> BNN103 under <i>dms</i> promoter control	67
Figure 2.4 Anaerobic growth of <i>E. coli</i> DSS301 containing Ynf plasmids at 30°C on glycerol-DMSO medium.....	68
Figure 2.5 Anaerobic growth of <i>E. coli</i> DSS301 containing chimeric plasmids at 30°C on glycerol-DMSO medium.....	70
Figure 2.6 Immunoblots of membrane and soluble fractions from <i>E. coli</i> DSS301 complemented with chimeric plasmids	73
Figure 2.7 Quenching of HOQNO fluorescence.....	75
Figure 2.8 Form A fluorescence of membranes expressing various chimeric enzymes	81

Figure 2.9 EPR spectra of dithionite-reduced membranes from *E. coli* DSS301 cells expressing chimeric Dms:Ynf proteins83

List of Abbreviations

ATP	adenosine triphosphate
BV	benzyl viologen
cAMP	cyclic adenosine monophosphate
CPNO	2-chloropyridine N-oxide hydrochloride
CRP	cAMP receptor protein
DMS	dimethyl sulfide
DMSO	dimethyl sulfoxide
DTT	dithiothreitol
<i>E.</i>	<i>Escherichia</i>
EPR	electron paramagnetic resonance
FAD	flavin adenine dinucleotide
Fe-S	iron sulfur centre
FMN	flavin mononucleotide
GD	glycerol dimethyl sulfoxide minimal media
GF	glycerol fumarate minimal media
GST	glutathione S-transferase
HOQNO	2-n-heptyl-4-hydroxyquinoline-N-oxide
HPNO	hydroxypyridine N-oxide
IPTG	isopropyl β -D-thiogalactoside
ISNO	isonicotinic acid N-oxide
kD	kilodalton
LB	Luria Bertani broth
MGD	molybdopterin guanine dinucleotide

Mo	molybdenum
MOPS	3-[N-morpholino] propanesulfonic acid
MPT	molybdopterin
MTT	membrane targeting and translocation system
NADH	nicotinamide adenine dinucleotide
PCR	polymerase chain reaction
PMF	proton motive force
PMSF	phenylmethyl sulfonyl fluoride
PNO	pyridine N-oxide
R.	<i>Rhodobacter</i>
TAT	twin-arginine translocation
TB	terrific broth
TCA	tricarboxylic acid cycle
TMA	trimethylamine
TMAO	trimethylamine N-oxide
TMS	transmembrane segment
TP	tryptone phosphate broth
TPP	thiamine pyrophosphate
W.	<i>Wolinella</i>

Chapter 1: Introduction

1.1. Introduction

Escherichia coli meets its energy needs by two biochemical mechanisms: fermentation and respiration. Fermentation is a wasteful means of deriving energy, as it is only generated from substrate-level phosphorylation reactions. Since the substrate is not completely oxidized, fermentation results in smaller amounts of energy than respiration. When exogenous electron acceptors are available, the cell switches to respiration. This process conserves the reducing equivalents in NADH or exogenous electron donors by coupling electron transfer reactions to the generation of a proton electrochemical potential gradient across the cell membrane (53). This gradient can be used for solute transport, flagellar rotation or ATP synthesis (53, 136, 180).

Respiration requires three main components: a membrane bound dehydrogenase, a quinone (a lipid soluble hydrogen carrier), and a terminal reductase. The primary dehydrogenase oxidizes the electron donor and reduces the quinone to quinol by passing the reducing equivalents from the oxidized substrate to the quinone. The reduced quinol acts as an intermediate electron carrier from the oxidase to the reductase. It passes two electrons to the terminal reductase to reduce the terminal electron acceptor. The terminal reductase oxidizes the quinol to quinone and reduces the terminal electron acceptor. The transfer of two protons from the cytoplasm to periplasm generates the proton motive force. Both the dehydrogenase and reductase catalyze two half reactions, often at different sites of the protein on opposite sides of the membrane (53). All

dehydrogenases are quinone reductases and all terminal reductases are quinol oxidases (53).

1.2. Respiration

Mitchell's chemiosmotic hypothesis (111) states that electron transport from oxidation-reduction reactions through the respiratory chain is coupled to the stoichiometric proton translocation across the membrane. This results in both a pH gradient (ΔpH) and electrical potential ($\Delta \psi$) across the membrane. This proton translocation can be mediated by one of two mechanisms. The scalar mechanism is when one half reaction consumes cytoplasmic protons and the other half reaction delivers them to the periplasm, i.e. the two half reactions occur on opposite sides of the membrane (53). Thus the proton gradient results from the chemistry occurring at two separated active sites so no proton channel is required (53). The vectorial mechanism occurs in an enzyme that has a proton pump that actively removes protons from the cytoplasm and delivers them to the periplasm (53).

1.3. Regulation

E. coli respiratory chains consist of at least 15 primary dehydrogenases and 10 terminal reductases (53). How the cell decides which chain to express is regulated at a number of levels. One level is determined by aerobiosis. In the presence of oxygen, ArcAB and FNR ensure that the cell will preferentially use oxygen as the terminal electron acceptor, as it generates the most energy. Under anaerobic conditions another level of regulation comes into play, mediated by

ArcAB, FNR and NAR. The better electron acceptors repress the expression of the respiratory chains for the poorer ones, i.e. the electron donor-acceptor with the greatest difference in midpoint potential will be used (70). Thus nitrate is a better substrate than fumarate and DMSO so NAR blocks the expression of their respiratory enzymes. This of course also depends on substrate availability.

The *E. coli* respiratory system is relatively simple and is set up as modules, meaning that different components can be substituted in place of or in addition to other components to make a functional respiratory chain (53). Many of the dehydrogenases can function with a variety of the terminal reductases depending on the availability of substrate and the potential difference between the donor-acceptor pair. This allows the cell to make minimal changes under different growth conditions (53). In the absence of electron acceptors the cell is forced to rely on the energetically less favourable fermentation (70).

1.3.1. ArcAB

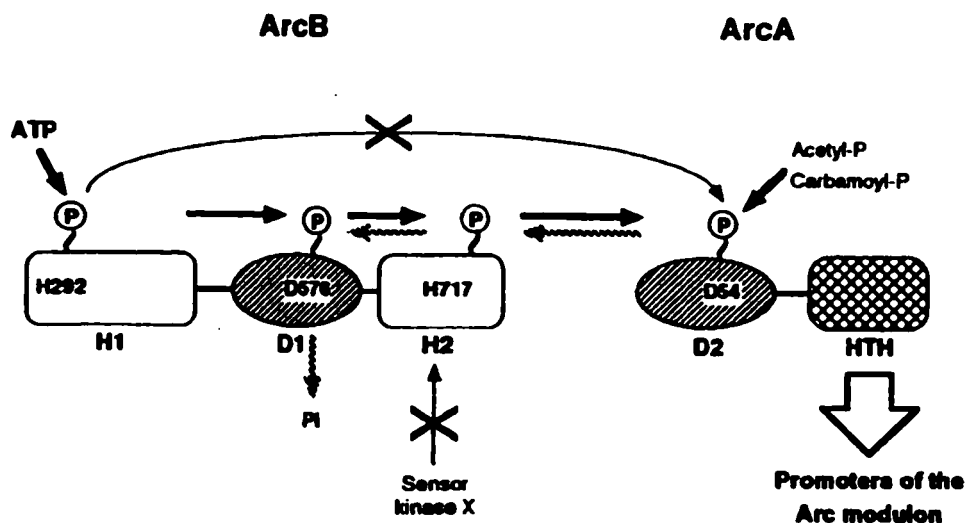
ArcAB or aerobic respiratory control, is a two-component regulatory system that, under anaerobic conditions, represses aerobically-expressed respiratory genes and activates some genes involved in anaerobic respiration (72, 181). ArcA is located at 0 minutes (70) and ArcB at 69.5 minutes on the *E. coli* chromosome (70). ArcA is a 28 kD transcriptional response regulator containing a helix-turn-helix DNA binding motif (70), with an N-terminal receiver domain and a C-terminal effector domain. ArcB is a 77 kD membrane sensor functioning as a sensory protein kinase (74). It has a transmitter and receiver domain with two

putative transmembrane segments near the N-terminus with a small portion of the protein periplasmically exposed (74).

ArcB controls ArcA activity through transphosphorylation reactions (68, 71, 73). ArcB autophosphorylates at His292 in the primary transmitter domain (68, 73), at the expense of ATP. This phosphoryl group is transferred to Asp576 in the ArcB receiver domain (68, 73, 91). At its C-terminus ArcB contains a third domain called the secondary transmitter domain (91). This domain contains His717, which receives the phosphate from Asp576. ArcA receives the phosphate from His717 at its Asp54 residue (see Figure 1.1).

Although the site of phosphate binding and the path it travels is fairly well understood, the original signal for the autophosphorylation of ArcB is not. It has been proposed to be redox state, metabolites generated by anaerobic respiration (9), respiration rate (3) or by proton motive force (21, 75).

Figure 1.1. Signal transduction by the Arc system (91).



1.3.2. FNR

Fumarate and nitrate reductase regulatory protein or FNR, is a positive regulator for the expression of many anaerobic respiratory enzymes (107, 181) and the repressor of some aerobic enzymes (51, 54). The protein acts like an anaerobic switch. In the absence of oxygen it functions as a positive gene activator, stimulating the transcription of a number of anaerobic proteins. FNR functions by binding DNA as a homodimer at the FNR box positioned -41bp upstream of the transcriptional start site (28) encoded by TTGAT-ATCAA (50). The two domain, 31 kD protein is encoded at 29.3 minutes (169), is constitutively expressed and is highly homologous to CRP, the cAMP receptor protein that is responsible for controlling catabolite repression in *E. coli*.

The FNR N-terminal domain contains a group of cysteine residues unlike CRP that coordinate a [4Fe-4S] centre. These cysteines are essential for FNR's ability to sense redox potential that results in FNR dimerization that is necessary for DNA binding where it exerts its activating effects (41, 86, 182, 191). Growth in iron-depleted media or removal of iron by chelating agents inactivates the regulator, indicating the importance of iron as a cofactor in FNR activation (86, 182, 191). FNR is inactivated by oxygen as it changes the iron centre to a [3Fe-4S] or [2Fe-2S] centre (198). The C-terminal domain of FNR is the DNA binding regulatory domain that is very homologous to CRP, with a helix-turn-helix motif characteristic of DNA binding proteins (170, 190, 197). FNR activates transcription initiation by interacting directly with the RNA polymerase at defined surface exposed activating regions (100, 209, 210).

1.3.3. NAR

Due to its relatively high midpoint potential, nitrate is the preferred electron acceptor in anaerobic cells. The presence of nitrate induces the nitrate respiratory chain and represses other anaerobic respiratory enzymes. The NAR system encodes two homologous two-component regulatory systems NarL/NarX and NarP/NarQ responsible for nitrate/nitrite regulation. Each is comprised of an integral membrane nitrate sensor and a transcriptional regulator. It is thought that both regulators interact with both sensors to control nitrate and nitrite-regulated gene expression.

NarX/NarL comprises one of the two regulatory systems. *narX* and *narL* are two adjacent genes encoding proteins of 66 kD and 23 kD respectively and are located at 27 minutes on the chromosome (84). NarL is the response regulator and NarX is the cognate sensor with histidine protein kinase activity. NarX detects the availability and changes in environmental signals like nitrate and NarL, on phosphorylation by NarX, activates/represses the transcription of sensitive genes by binding specific DNA sequences (72, 84). NarL activates the *narGHJ* operon that encodes the major nitrate reductase and *fdnGHI* that encodes the formate dehydrogenase associated with nitrate reduction (11, 184). NrfABCDEFG, the formate-dependent nitrite reductase is repressed by NarL in the presence of nitrate but is activated by NarL and NarP in the presence of nitrite (133, 195).

The second regulation system is comprised of NarQ, the membrane sensor and NarP the transcriptional response regulator. *narQ* is located at 53 minutes and *narP* at 46 minutes (49, 53, 134).

In response to nitrate or nitrite, NarL and NarP are phosphorylated by their membrane-bound sensor kinase proteins NarX or NarQ, respectively. The phosphorylated NarL and NarP then bind to specific heptamer sequences at target promoters and either up- or downregulate transcriptional initiation at these promoters (195).

1.4. Prosthetic Groups

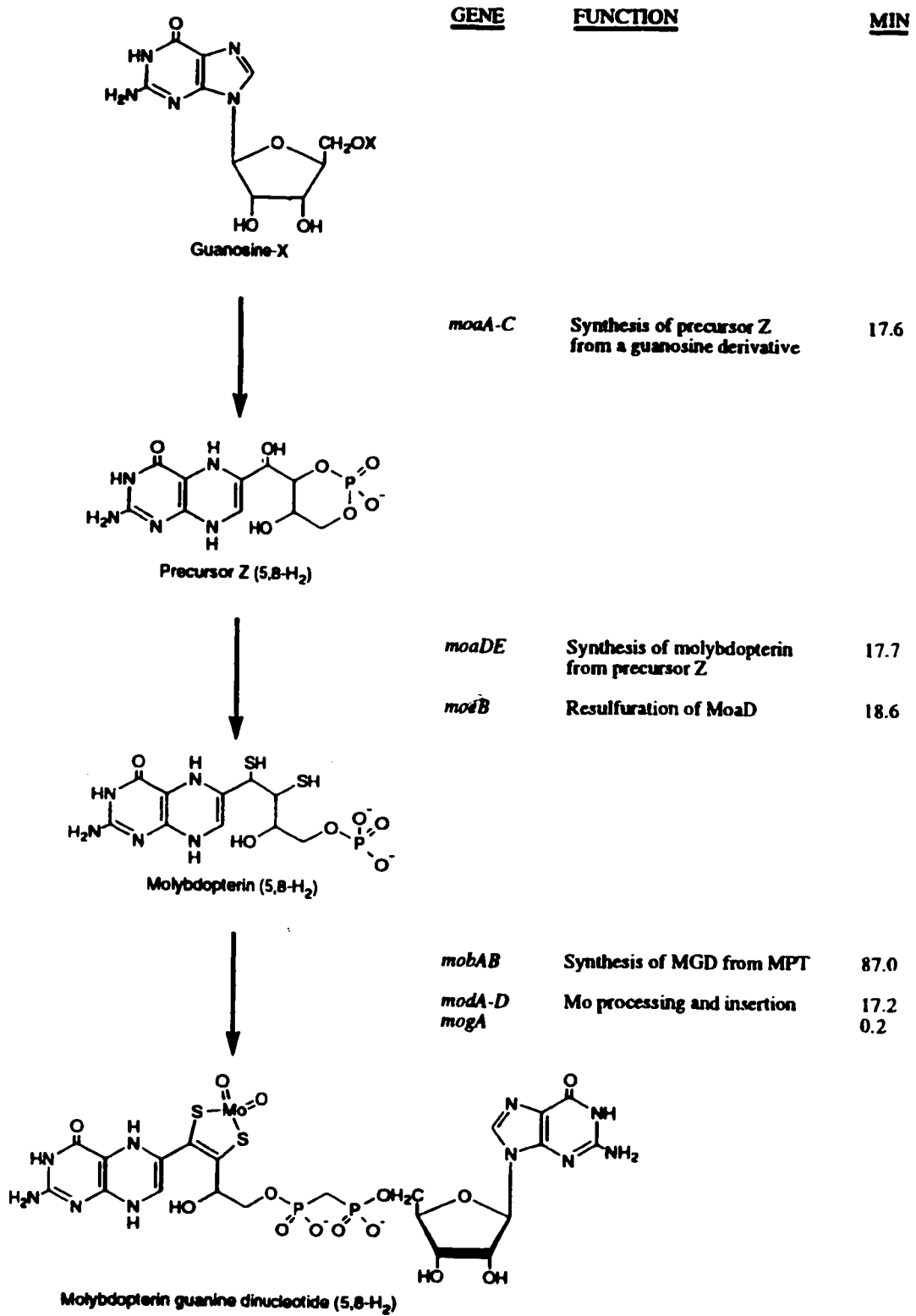
Electron transport is fundamental in respiration and requires redox centres in the respiratory proteins involved. These redox centres include molybdenum cofactor (moco), heme, iron-sulfur (Fe-S) centres, flavin adenine dinucleotide (FAD), flavin mononucleotide (FMN), nickel-metal (Ni-M) dinuclear centres, polynuclear copper (Cu) sites, and pyrroloquinoline quinone (PQQ) (12).

1.4.1. Molybdenum Cofactor

The functional form of the molybdenum cofactor found in enterics is molybdopterin guanine dinucleotide (Mo-MGD) (53). The synthesis of the cofactor in *E. coli* occurs in four stages prior to insertion into the enzyme, involving 5 genetic loci *moa*, *mob*, *mod*, *moe* and *mog* (48) (see Figure 1.2). Biosynthesis of precursor Z and its conversion to MPT requires the *moa* and *moe* loci (48). *MoaABC* convert guanosine-X to precursor Z and *MoeB* and *MoaDE*

are thought to be involved in the addition of sulfur in MPT (179). The *mod* locus encodes a high affinity molybdate-specific uptake system (48). The products of the *mob* locus are required for the final step of Mo-MGD biosynthesis, the attachment of the GMP to MPT (48). MobB likely binds the guanine nucleotide that is incorporated into the final product.

Figure 1.2. Molybdenum cofactor biosynthesis (135).



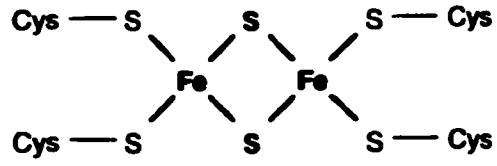
1.4.2. Hemes

Hemes are electron transfer moieties often found in respiratory enzymes. Heme *b* is commonly found in intrinsic membrane proteins where it mediates electron transfer between quinone pools and its respective enzyme. Heme b_{556} is present in nitrate reductases NRA and NRZ, in formate dehydrogenases -N and -O (53), and in aerobic succinate dehydrogenase (88). Heme *c* is periplasmically localized in anaerobic respiratory enzymes, some are soluble and others are membrane anchored but they always face the periplasm. Heme *c* is found in nitrite reductase (NrfAB), periplasmic TMAO reductase (TorCAD) and in periplasmic nitrate reductase (NapABC) (53). Heme *d* and *o* are only found in two terminal oxidases Cyd and Cyo respectively (53).

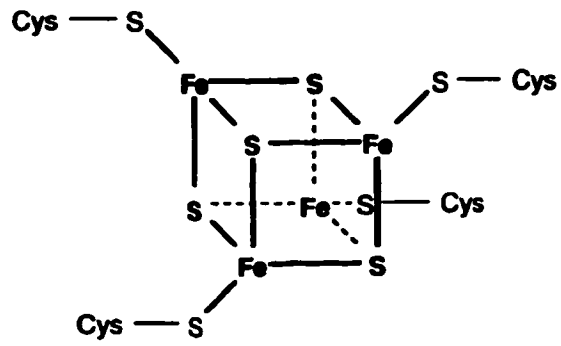
1.4.3. Iron-Sulfur Centres

Iron-sulfur centres are involved in single electron transfer reactions (29). These assemblies contain covalently bonded iron and sulfur with additional covalent bonds between iron and specific cysteine residues in the protein. Binuclear centres [2Fe-2S] have 2 iron and 2 sulfur atoms with each iron bonded to one or two cysteines. Tetranuclear [4Fe-4S] centres have 4 atoms of each displaying a cubane pattern (Figure 1.3) with each iron additionally bonded to a single cysteine. [3Fe-4S] centres resemble the structure of the [4Fe-4S] except one of the cysteines is not present and therefore one of the iron atoms is not present (193). The amino acid sequence that specifies a [4Fe-4S] centre contains clusters of 4 cysteines where the first three ligate the centre and the fourth ligates an iron for a second cluster (141, 206).

Figure 1.3. Structures of iron-sulfur clusters (53).



[2Fe-2S] Cluster



[4Fe-4S] Cluster

1.4.4. Flavins

Flavins in the form of FAD or FMN are components involved in electron transport. They transfer one or two electrons to and from redox centres. They are rarely covalently attached to proteins through a linkage. $\delta\alpha$ -(N3-histidyl) FAD is at the active site of all fumarate reductases and succinate dehydrogenases (137). FAD is present in NADH dehydrogenase II and FMN is in NADH dehydrogenase I.

1.5. Dehydrogenases

1.5.1. NADH Dehydrogenase

There are two NADH dehydrogenases in *E. coli*, NDH-I and NDH-II, both of which are membrane bound and contain noncovalently bound FMN or FAD respectively (77). Oxidation of NADH is used to feed electrons to the respiratory chain (53). NDH-I is a primary proton pump that translocates protons in a vectorial manner (53). It is a homologue of the mitochondrial complex I (201) and is composed of 14 subunits, *nuoABCDEFGHIJKLMN*, encoded at 49 minutes on the chromosome (97, 201). Seven of the 14 subunits contain TMS (transmembrane segments). Not all subunits have a known function but NuoF is 50 kD, is the NADH and FMN binding site and contains one [4Fe-4S] centre. NuoH is 36 kD, contains 8 TMS and is the quinone binding site.

NDH-II is a 47 kD single subunit peripheral membrane enzyme with no TMS (77) that oxidizes NADH on the cytoplasmic side of the membrane. It is not coupled to the generation of a proton electrochemical gradient.

1.5.2. Formate Dehydrogenase

There are three formate dehydrogenases in *E. coli*, formate dehydrogenase-H (*fdnF*), -N (*fdnGHI*) and -O (*fdoGHI*) (53). All three are involved in formate-nitrate respiration although formate dehydrogenase-O is minor and formate dehydrogenase-H is usually considered a fermentative enzyme (53). All three also contain a selenocysteine amino acid encoded by an opal codon (UGA) (53) and a molybdenum cofactor (98, 123). Formate oxidation in nitrate-grown cells results in transmembrane proton translocation by the scalar mechanism (79) that contributes to the proton motive force.

Formate dehydrogenase-H is 80 kD, encoded by *fdnF* at 92 minutes on the chromosome (10) and is a component of the formate-hydrogen lyase enzyme complex. The complex consists of the molybdoenzyme FdhF and hydrogenase 3 (HycB) (167), and is expressed when cells are grown anaerobically in the absence of exogenous electron acceptors (53).

The nitrate inducible formate dehydrogenase-N is expressed from *fdnGHI* at 32 minutes on the chromosome (10, 192, 194) when cells are grown anaerobically in the presence of nitrate (10, 194). This enzyme serves as a major electron donor for nitrate respiration (10). FdnG (α_N) is a large 110kD selenomolybdoprotein containing MGD at its active site and is homologous to FdnF (10). FdnH (β_N) is 32 kD and contains 4 cysteine clusters ligating 4 [4Fe-4S] centres and functions as the electron transfer subunit between FdnG and FdnI (10). FdnI (γ_N) is 20 kD and encodes cytochrome b_{Fdn556} (10, 205) and three transmembrane segments

characteristic of *b*-type hemoproteins (10). Two of the TMS contain a histidine residue, which likely are ligands for the heme (10). This subunit is responsible for the electron transfer from FdnH to the quinone pool.

Formate dehydrogenase-O is synthesized at low levels regardless of aerobiosis and nitrate (125). It is encoded by *fdoGHI* at 88 minutes (125) and is structurally similar to FdnGHI (124, 125). It may serve to couple formate oxidation to the reduction of a number of electron donors, i.e. oxygen (53).

1.5.3. Glycerol-3-Phosphate Dehydrogenase

There are two glycerol-3-phosphate dehydrogenases expressed in *E. coli* (53). Both oxidize glycerol-3-phosphate to dihydroxyacetone phosphate and reduce quinone. The function of these enzymes is to salvage the glycerol and glycerol phosphate that is produced by phospholipid and triacylglycerol breakdown (53).

The aerobic glycerol-3-phosphate dehydrogenase (GlpD) is a 57 kD membrane associated, FAD-containing homodimer (166) that catalyzes the oxidation of glycerol-3-phosphate with oxygen or nitrate as the electron acceptor (53). The *glpGED* operon is encoded at 75 minutes on the chromosome and its expression is controlled by glycerol and catabolite repression (216).

The anaerobic glycerol-3-phosphate dehydrogenase is a three subunit enzyme loosely associated with the membrane that oxidizes glycerol-3-phosphate but uses an electron acceptor other than oxygen (53). The operon encoding the enzyme is *glpACB* located at 49 minutes on the *E. coli* chromosome (90). Its

expression is induced anaerobically in the presence of fumarate and is mediated by FNR (69). GlpA is a 62 kD protein that contains noncovalently bound FAD, GlpB is a 44 kD protein encoding the membrane anchor subunit and GlpC is 41 kD.

1.5.4. Hydrogenase

Hydrogen is an important electron donor in anaerobic respiration with nitrate, DMSO, TMAO and fumarate as electron acceptors (104, 162, 211, 214). The oxidation of hydrogen contributes to the transmembrane proton translocation by the scalar method (53). There are three membrane-bound nickel-containing hydrogenases in *E. coli*, hydrogenase-1 (HyaABC), hydrogenase-2 (HybABC), and hydrogenase-3 (HycEG) (53). Hydrogenases 1 and 2 oxidize dihydrogen to protons and donate the electrons to the quinone pool. Both menaquinone and demethylmenaquinone are electron acceptors for dihydrogen oxidation (53). Hydrogenase-3 is a component of the formate-hydrogen lyase complex involved in pH balance during fermentative growth (53).

The physiological role of hydrogenase-1 is unclear as it only minimally contributes to the hydrogenase activity. It is encoded at 22 minutes by *hyaABCDEF* where HyaABC make up the enzyme and HyaDEF are involved in the maturation of the enzyme. HyaA is a 41 kD protein that contains a signal sequence that is responsible for membrane targeting (53). HyaB, based on its sequence, probably contains 2 [4Fe-4S] centres (109) and HyaC may be cytochrome *c* (108).

Hydrogenase-2 is responsible for the majority of a cell's hydrogenase activity especially in glycerol-fumarate respiring cells (53). It is encoded by *hybABCDEFG*. HybABC make up the enzyme and HybDEFG are involved in enzyme maturation. HybA has an N-terminal signal sequence (53) so probably targets the enzyme to the membrane, HybB sequence predicts 4 [4Fe-4S] centres and HybC is predicted to be cytochrome *b* (108). Synthesis only occurs under anaerobic conditions and is repressed in the presence of nitrate (161, 162).

1.5.5. Pyruvate Dehydrogenase

Pyruvate dehydrogenase is a peripheral membrane flavoprotein that catalyzes the oxidation of pyruvate to acetate and carbon dioxide with the concomitant reduction of quinone (57). The enzyme is encoded by *poxB* at 19 minutes on the *E. coli* chromosome and is maximally expressed during early stationary phase (57). It is composed of four identical 62 kD subunits that contain tightly bound FAD and loosely bound TPP (thiamine pyrophosphate) (57). In the presence of pyruvate and TPP a conformational change occurs that exposes a hydrophobic lipid binding site (148). This site is important as the enzyme is dramatically activated by lipids and this is thought to be important for access to ubiquinone-8 in the membrane (57). The enzyme is thought to shuttle between the cytosol and membrane depending on the presence of pyruvate (37). When pyruvate levels are low, the enzyme is inactive and soluble but when levels are high it triggers the conformational change that exposes the C-terminal lipid-binding domain that inserts into the lipid bilayer (37). The enzyme can alternatively be activated by proteolytic clipping of a small 2.6 kD peptide from the C-terminus (57). Both

types of activation require TPP and pyruvate and prevent the C-terminal domain from interacting with the active site where it usually blocks pyruvate from binding (37).

1.5.6. Succinate Dehydrogenase

Succinate dehydrogenase is an aerobically expressed flavoprotein involved in the oxidation of succinate to fumarate, and is a critical component of the TCA cycle (53). It is similar in composition and subunit structure to fumarate reductase. The *sdhCDAB* operon (60) located at 17 minutes on the *E. coli* chromosome, encodes a membrane localized enzyme that catalyzes the two electron transfer between succinate and quinone, transferring the reducing equivalents to ubiquinone as part of the aerobic respiratory chain.

SdhA is a 64 kD catalytic subunit containing the covalently bound FAD and dicarboxylate binding site (63). SdhB is the 26 kD electron transfer subunit that contains 3 iron-sulfur clusters (63). SdhC (14 kD) and SdhD (12 kD) are the membrane anchor subunits required for quinone binding. The two also share a heme b_{556} cofactor that is involved in assembly and structure of the membrane anchors as it bridges the two (53).

1.6. Quinones

Quinones are membrane soluble electron carriers that couple proton and electron transfer between protein components of the respiratory chain (53). There are three types of quinones in *E. coli*, all containing an octaprenyl side chain (C40):

benzoquinone, ubiquinone, and two naphthoquinones, menaquinone and demethylmenaquinone (53). Oxygen respiration makes use of ubiquinone, nitrate respiration ubiquinone and menaquinone, and anaerobic respiration with acceptors other than nitrate use both menaquinone and demethylmenaquinone (53). These preferences are reflected in quinone abundance under different conditions. Aerated cells contain 4-5 times more ubiquinone than menaquinone and demethylmenaquinone and anaerobic cells have about one third of the ubiquinone (10 fold decrease) as menaquinone and demethylmenaquinone (53, 200, 212). These ratios also make sense with respect to midpoint potentials as menaquinone/menaquinol has a 200mV lower potential than ubiquinone/ubiquinol (53), which makes menaquinone a better choice for anaerobic respiratory chain enzymes, which have lower potential electron acceptors (53).

1.7. Oxidases

1.7.1. Cytochrome *bd* Oxidase

Cytochrome *bd* oxidase is an ubiquinol-8 oxidase that reduces oxygen to water and is maximally expressed in limited aeration (61). It generates PMF by translocating substrate protons in a scalar manner (46, 47). The enzyme may be responsible for scavenging oxygen to prevent the degradation of oxygen sensitive enzymes (65). It is made up of two subunits, CydAB encoded at 16 minutes on the chromosome (25) that are regulated by FNR (53). Both subunits contain TMS (117) and are integral membrane proteins (55). CydA is the 58 kD protein that contains heme b_{558} where quinol oxidation occurs (62) and shares

heme b_{595} and heme d with CydB, which is a 42 kD protein of unknown function (101). Heme d is the site of oxygen binding but the role of heme b_{595} is unknown but it has been proposed to interact with heme d to jointly reduce oxygen to water (64).

CydCD, located at 19 minutes are required for assembly of CydAB (56, 127, 215), specifically for the insertion of heme d (56, 215) and may affect heme b_{558} and b_{595} (127). These two proteins encode an ATP dependent transporter in the cell membrane (127) so their actual function may be to transport the hemes to the periplasm where they are incorporated into the enzyme (127).

1.7.2. Cytochrome bo_3 Oxidase

Cytochrome bo_3 oxidase is a membrane-bound terminal oxidase that is expressed when cells are grown under high aeration conditions (52). It oxidizes ubiquinol and reduces oxygen to water and in the process translocates protons across the cell membrane in a vectorial manner (52, 53). The operon encoding the enzyme, *cyoABCDE* is at 10 minutes on the chromosome and is regulated by ArcAB (53). All four subunits (CyoABCD) contain transmembrane segments and are integral membrane proteins (103). CyoA (subunit II) is a 35 kD quinol oxidase (103) with two TMS and a cleavable signal sequence. It is covalently modified by the attachment of lipids at the new N-terminus (103). CyoB (subunit I) is 75 kD, contains heme b_{562} , heme o_3 and cu_B . It has 12 predicted TMS, is the site of oxygen binding and reduction and acts as a proton pump (53). CyoC (subunit III) is 23 kD and CyoD (subunit IV) is 12 kD. Both proteins are components of the final

enzyme complex and contain TMS (103). CyoE (32 kD) is involved in heme *o* synthesis (farnesyltransferase) (53, 103).

1.8. Reductases

1.8.1. Fumarate Reductase

Fumarate reductase is an integral membrane protein involved in anaerobic respiration where it oxidizes menaquinol and reduces fumarate to succinate. The *E. coli* enzyme consists of four subunits, FrdABCD encoded at 94.4 minutes on the chromosome. FrdA is a 66 kD flavoprotein containing a covalently $\delta\alpha$ -[N ϵ -histidyl]-linked FAD, the catalytic site for fumarate reduction and succinate oxidation (44, 199). FrdB is the 27 kD protein containing 3 iron-sulfur centres, a [2Fe-2S], a [4Fe-4S] and a [3Fe-4S] centre. FrdAB are soluble hydrophilic subunits localized to the cytoplasmic side of the membrane by two membrane anchors, FrdC (15 kD) and FrdD (13 kD). These subunits function not only as anchors but also in menaquinol oxidation as there are at least two quinone binding sites associated with them (149, 151, 207), although only the proximal quinol binding site is involved in electron transfer reactions.

A structural study on the *E. coli* enzyme at 3.3 Å (76) demonstrated that the four subunits are arranged in a 'q' like configuration, with the top of the 'q' formed by the two hydrophilic subunits (70 Å in diameter) and the tail (110 Å long) by the hydrophobic subunits.

A higher resolution structure (2.2 Å) of *Wolinella succinogenes* fumarate reductase (95) gives further insight into the enzyme structure. It can be compared to the *E. coli* enzyme as all amino acids implicated in substrate binding and catalysis are conserved at the structural level, indicating a common mechanism in both enzymes (165). The major differences between the *W. succinogenes* and *E. coli* enzymes is that the former has only three subunits (one membrane anchor with five TMS) and within this anchor there are two heme *b* groups which are absent from the *E. coli* FrdCD. Because of the differences in the membrane anchor(s) the relative orientation of the soluble and membrane-bound subunits is dissimilar. The other variation between the two enzymes is that the *Wolinella* enzyme forms a dimer connected at the membrane anchor subunit, which does not occur in the *E. coli* enzyme.

The *Wolinella* structure revealed that FrdA consists of four domains, the large FAD-binding domain, the capping domain, the helical domain and the C-terminal domain. Upon superimposition of the enzymes of the two bacteria, a high degree of structural similarity was observed in the first three domains of this subunit. The study demonstrated that the fumarate binding site is located between the FAD-binding and capping domains next to the plane of the FAD isoalloxazine ring. It also revealed that His A43 is the residue that covalently binds the isoalloxazine ring of FAD. The flavin is additionally hydrogen bonded by a number of other residues throughout FrdA. An additional metal binding site tentatively assigned to a calcium ion was found in the FAD binding domain.

The dicarboxylate-binding site is primarily formed by the FAD isoalloxazine ring, two arginine side chains (A301 and A404), one histidine side chain (A369) and a phenylalanine side chain (A141).

The iron-sulfur subunit of *W. succinogenes* can be superimposed well with the *E. coli* FrdB indicating that this subunit is structurally very similar in both enzymes (95). The *E. coli* structure (76) demonstrated that the iron-sulfur protein, FrdB is a two domain structure. The N-terminal domain, formed by B1-B91, is characteristic of plant-ferredoxin domains and binds the [2Fe-2S] centre. The C-terminal domain consisting of B145-B221 is characteristic of bacterial ferredoxins and binds the [3Fe-4S] and [4Fe-4S] centres. The [2Fe-2S] centre is coordinated by cysteines B57, B62, B65 and B77, the [4Fe-4S] by Cys B148, B151, B154 and B214 and the [3Fe-4S] centre by Cys B158, B204 and B210.

The two membrane anchors FrdC and FrdD each contain three TMS designated I-VI. The two menaquinone sites are on opposite sides of the membrane-spanning region. The proximal quinone Q_p is close to the [3Fe-4S] centre of FrdB and is located in the relatively polar pocket formed by helices I, II, IV and V. The distal quinone Q_D is 27 Å away from Q_p and binds the relatively hydrophobic pocket near the ends of the same helices.

The six cofactors in the enzyme are arranged linearly, forming the path of electron transfer (from the menaquinol oxidation site to the flavin), Q_D - Q_p -[3Fe-4S]-[4Fe-4S]-[2Fe-2S]-FAD. A common separation distance of 11-14 Å observed

in multicentred electron transfer proteins is observed in this enzyme except between the two quinone binding sites.

Fumarate to succinate conversion also requires hydride transfer from N5 of flavin to fumarate and protonation of fumarate by an active site acid as of yet unidentified. This residue had previously been proposed to be (*Shewanella* numbering) H365 (165), H504 (7) and R402 (99, 189), all of which are conserved in known fumarate reductases. A crystal structure of *Shewanella* fumarate reductase, a soluble, periplasmic flavocytochrome c_3 , revealed that this function is served by the arginine side chain of A402, equivalent to the arginine residue in *E. coli* A287 and *W. succinogenes* A301 (45, 116, 137). This means that fumarate is reduced to succinate by direct hydride transfer from N5 of the reduced FADH[•] to one fumarate methenyl C atom and the other fumarate methenyl C atom is protonated by the side chain of an arginine (A287 in *E. coli*). Release of the product, succinate, could then be facilitated by the movement of the capping domain away from the dicarboxylate site (94, 95).

In addition to electron transfer and binding of two protons on fumarate reduction, two protons are liberated on menaquinol oxidation (in *W. succinogenes*). Glu C66, an essential residue for menaquinol oxidation by *W. succinogenes* fumarate reductase (93) probably accepts a proton formed by menaquinol oxidation. This residue is located within a cavity that extends to the periplasmic aqueous phase. This suggests that the protons liberated during menaquinol oxidation are released on the periplasmic side of the membrane. This in turn implies that, because of the location of the catalytic and menaquinol

oxidations sites, that quinol oxidation by fumarate is an electrogenic process in *W. succinogenes* (147). On the other hand in *E. coli*, due to the large distance between quinone sites (76) it is unlikely transmembrane electron transfer occurs so it is most likely that quinol oxidation occurs at the Q_p site (147) and there is no proton translocation.

1.8.2. Nitrate Reductase

There are three nitrate reductases in *E. coli*, NRA, NRZ and NAP. NRA is the predominant enzyme that is expressed when the cell experiences high concentrations of nitrate (183). At very low levels of nitrate the periplasmic NAP is produced (132). NRZ is expressed during the early stationary phase of growth irrespective of the presence of nitrate (36).

NRA and NRZ are 73% homologous, are both 3 subunit membrane-bound enzymes that face the cytoplasm, require a molybdenum cofactor and contain heme iron (19). The electron donor for nitrate reduction is ubiquinol or menaquinol and the reduction is associated with the generation of a transmembrane pH gradient by the scalar mechanism, which can be used to drive ATP synthesis (38, 80, 81, 110, 113).

Nitrate reductase A (NRA) is encoded by *narGHJI* at 27 minutes on the *E. coli* chromosome (18, 25, 178, 185). It is positively regulated under anaerobic conditions by FNR and requires nitrate for expression (19). Under anaerobic conditions it is the most energetically favourable respiratory enzyme so it has an

additional regulatory system NarL which, when phosphorylated activates its expression (131).

NarG (α_A) is a soluble 145kD protein that is homologous to a number of other *E. coli* molybdoproteins (18). It contains Mo-bisMGD at the active site (18, 139).

NarH (β_A) is the 58 kD electron transfer subunit that contains 15 cysteine residues in four groups that coordinate 4 iron-sulfur centres (6, 18, 19, 59). It also participates in the attachment of the catalytic dimer (NarGH) to the membrane (18). The iron-sulfur centres are as follows: centre 1 [4Fe-4S] is the highest potential centre of 80mV, centre 2 [3Fe-4S] (60mV), centre 3 [4Fe-4S] (-200mV), and the lowest potential centre 4 [4Fe-4S] (-400mV) (30). Centres 1 and 2 both are competent for intramolecular electron transfer between the γ subunit (NarI) and the catalytic site in the α subunit (58, 59). Centre 2 is believed to be located at the NarGH-NarI interface (139) so it is probably the first cluster accepting electrons from NarI. Centre 1 is close to the Mo-bisMGD of NarG (139) so it probably passes electrons to the cofactor. The role of lower potential centres 3 and 4 is unknown with respect to electron transfer but it is believed that they serve a structural role in stabilizing the $\alpha\beta$ complex (6).

NarI (γ_A) is a 24 kD protein (19) containing diheme cytochrome b_{556} (19, 205) that transfers electrons to the $\alpha\beta$ complex (18) and anchors the complex by virtue of its five TMS (139). Heme b_L is located on the periplasmic side of NarI and heme b_H is on the cytoplasmic side, at the interface of NarGH-NarI (139). They are

coordinated between TMS 2 and 5 of NarI. The dissociable quinone site for menaquinol binding and oxidation is in this subunit near heme b_L (139). An additional quinone-binding site has been proposed to be in the NarGH dimer (139).

The final gene in the operon, *narJ* is 25.5 kD and is not part of the holoenzyme. It has been recently shown to be a private chaperone for NRA (138).

The NRA homologue, NRZ is negatively controlled by FNR under anaerobic conditions (67). These low levels could allow some nitrate reduction during sudden shifts from aerobic to anaerobic environments (53) thereby providing energy to synthesize NRA. It is expressed from the *narZYWV* operon where *narZ* is the *narG* homologue, *narY* the *narH* homologue, *narV* the *narI* homologue and *narW* the *narJ* homologue. NRZ subunits, based on their high sequence homology, are proposed to serve the same functions as their NRA counterparts. One difference is that the midpoint potentials of the iron-sulfur clusters in NarY are negatively shifted by about 100mV compared to their NarH homologue (58).

NAP, the nitrate reductase in the periplasm, is encoded by *napFDAGHBC* at 47 minutes on the *E. coli* chromosome (131). It is a two subunit complex in the periplasm that is coupled to quinol oxidation by its membrane anchored tetraheme cytochrome (138). This nitrate reductase is very different than the two NAR enzymes and the physiological role of NAP is scavenging very low levels of nitrate (130). NapA encodes the molybdoprotein, and NapB (diheme) and NapC (tetraheme) are two *c* type cytochromes. NapD may be a private chaperone

involved in NapA maturation (138). NapF, NapG and NapH are predicted to be nonheme iron-sulfur proteins (130). NapG is predicted to be soluble and periplasmic and NapH is found in the cell membrane with its iron-sulfur centres facing the cytoplasm (130).

1.8.3. Nitrite Reductase

There are two nitrite reductases in *E. coli*, NirBD and NrfAB. NirBD is the major anaerobic nitrite reductase in most enterics and contains FAD, siroheme and two iron-sulfur clusters (53). This enzyme is at 72 minutes on the chromosome (121) and is induced anaerobically by nitrite or nitrate but serves no respiratory function (128). It uses NADH in the cytoplasm to reduce nitrite (130), with no energy conservation. It is responsible for regenerating NAD⁺ and detoxifying the nitrite generated from nitrate respiration (39, 120, 146).

NrfAB (“nitrite reduction by formate”) is part of the *nrfABCDEFG* operon at 92 minutes on the *E. coli* chromosome (177), and is the respiratory nitrite reductase. It is a periplasmic, tetraheme cytochrome *c*₅₅₂ (40, 43) that is expressed anaerobically when nitrite is present and is repressed by NarL when nitrate is present (130). Reduction results in the generation of PMF (115, 129) although the mechanism is unknown.

NrfA is the 50 kD soluble periplasmic nitrite reductase, NrfB is a 18 kD cytochrome *c* proposed to be the electron donor for NrfA (177). NrfC is a 24 kD membrane bound iron-sulfur protein and NrfD is a 37 kD hydrophobic protein

proposed to react with the quinone pool (177). NrfEFG function in cytochrome *c* biogenesis and in the maturation of NrfA (177).

1.8.4. TMAO Reductase

TMAO is widely distributed in nature as a normal component of excreta and of muscles (171). It is also in marine animals including invertebrates and in fish where it acts as an osmostabilizer (8). Post mortem, TMAO is reduced by bacteria to TMA, which gives rise to the characteristic off-flavour and smell of marine fish in the early stages of decay (187).

TMAO reductase is encoded by *torCAD* at 28 minutes on the chromosome (154, 205), is induced by TMAO (205) and generates proton motive force (188). TMAO reduction requires TorA, a 97 kD soluble, periplasmic molybdoenzyme and TorC, a 43 kD membrane-anchored pentaheme *c*-type cytochrome involved in electron transfer to TorA (5, 126). TorD is a 22 kD cytoplasmic TorA-specific chaperone (126). Substrate specificity of the enzyme includes TMAO, adenosine N-oxide and other N-oxides but not S-oxides (154).

TMAO regulation is believed to be mediated by three proteins, a two component system comprised of a sensor kinase TorS (82) and a response regulator TorR (176), and TorT (83), a periplasmic inducer-binding protein that interacts with the periplasmic region of TorS to stimulate *tor* induction (82). TorS is a transmembrane sensor that detects TMAO in the medium. Once activated it transphosphorylates TorR, which triggers the transcription of the *tor* operon by

binding four decameric boxes located in the promoter (5). An additional level of regulation is mediated by *torC*, which negatively controls its own synthesis by TorS/TorR.

1.8.5. Biotin Sulfoxide Reductase

There are two biotin sulfoxide reductases in *E. coli* encoded by *bisC* and *bisZ* (32, 33). They reduce biotin sulfoxide to biotin in a manner dependent on a thioredoxin-like protein moiety, protein (SH)₂ which functions as a source of reducing equivalents, and an unidentified flavoprotein (33). BisC and BisZ are soluble, monomeric molybdoenzymes homologous to *dmsA* that are not involved in respiration. Their function has been proposed to be scavengers of biotin sulfoxide, allowing cells to use this as a source of biotin and protectors from oxidative damage by restoring activity to enzymes that have been inactivated by spontaneous oxidation of the biotin cofactor.

1.8.6. Methionine Sulfoxide Reductase

Methionine sulfoxide reductase (MrsA) (114) reduces methionine sulfoxide to methionine, in a thioredoxin-dependent manner (27). Other enzymes can also perform this function including DMSO reductase. It is a small cytosolic enzyme not involved in respiration, and is highly conserved in bacteria, plants and mammals, as its sequence is 60% identical between *E. coli* and mammalian cells (26, 66). The proposed function of this enzyme is to protect cellular enzymes from oxidative damage when their methionine groups have been oxidized to

methionine sulfoxide resulting in loss of function and activity (much like biotin sulfoxide reductase) (27).

1.8.7. DMSO Reductase

1.8.7.1. Introduction

Dimethyl sulfide (DMS) is a volatile natural sulfur compound that transfers sulfur from oceans through the air to the land (102). It is ubiquitous in the biosphere (102) and is estimated to account for almost half of the global biogenic input of sulfur to the environment (87, 218). DMS is emitted from the oceans and is involved in the control of the global climate (85, 87, 102). The level of DMS in the oceans is controlled by microbial consumption (87).

Dimethyl sulfoxide (DMSO) is a hygroscopic compound that is part of the global sulfur cycle and is produced naturally from photooxidation of DMS in the atmosphere or from phytoplankton degradation in marine environments (4). DMSO is a waste product of paper mills, used as a solvent, is found in pesticides (221), and in the past was used as a vehicle for drug administration (96). When in pesticides in sulfoxide form DMSO is highly toxic to mammals so microbial reduction may detoxify them (2). Enterics, *Pseudomonas aeruginosa*, and *Bacillus subtilis* are the greatest microbial DMSO reducers (221). This reduction also occurs in the cat, cow and other animals and plants (221).

1.8.7.2. *Rhodobacter* DMSO Reductase

The DMSO reductases of *Rhodobacter sphaeroides* and *R. capsulatus* are 86 kD soluble, monomeric enzymes that are periplasmically localized and function during anaerobic photosynthetic growth (1). They are oxotransferases with 77% sequence identity that catalyze the transfer of an oxo group between the substrate (DMSO or TMAO) and water in a two-electron redox reaction. Because they are soluble enzymes, electrons from the quinol are transferred via a membrane-bound *b*-type cytochrome that interacts with the periplasmically localized cytochrome c_{556} that transfers the reducing equivalents to the DMSO reductase (164), thereby generating membrane potential. During this redox reaction the molybdenum atom at the active site of the enzyme cycles between Mo^{IV} and Mo^{VI} via a Mo^{V} intermediate since electrons are transferred singly.

Crystal structures of the two enzymes have been published (106, 163, 164) and provide insight into their structure (Figure 1.4) and the mechanism (Figure 1.5) of DMSO reduction. These studies revealed that DMSO reductase contains two molybdopterin guanine dinucleotide molecules, termed the P and Q pterins (163) (Figure 1.4) that asymmetrically coordinate the molybdenum atom through their dithiolene groups. The enzyme itself is divided into four domains, I – IV, that are formed by noncontiguous regions of the protein grouped around the cofactor.

The residues that ligate the cofactor are dispersed throughout domains II, III and IV. Domain I (the N-terminal region) is the only domain with no direct

interaction with the molybdenum cofactor. The molybdenum atom is located at the base of a 35 Å funnel, on one side of the enzyme. A section of domain II forms part of the funnel wall and domain III is on the opposite side of the cofactor as domain II. Both domains interact with the guanosine moiety, domain II mainly with the P pterin and domain III with the Q pterin. Domain IV consists of the C-terminus of the protein and is located between domains II and III on the opposite side of the enzyme as the funnel. Part of this domain binds the two pterins of the cofactor.

The molybdenum is coordinated differently in the oxidized and reduced states. The side chain of Ser147 is involved in coordination in both states. In the oxidized form (Mo^{VI}), the molybdenum is coordinated by the four dithiolene sulfur atoms of the two molybdopterin, one oxo group and the side chain of O γ of Ser147 (163).

The substrate binds the reduced (Mo^{IV}) form of the enzyme. Although there are no major conformational changes in the protein structure upon substrate binding, there are significant changes at the active site. The oxo ligand is lost and the coordination of the molybdenum by the pterin S atoms changes so that only three sulfur ligands remain, two from the P pterin and one in the Q pterin (163). The ligand from Ser147 is shifted and the Q pterin undergoes a conformational change. The ribose and guanine are coordinated by Asn221 and Asp243 in the Q pterin and by Asp459 and Asp511 in the P pterin respectively.

The mechanism of DMSO reduction consists of two half reactions, an oxidative and reductive half cycle (Figure 1.5). During the oxidative stage the reduced enzyme binds the substrate at Mo^{IV} either through its O atom or through both O and S atoms, which results in a weakening of the sulfur oxygen double bond in the substrate (163). The Q pterin then shifts towards the molybdenum, liberating the DMS by electronic and steric forces. During this time the molybdenum is oxidized to its +VI state where it forms a double bond to the oxo ligand. This completes the oxidative cycle, with molybdenum coordinated to an oxo ligand, O_y of Ser147 and asymmetrically to four dithiolene sulfur atoms.

The reductive stage involves two cycles of electron donor binding to Mo^{VI}, each cycle transferring one electron to the active site. Two protons are also transferred to the metal centre yielding water and restoring the Mo^{IV} state of the enzyme. *b*- and *c*-type cytochromes have been proposed as the external electron donor. An important residue involved at this stage is Trp388, which acts as a lid on the active site that when both electrons are transferred to the molybdenum cycling it back to Mo^{IV}, undergoes a conformational change that could allow substrate entry to the active site.

In this mechanism O atom transfer occurs from the substrate to water. The oxo group bound to molybdenum is the O atom that is transferred to water. Tyr114 is proposed to participate in the proton transfer to produce water.

The two crystal structures of *Rhodobacter capsulatus* (106, 164) differ from the *R. sphaeroides* structure results described above as these authors proposed that the

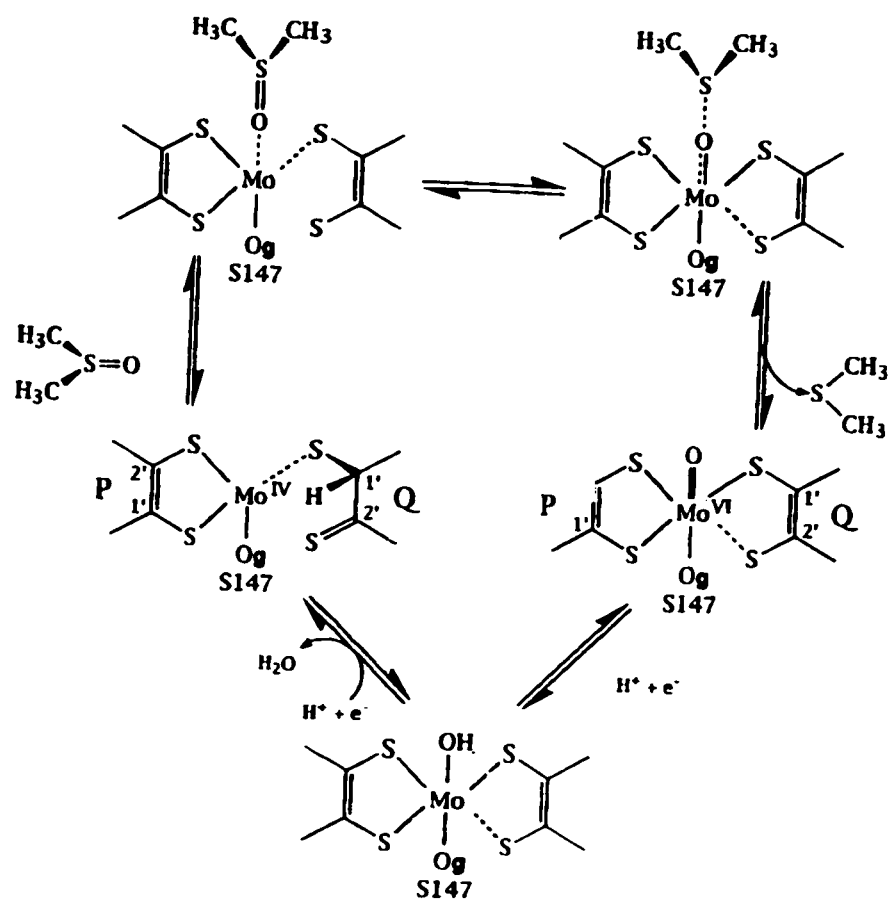
molybdenum coordination in oxidized form includes not one but two oxo groups. The study by Schneider and coworkers (164) reported that only the P pterin binds the molybdenum atom and that only part of the Q pterin is involved in the electron transfer from the electron donor to the redox centre. This conclusion was based on structural findings that the molybdopterin of the P pterin and guanine nucleotides of both the Q and P pterins are buried in the protein. This results in a very different proposed mechanism for DMSO reduction.

These structures are more universal in their application as sequence comparisons between the *Rhodobacter* DMSO reductase and a variety of bacterial oxotransferases containing molybdopterin guanine dinucleotide suggests a similar polypeptide fold and an active site containing two molybdopterin guanine dinucleotides (163).

Figure 1.4. Crystal structure of DMSO reductase from *Rhodobacter sphaeroides*, looking down the active site funnel (used with permission from Kerensa Heffron).



Figure 1.5. Mechanism of DMSO reduction (163).



1.8.7.3. *Escherichia coli* DMSO Reductase

DMSO reductase of *Escherichia coli* is an iron-sulfur molybdoenzyme that is a terminal reductase in the anaerobic respiratory chain. The *dms* operon is comprised of three genes, *dmsABC*, located at 20 minutes on the *E. coli* chromosome. It is expressed constitutively under anaerobic conditions and is induced 65 fold by the global regulator protein FNR due to increased *dms* mRNA transcription (13, 50). The operon is repressed in the presence of oxygen by *arcAB*, and by nitrate by NarL (53). Coupled to a dehydrogenase DMSO reduction contributes to the proton motive force across the cell membrane (14, 16, 31, 205). There is controversy over this point however, as it has been suggested that proton release during menaquinol oxidation and proton consumption during DMSO reduction both take place at the cytoplasmic side of the membrane (196) so there is no net proton release.

The enzyme is able to reduce a wide variety of S- and N-oxides (174, 204) including DMSO, TMAO and several pyridine N-oxides. When *E. coli* is grown anaerobically, DMSO reductase accounts for 90% of the TMAO activity observed (153) and it is the only enzyme capable of sustaining anaerobic growth on DMSO, methionine sulfoxide (154) and sulfoxides (174).

When the *dms* operon was initially cloned and sequenced (13, 15) a start site was assigned such that there were 16 amino acids cleaved to give rise to the mature polypeptide. This was based on the comparison of the N-terminal sequence of DmsA from the automated Edman degradation and the translated DNA coding

sequence. Years later a different N-terminus was suggested by Berks (12) who was examining a series of complex redox cofactor-containing periplasmic proteins. He found that most of these proteins contained an unusually long signal sequence with what he coined as a 'double-arginine motif' of (S/T) RRxFLK. Based on this finding he suggested these proteins share a common export path across the cell membrane.

E. coli DMSO reductase was the exception to his list of redox proteins due to its cytoplasmically oriented localization (13, 153, 206). By reassigning the start site of DmsA, Berks found that it too contained a plausible double-arginine signal sequence. It has since been confirmed by the Weiner group (203) that DmsA has a 45 amino acid signal sequence that is responsible for targeting itself along with DmsB to the MTT (Membrane Targeting and Translocation) system.

The topology of DMSO reductase is based on a number of experiments including biochemical, immunological and electron microscopic techniques (153). DmsAB form a 50 Å (145) soluble dimer that take up a side-by-side conformation that is anchored to the inner side of the cell membrane facing the cytoplasm by the integral membrane subunit, DmsC (153, 205).

The catalytic subunit DmsA is a 90.4 kD molybdoprotein that contains a Mo-bisMGD cofactor at its active site (13, 141, 193, 205). DmsA shares six blocks of sequence similarity and organization with catalytic subunits in a number of molybdoenzymes (193, 205) including enzymes that reduce nitrate (18, 19), biotin

sulfoxide (122), and polysulfide (89) and enzymes that oxidize formate (10, 22, 160, 172, 208, 222). The order of the blocks is consistent but the spacing between them varies greatly (193). The site of the molybdenum cofactor binding is contained within these blocks (163). The N-terminal block contains conserved residues, Cys38, Cys42, and Arg77 shown to be important in electron transfer from the quinol pool to dimethyl sulfoxide (193).

DmsA is 54.4% similar and 32% identical to the *Rhodobacter sphaeroides* counterpart (192) so the crystal structure previously described provides information about the *E. coli* enzyme. Based on sequence alignment with *R. sphaeroides*, the molybdenum ligation sphere of the *E. coli* DMSO reductase includes four sulfur atoms from the 2 MPTs, 1 oxo ligand and the side chain of O γ from Ser205. Based on alignment the residues involved in coordinating the MGD ribose and guanine are Asp271 and Asp293 for the Q pterin and Asp501 and Ile566 for the P pterin, respectively.

DmsA also contains a vestigial [4Fe-4S] cluster-binding motif near the C-terminus of the protein but there is no EPR detectable cluster (142). This motif has been shown to be important in the electron transfer from the -120 mV [4Fe-4S] cluster of DmsB to the Mo-bisMGD cofactor Mo^V in DmsA (142).

Reduction of DMSO to DMS requires two electrons provided by Mo^{IV} in DmsA (205). The molybdenum exists as oxidized Mo^{VI}, partially reduced Mo^V and fully reduced Mo^{IV} (202, 205). The intermediate state allows molybdenum to receive electrons from the -120 mV [4Fe-4S] centre in DmsB.

The active site is accessible through a narrow 35 Å channel from the surface of the protein to the molybdenum, located at the bottom of the funnel (163) so bulky substrates are not used (174). Based on the sequence similarity of the DMSO reductase of *E. coli* and those of *Rhodobacter capsulatus* and *R. sphaeroides*, whose DMSO reductases have been characterized (106, 163, 164), it has been proposed that DmsA residues 142-219 may be important for substrate binding (175). Based on its sequence it has also been hypothesized that DmsA-M14, T148 and R149 potentially form a large portion of the bottom layer of the funnel leading to the active site (175).

DmsB is a 23 kD iron-sulfur containing electron transfer subunit. It contains 16 cysteine residues arranged in four groups (I-IV) (31) that ligate 4 [4Fe-4S] centres with midpoint potentials of -50, -120, -240 and -330 mV (144). This subunit is responsible for transferring electrons from DmsC to the active site in DmsA. Only the two highest potential clusters (-50 and -120 mV) are believed to be involved in this transfer (31). The two low potential clusters (-240 and -330 mV) may play a role in the overall structure of the subunit, but their large negative midpoint potentials probably preclude them from any role in electron transfer (142).

The -50 mV centre 1 is functionally and conformationally linked to DmsC-His65 which is believed to be the menaquinol binding site (142, 144). This [4Fe-4S] centre is 21 Å below the cytoplasmic side surface of DmsABC, close to the

membrane surface, which is consistent with its role in electron transfer from the DmsC menaquinol binding site (144).

Following the electron transfer from menaquinol to the -50 mV cluster, electrons are passed to the -120 mV cluster (15 Å away from molybdenum) and finally onto the Mo-bisMGD of DmsA through the vestigial [4Fe-4S] cluster binding motif (142). DmsA-R77 defines the interaction pathway between the -120 mV cluster and Mo^{V} of DmsA (142). It is likely that the pterins provide a conduit for electron transfer to molybdenum (142).

A second function of DmsB is to facilitate the membrane assembly of the catalytic dimer (155). The C-terminal 30 amino acids of DmsB interact with DmsC to anchor the dimer to the membrane (which allows the electron transfer to occur).

DmsC is the 30.8 kD membrane integral subunit. It has 8 TMS with both N- and C-termini exposed to the periplasm and has three large periplasmic and four cytoplasmic loops (206). It is required for anchoring and stability of the DmsAB catalytic subunit, and for menaquinol binding and oxidation (156, 205). When this subunit is expressed alone it is lethal and this has been proposed to be due to it acting as a proton channel (194). Without the soluble dimer blocking the cytoplasmic side of the protein, ATP depletion occurs as the cell tries to maintain the proton motive force (194).

DmsC may have two quinone sites (142) but has a single dissociable site at His65 where menaquinol binding and oxidation occur. His65 is in TMS2 of DmsC and is close to the periplasmic side of the membrane (144). Once it receives the reducing equivalents from the menaquinol or demethylmenaquinol they are transferred to the -50 mV cluster of DmsB.

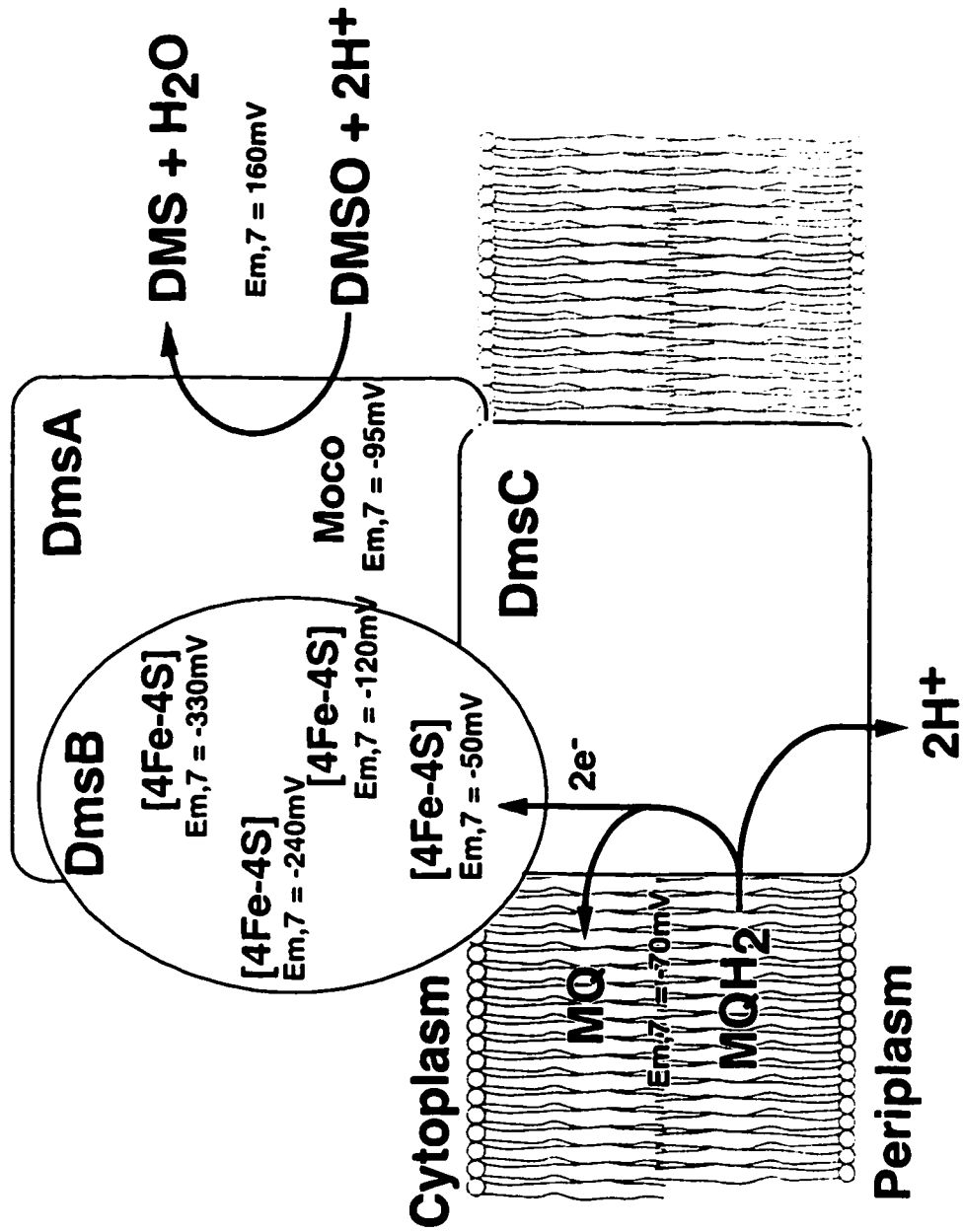


Figure 1.6. Proposed topology of *Escherichia coli* DMSO reductase.

1.9. Translocation

1.9.1. Membrane Targeting and Translocation System (MTT)

The MTT or membrane targeting and translocation system (also known as TAT) is a Sec-independent system that interacts with cofactor-containing redox proteins bearing the (S/T) RRxFLK 'twin-arginine' leader motif (158, 203). These proteins contain cofactors that are incorporated prior to membrane targeting and translocation. This fully folded form means that they are much too large for Sec translocation so they rely on the MTT system, encoded by *mttA₁A₂BC* (or *tatABCDE*), a complex of approximately 600 kD in the cell membrane (23). Over 150 of these proteins have been identified from very diverse sources ranging from bacteria and plants to humans and a few have been discussed earlier in this chapter including TMAO and DMSO reductase.

1.9.2. YnfI

YnfI was recently identified as a result of the *E. coli* genome sequencing project (20). It is located at 36 minutes on the chromosome and encodes a 23 kD protein that is very rich in proline and tryptophan residues (119). It has internal homology between its first and second half, which is characteristic of many peptide-binding proteins (119). A recent study by Turner's group revealed that YnfI is a twin-arginine leader binding protein that escorts MTT proteins from the ribosome to the Sec-independent translocase. YnfI was renamed DmsD (119).

1.10. Thesis Introduction and Objectives

The *ynf* operon was discovered as the result of the *Escherichia coli* genome sequencing project. It is a five gene operon that is very homologous to DMSO reductase so we were very interested in its function as our laboratory has studied DMSO reductase over a number of years.

The first *ynf* gene to be studied was *ynfI*. It was found by Dr. Raymond Turner's laboratory (119) by immobilizing MTT-specific leader sequences on a GST column and running *E. coli* cell extracts down the column to determine if there were any proteins that would bind to them. The reasoning behind this experiment was that there is still much to be learned about the MTT translocation system, including whether there are chaperones that bind the MTT-specific leader sequences to target them to the translocation system. The result of the GST experiment was the discovery of YnfI, the protein encoded by the fifth gene of the then uncharacterized *ynf* operon. They found that the protein only bound the precursor forms of the MTT-dependent proteins (DMSO and TMAO reductases) and that a *ynfI* deletion strain resulted in the inability of cells to grow on DMSO, indicating that the protein is required for targeting the enzyme to the membrane for proper functioning. YnfI homologues are found in a number of Enterobacteriaceae and Archae.

On examination of protein databases, one homologue of the *ynf* operon has been found (i.e. one that contains two catalytic subunits like the *ynf* operon). This

homologue is in *E. coli* 0157:H7, the bacterium responsible for hamburger disease.

Based on these two findings, that YnfI is required for the targeting of (at least some) MTT-dependent enzymes and that a *ynf* homologue is present in the pathogenic bacterium 0157:H7, YnfEFGHI is potentially a very important enzyme.

The objectives of this thesis were:

1. Cloning of the contiguous YnfEFGH operon into an expression vector.
2. Optimization of YnfEFGH protein expression and determination of their cellular localization.
3. Determination of YnfEFGH complementation profile in a DMSO reductase deletion strain (DSS301).
4. Construction of Ynf:Dms chimeric plasmids.
5. Expression of chimeric proteins.
6. Complementation and growth profile determination.
7. Examination of YnfEFGH substrate specificity.

This thesis centres on the elucidation of the function of the Ynf operon. Because the *ynf* promoter(s) are not understood the proteins were expressed from the *tac* and native *dms* promoters. Ynf proteins were examined for glycerol-DMSO complementation in a DmsABC deletion strain and their localization was studied. Substrate specificity was investigated to help determine the natural function of the enzyme. Each individual subunit was also examined for similarities to, and ability to substitute for, their Dms counterparts. This work

constitutes a preliminary characterization of the Ynf operon and will assist in understanding it's the natural function.

Chapter 2: Investigation of Expression, Localization and Function of the YnfEFGH Operon

2.1. Introduction

Dimethyl sulfoxide (DMSO) reductase (DmsABC) is a terminal electron transfer enzyme that allows *Escherichia coli* to grow anaerobically on DMSO and many S- and N-oxides as terminal electron acceptors (13, 15, 150, 154, 173, 204, 213). The enzyme is located on the cytoplasmic surface of the inner membrane (153, 206). It consists of a bis-molybdopterin guanine dinucleotide cofactor-containing catalytic subunit (DmsA, 90.4 kDa), a 4 [4Fe-4S] cluster electron-transfer subunit (DmsB, 23.1 kDa) and a hydrophobic, membrane-spanning anchor subunit (DmsC, 30.8 kDa). DmsABC is a member of an emerging family of closely related electron transfer enzymes found in a large number of prokaryotes which reduce DMSO, TMAO (8, 154), nitrate (8, 18, 19, 154), and polysulfide (89) or which oxidize formate (10, 22, 160, 172, 208, 222).

When the *E. coli* genome sequence was published (20) an operon consisting of five open reading frames, *ynfEFGHI*, and bearing very strong similarity to *dmsABC* was identified. There was no gene in the *dmsABC* operon similar to the fifth gene, *ynfI*. *ynfI* (*dmsD*) has recently been shown to code for a twin-arginine leader binding protein for Sec-independent targeting of DmsA by the Mtt/Tat system (119).

The presence of this operon on the chromosome was surprising to us, as we have previously characterized a deletion of *dmsABC* (DSS301) (156), which is unable to grow on DMSO and related substrates. This mutant did not express any DMSO reductase activity or any proteins that cross-reacted with anti-DmsAB antibodies. However, *E. coli* does encode two related nitrate reductases that probably arose by gene duplication. *narGHJI* encodes the major nitrate reducing enzyme but the *narZYWV* (19) operon can express a low level of nitrate reductase and is regulated differently than *narGHJI* (18, 24). It was possible that *dmsABC* and *ynfEFGH* encoded a similar pair of enzymes.

We decided to examine the expression and function of the *ynfEFGH* holoenzyme and constituent subunits using a cassette cloning strategy. In this study we demonstrate that YnfEFGH can be expressed using the *tac* or *dms* promoters and the membrane-bound enzyme has N-oxide reductase activity. *ynfH* can replace *dmsC* and *ynfG* can replace *dmsB* resulting in fully functional enzymes with *dmsA*. *ynfE* and *ynfF* are poorly expressed, tend to form inclusion bodies and poorly complemented *dmsA*.

2.2. Material and Methods

2.2.1 Materials

Oligonucleotides were purchased from the DNA core facility, Department of Biochemistry, University of Alberta, Edmonton, Canada. All molecular biology reagents were purchased from GibcoBRL except cloned Pfu DNA polymerase, which was purchased from Stratagene/Perkin-Elmer Corp. (Alameda, California). ECL Western blotting detection reagents were purchased from Amersham Life Sciences. Benzyl viologen (BV), dithiothreitol (DTT), isonicotinic acid N-oxide (ISNO), hydroxypyridine N-oxide (HPNO), 2-chloropyridine N-oxide hydrochloride (CPNO), pyridine N-oxide (PNO), 3-[N-morpholino] propanesulfonic acid (MOPS), trimethylamine N-oxide (TMAO), fumarate, phenylmethyl sulfonyl fluoride (PMSF), kanamycin sulfate, ampicillin and potassium tetrathionate were obtained from Sigma Chemical Co. (St. Louis, Missouri). Dimethyl sulfoxide (DMSO) was obtained from Fisher Scientific Ltd. (Edmonton, Alberta). All other reagents were of analytical grade.

2.2.2 Cloning Strategy

Using the polymerase chain reaction we individually amplified each of the *ynf* and *dms* genes or segments of the *ynf* operon and cloned them in the *tac* promoter expression vector pMS119HE (186) or behind the *dms* promoter substituted for the *tac* promoter in the same vector background. Individually cloned genes were constructed with convenient restriction sites at the 5' and 3' ends to simplify sequential construction and gene substitution between the *ynf* and *dms* genes. The entire *ynf* and *dms* operons were first constructed, then by

making use of the restriction sites the homologous genes were substituted (i.e. *dmsABC* → *dmsABynfH*). A list of plasmid derivatives can be found in Table 2.1 and the appropriate PCR oligonucleotides used for their construction are listed in Table 2.2. Each gene (or combination thereof) was amplified by PCR from HB101 chromosomal DNA. Each sense primer incorporated a Shine-Dalgarno sequence (GGAG) and spacer (17). Following PCR amplification, products were purified with cetyl trimethyl ammonium bromide (219), digested, run on an agarose gel and gel purified (using the glass milk procedure) (35), ligated into digested and dephosphorylated pMS119HE or pSPL-119HE vector and transformed into *E. coli* TG1.

Table 2.1. Bacterial strains and plasmids used in this study

Strain/Plasmid	Genotype/Description	Reference
TG1	K12 $\Delta(lac-pro)supEF'traD36$ $proABlac^{\dagger}\Delta lacZM15$	Amersham Corp.
DSS301	K12 $\Delta(lac-pro)supEF'traD36$ $proABlac^{\dagger}\Delta lacZM15 \Delta dmsABC, Kan^r$	(155)
BNN103	(<i>lacIPOZYA</i>) U169 $proA^+ \Delta lon$ $araD 139 strA thi hflA 150 [chr::Tn10]$	(217)
pBR322	$Amp^r lacZ'$	Pharmacia
pDMS160	pBR322 $Amp^r (dmsABC)^r$	(143)
pMS119HE	<i>tac, lacIq, Amp^r</i>	(186)
pSPL-119HE	pMS119HE without <i>Sall</i> and <i>SphI</i> sites	this study
pSPL-119HE/dmsP	pSPL119HE with the <i>dmsP</i>	this study
pTDMS28/Kan	<i>ynfI</i> under <i>tac</i> control	(119)
pSPL-(FG)	pSPL-119HE/ <i>ynfFG</i> contiguous	this study
pSPL-(H)	pSPL-119HE/ <i>ynfH</i> contiguous	this study
pSPL-(FGH)	pSPL-119HE/ <i>ynfFGH</i> contiguous	this study
pSPL-(EFGH)	pSPL-119HE/ <i>ynfEFGH</i> contiguous	this study
pSPL-d(FGH)	pSPL-119HE/ <i>dmsP/ynfFGH</i> contiguous	this study
pSPL-d(EFGH)	pSPL-119HE/ <i>dmsP/ynfEFGH</i> contiguous	this study
pSPL-dFGH	pSPL-119HE/ <i>dmsP ynfFGH</i> individual	this study
pSPL-dEFGH	pSPL-119HE/ <i>dmsP ynfEFGH</i> individual	this study
pSPL-dABC	pSPL-119HE/ <i>dmsP dmsABC</i> individual	this study
pSPL-dABH	pSPL-119HE/ <i>dmsP dmsABynfH</i> chimera	this study
pSPL-dEBC	pSPL-119HE/ <i>dmsP ynfEdmsBC</i> chimera	this study
pSPL-dFBC	pSPL-119HE/ <i>dmsP ynfFdmsBC</i> chimera	this study
pSPL-dFGC	pSPL-119HE/ <i>dmsP ynfFGdmsC</i> chimera	this study
pSPL-dEFGC	pSPL-119HE/ <i>dmsP ynfEFGdmsC</i> chimera	this study
pSPL-dAGH	pSPL-119HE/ <i>dmsP dmsAynfGH</i> chimera	this study
pSPL-dEGH	pSPL-119HE/ <i>dmsP ynfEGH</i> chimera	this study

The *ynf* genes were cloned by PCR as described in Methods into either pSPL-119HE or pSPL-119HE/*dmsP*, where *dmsP* represents the *dms* promoter. Plasmids that carry the *ynf* genes as contiguous PCR products are denoted with brackets e.g. (FGH), all others contain individually cloned genes. Plasmids with the *ynf* and/or *dms* genes under *dms* promoter control are preceded by a (d).

Table 2.2. PCR primers used to amplify *ynf* and *dms* genes

Gene	Product Length (bp)	Sense Primer	Antisense Primer
<i>ynfE</i>	2462	5'-gct <u>cta gaa</u> agg aga aat att ATG TCC AAA AAT GAA-3'	5'-gcg <u>aat tcg cat gcT</u> TAT ATT TTT TCG ATC TCG ACC-3'
<i>ynfE2</i>	2462	5'-gct <u>cta gaa</u> agg aga aat att ATG TCC AAA AAT GAA-3'	5'-gcg <u>aat tcg tcg acT</u> TAT ATT TTT TCG ATC TCG ACC-3'
<i>ynfF</i>	2465	5'-gct <u>cta gag cat gca</u> agg aga aat aat ATG AAA ATC CAT CA-3'	5'-gcg <u>aat tcg tcg acT</u> TAA ACC TTT TCG AT-3'
<i>ynfG</i>	659	5'-gct <u>cta gag tcg aca</u> agg aga aat aat ATG ACC ACA CAA TAT GGA-3'	5'-gcg <u>aat tcg cta gcT</u> TAC ACT TCC TCC GG-3'
<i>ynfH</i>	890	5'-gct <u>cta gag cta gca</u> agg aga aat aat ATG GGA AAT GGA TG-3'	5'-gcg <u>aat tcT</u> TAA CCT GCA ATA GCC A-3'
<i>dmsA</i>	2486	5'-gct <u>cta gag cat gca</u> agg aga aat aat ATG AAA ACG AAA ATC CCT-3'	5'-gcg <u>aat tcg tcg acT</u> TAC ACC TTT TCA ACC TGA-3'
<i>dmsB</i>	659	5'-gct <u>cta gag tcg aca</u> agg aga aat aat ATG ACA ACC CAG TAT GGA-3'	5'-gcg <u>aat tcg cta gcT</u> CAC ACC TCC TTC GGG TTT-3'
<i>dmsC</i>	899	5'-gct <u>cta gag cta gca</u> agg aga aat aat ATG GGA AGT GGA TGG CAT-3'	5'-gcg <u>aat tcT</u> TAG CTT GCG ACG GCC ATC-3'
<i>dms</i> Promoter	793	5'- <u>cga cgc gta</u> tca tcg ATG AAG ATG ATC TGC-3'	5'-tgc <u>tct aga</u> TGG CTC ACT CAA GCT TGC-3'

Lower case letters represent extra nucleotides introduced into the primer that are not part of the *ynf* or *dms* gene (including restriction sites, which are underlined).

Upper case letters are nucleotides of the *ynf* or *dms* gene. There are two *ynfE* antisense primers, differing only in the restriction site incorporated. This is to allow cloning upstream of *ynfF* (*ynfE*) which has the *SphI* site at its 5' end, or upstream of *ynfG* (*ynfE2*) which has the *Sall* site at its 5' end.

Cloning *ynf* genes downstream of the *dms* promoter was achieved by replacement of the *tac* promoter in pSPL-119HE using *MluI* and *XbaI*. An 81 bp fragment encompassing the *dms* promoter was PCR amplified from HB101 chromosomal DNA with an *MluI* site at the 5' end and an *XbaI* site at the 3' end. The *tac* promoter was digested from the plasmid using *MluI* and *XbaI* and replaced with the *dms* promoter.

The plasmid pSPL-(EFGH) was constructed as follows: pSPL-(FGH) was digested with *XbaI* (5' end of *ynfF*) and *BglII* (a natural internal site near the 5' end of *ynfG*) to remove *ynfFG'*. *ynfEFG* was amplified from HB101 chromosomal DNA, digested with the same enzymes, and the *ynfEFG'* fragment ligated into the digested and dephosphorylated pSPL-(FGH) to create pSPL-(EFGH). Figure 2.1 shows composites of the pSPL-dEFGH and pSPL-dABC plasmids with the key restriction sites indicated.

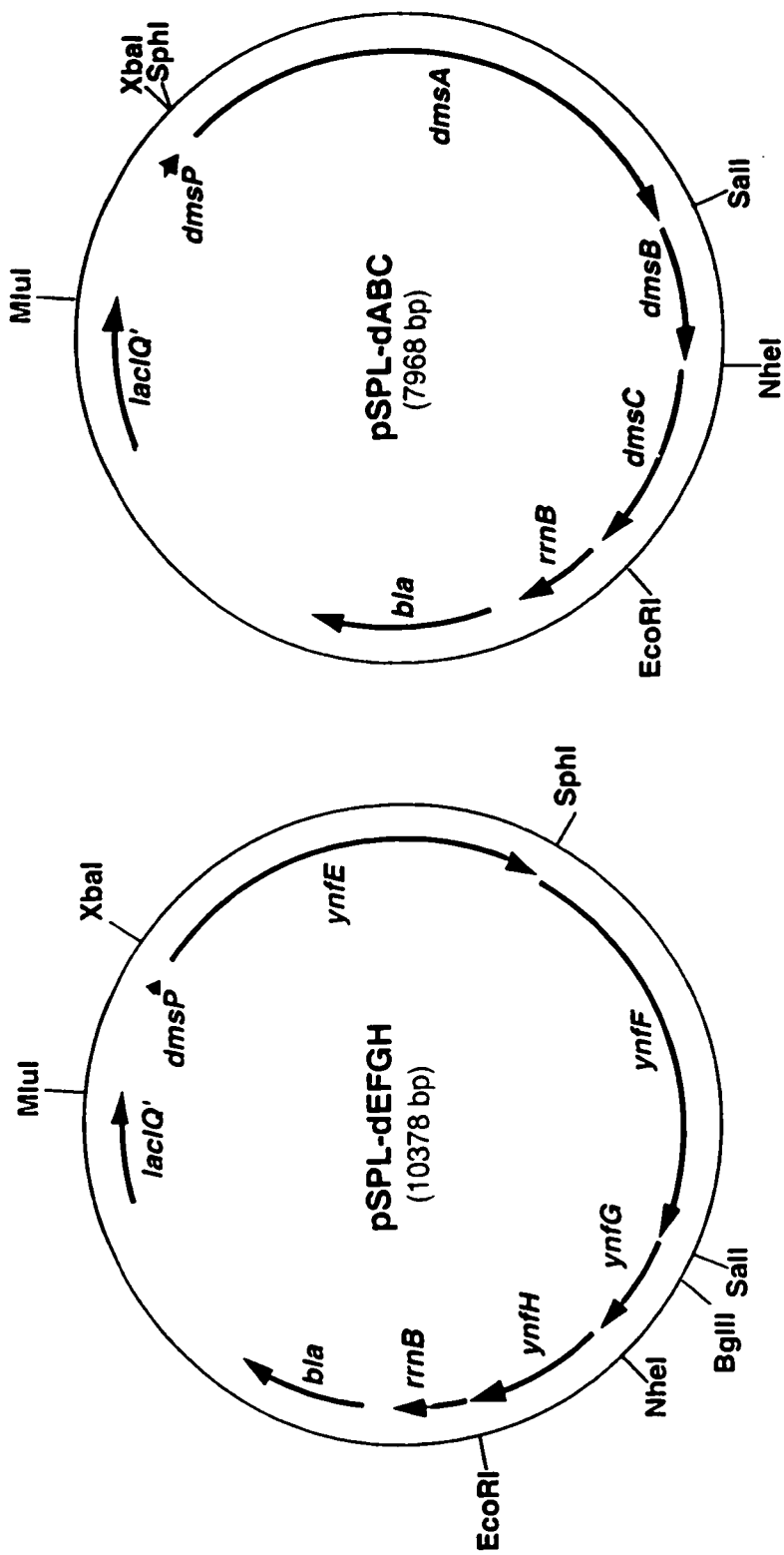


Figure 2.1. Restriction map of cassette plasmids pSPL-dEFGH expressing the *ynf* genes and pSPL-dABC expressing the *dms* genes under *dms* promoter control. *bla* is b-lactamase. See Methods for the construction of the plasmid.

2.2.3. Aerobic Growth

To examine the expression of the *ynf* genes, cells were grown on Terrific Broth (TB) (157), Luria Bertani Broth (LB) (157) or tryptone phosphate media (TP) (112), supplemented with 10 µg/ml thiamine and with antibiotics as required (100 µg/ml ampicillin, 40 µg/ml kanamycin) at either 37°C or 30°C. Inocula were grown overnight in LB supplemented with 10 µg/ml thiamine and antibiotics as required and inoculated at a 1:100 dilution into the appropriate media. Cultures were induced with 0.1 mM IPTG and 1 ml aliquots were withdrawn at 0, 2 and 4 hours. Cells were washed in 50 mM MOPS-0.2 mM IPTG and 0.5 mM DTT and resuspended in the same buffer. Whole cell immunoblots were run with 25 µg of protein of each sample.

2.2.4. Anaerobic Growth

Cells grown aerobically overnight in LB Broth were used to inoculate glycerol-fumarate media (GF) at a 1:100 dilution for 24 or 48 hours at 30°C using flasks filled to the top. For growth experiments DSS301 construct-containing strains were inoculated with 12-hour LB grown cells at a 1:100 dilution and grown anaerobically in Klett flasks at 30°C (154). Growth was monitored with a Klett spectrophotometer.

2.2.5. Preparation of Membranes and Soluble Fractions

Membrane and soluble fractions were prepared as follows. GF grown cells, grown for 48 hours, were harvested and washed in 50 mM MOPS, pH 7.0 - 0.2

mM PMSF - 0.5 mM DTT, and disrupted by French press lysis as previously described (153).

2.2.6. Polyacrylamide Gel Electrophoresis and Immunoblotting of Ynf Proteins

Samples, 25 µg (unless otherwise indicated), were prepared by boiling in Laemmli SDS sample buffer for 5 minutes and analyzed by electrophoresis (200V for approximately 45 minutes or until dye front reached that bottom of glass plates) using a Laemmli buffer system as described (92). Immunoblotting was carried out as previously described (155) with a 1:25 dilution of polyclonal anti-DmsA and anti-DmsB antibodies.

2.2.7. Protein Determination

Protein concentration was determined using a modified Lowry protein assay, using Bovine Serum Albumin as the standard (105).

2.2.8. Benzyl Viologen Enzyme Assays

Reductase activity was monitored spectrophotometrically at 570 nm by the substrate-dependent oxidation of reduced benzyl viologen at room temperature (153, 204). The terminal electron acceptors used were 72 mM TMAO, 21 mM DMSO, 5.4 mM isonicotinic acid N-oxide, 18 mM hydroxypyridine N-oxide, 18 mM 2-chloropyridine N-oxide hydrochloride, 72 mM pyridine N-oxide in 50 mM MOPS, pH 7.0. One unit represents 1 µmol of benzyl viologen oxidized/min.

2.2.9. Lapachol Enzyme Assays

Quinol : TMAO oxidoreductase activity was monitored spectrophotometrically at 481 nm by the TMAO-dependent oxidation of the menaquinol analogue, lapachol as described previously (140).

2.2.10. Fluorescence Analysis of Molybdopterin Cofactor

Membrane samples (10 mg) were centrifuged at 95,000 RPM for 25 minutes using a Beckman TL100 ultracentrifuge with a Ti100.3 rotor. Membranes were resuspended in 300 μ l water with a Teflon homogenizer. 6N HCl (200 μ l) was added and the samples were vigorously shaken using a Vortex mixer, followed by the addition and vortex of 800 μ l 2%/4% I₂/KI. Samples were boiled for 25 minutes and cooled on ice for 2 minutes. Samples were centrifuged in an Eppendorf centrifuge at 13, 000 RPM for 15 minutes and supernatants transferred to new tubes. Fluorescence was measured by adding 200 μ l sample to 3.5 ml 1 M NH₄OH. Excitation spectra were recorded from 240 - 420 nm with an emission wavelength of 442 nm and emission spectra from 410 - 520 nm with an excitation wavelength of 395 nm (78).

2.2.11. 2-*n*-hepty-4-hydroxyquinoline-N-oxide (HOQNO) Fluorescence

Binding

Membrane samples containing 1 mg protein in 3.5 ml of 50 mM MOPS buffer pH 7.0 were assayed for HOQNO binding (118) by adding 2 μ l aliquots of 0.1 mM HOQNO in 95% redistilled ethanol, inverted 3 times, and examined spectrophotometrically at an excitation wavelength of 341 nm and emission

wavelength of 479 nm in a Perkin Elmer LS50B. Plots of fluorescence intensity versus [HOQNO] were analyzed as previously described (144) yielding an estimate of specific enzyme concentration (nM) and the K_d of HOQNO binding.

2.2.12. EPR Spectroscopy

Levels of iron-sulfur clusters in DSS301 strains were determined by measuring membrane samples prepared as previously described (31) using a Bruker Spectrospin ESP300 EPR spectrophotometer and conditions also described earlier (143). EPR spectra were recorded under the following conditions: temperature, 12K; microwave power, 20mW at 9.47GHz; modulation amplitude, 10G_{pp} at 100KHz. Spectra were corrected for EPR tube calibrations and normalized to a nominal protein concentration of 30mg mL⁻¹. g-values are indicated by vertical lines above the spectra.

2.3. Results

2.3.1. A paralogue of the *dmsABC* operon in *E. coli*

The *ynfEFGHI* operon was identified during the course of the *E. coli* genome sequencing project (20). The operon, located at 35 minutes on the chromosome, consists of five open reading frames, the first four of which are surprisingly similar to those of the *E. coli dms* operon. The first two genes, *ynfE* and *ynfF*, are each homologous to *dmsA* and appear to result from a tandem duplication. YnfE is 66.7% identical and a further 15.1% similar to DmsA and YnfF is 66.4% identical and an additional 15.8% similar to DmsA. *ynfE* and *ynfF* are also very similar to *dmsA* at the DNA level, 66% and 65% identical respectively. Both YnfE and YnfF possess a twin-arginine leader, that in the case of DmsA has been shown to be essential for membrane targeting and assembly of the holoenzyme (158, 159, 168, 204), and conserve all the residues known to be essential for DmsA molybdopterin binding (205). YnfG is 94.1% identical and a further 2.9% similar to DmsB (81% identical at the DNA level) and contains four Cys motifs that coordinate the 4 [4Fe-4S] clusters. YnfH is the least conserved member of the operon but it is clearly an integral membrane protein related to DmsC. Like DmsC it encodes eight potential transmembrane α -helices and is 57.4% identical and an additional 14.8% similar to DmsC (61% identical at the DNA level). The arginine and glutamate residues known to be essential for menaquinol binding and reductase activity are conserved (206). The fifth gene of the operon, *ynfI* (*dmsD*), encodes a twin-arginine leader binding protein and plays a role in the targeting of DmsABC and YnfEFGH to the membrane (119).

The *ynfEFGHI* and *dmsABC* operons are very similar in their architecture. The molybdopterin-containing subunit(s) is at the 5' end of the operon, followed by the iron-sulfur cluster-containing subunit, and the membrane anchor. The major differences between the two operons include the presence of two tandem *dmsA* paralogues in the *ynf* operon, and the absence of a *ynfI* paralogue in the *dms* operon.

There are two possible σ_{70} promoters in the *ynf* operon, one upstream of *ynfE* and the other upstream of *ynfF*. Based on a computational prediction (152) the *ynfE* promoter begins 102 bp upstream of the initiating methionine and is 81 bp in length. Just upstream of this promoter is a good FNR box (53). Based on the same prediction, the possible *ynfF* promoter is contained entirely within the 3' end of *ynfE* but does not contain an obvious FNR box. It is 81 bp in length and begins 148 bp upstream of the initiating methionine of *ynfF*. There is a good Shine-Dalgarno site 6 bp upstream of the initiating ATG of *ynfE* (GGAG) and a reasonable site 5 bp upstream of *ynfF* (TGAG).

2.3.2. Detection of the products of the *ynf* Open Reading Frames

E. coli DSS301, deleted for the *dmsABC* operon eliminated DMSO reductase activity, growth on DMSO and immunostaining protein with anti-DmsA and anti-DmsB antibodies (153). DmsC cannot be detected as we have been unsuccessful in making an anti-DmsC antibody (153). We confirmed the absence of anti-DmsA and anti-DmsB immunoreactive protein in DSS301 by Western blotting of cells grown aerobically and anaerobically in TB (157), LB (157) or TP media (112) (data not shown). This suggested that YnfEFG were either not

expressed under these conditions, or were expressed at a level below our detection limit. It was also possible that YnfEFG did not cross-react with the antibodies.

To examine this we cloned various combinations of the *ynf* genes behind the IPTG-inducible *tac* promoter and examined expression in TG1 (wild-type), DSS301 ($\Delta dmsABC$) and a protease-deficient *lon*⁻ mutant, BNN103. We immunoblotted these whole cells following IPTG induction and tested the ability of anti-DmsA to detect YnfE and YnfF and anti-DmsB to detect YnfG. Figure 2.2 shows a typical aerobic expression in TG1 after IPTG induction. A small amount of DmsA resulting from the chromosomal *dms* operon is visible in TG1. Polypeptides cross-reacting with anti-DmsA and anti-DmsB were clearly visible in cells complemented with pSPL-(EFGH) (lane B). When cells were complemented with pSPL-(FGH), expression of YnfF was very poor compared to YnfE (more than twice as much YnfEF when compared to YnfF alone) (cf. lane B pSPL-(EFGH) and lane C pSPL-(FGH)). There was good expression of YnfG from both YnfEFGH and YnfFGH. The apparent anomalous migration of YnfG is an artifact of electrophoresis and is dependent on protein concentration. We attribute this to the large number of cysteine residues in YnfG, which are required for ligating the iron-sulfur centres. With decreased concentrations of protein (and therefore relative increased levels of reducing agent, DTT), the YnfG band ran faster, indicating that the reducing agent at higher protein levels was unable to reduce all inter- and intramolecular disulfide bonds resulting in multimers of YnfG.

We could not observe YnfEFGH or YnfFGH by direct Coomassie blue staining of induced cells indicating that overall expression was much lower than observed with DmsABC which can constitute as much as 30% of the membrane protein (data not shown).

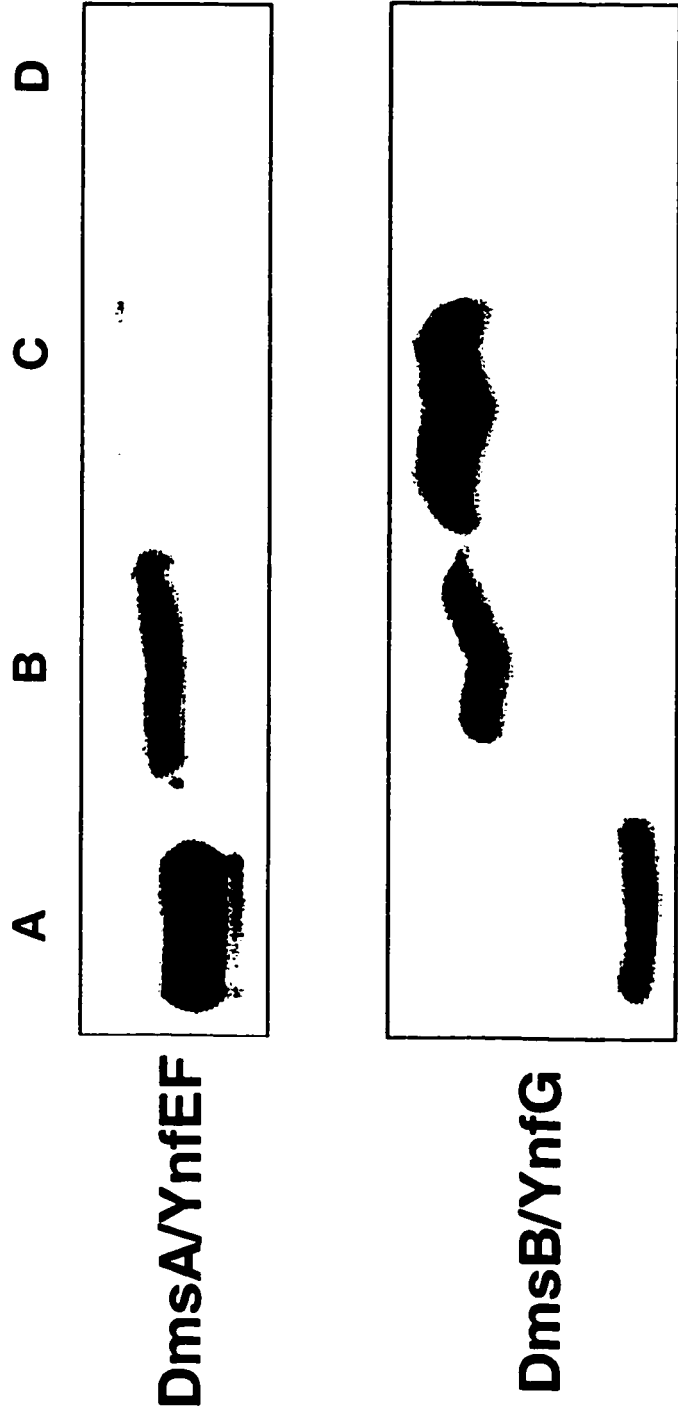


Figure 2.2. Western blot of *E. coli* TG1 whole cells expressing the *ymf* operon. Cells were grown aerobically on LB and induced with 0.1 mM IPTG. After 4 hrs the cells were harvested and directly examined by immunoblotting with anti-DmsAB antibodies. Lane A, purified standard DmsAB dimer; lane B /pSPL-(EFGH); lane C, /pSPL-(FGH); lane D, TG1. 30 mg of whole cell protein were loaded on each lane.

2.3.3. Localization of YnfEFGH

The localization of the Ynf proteins expressed from the *tac* promoter was examined by separating the whole cell lysate into soluble cytoplasmic/periplasmic fraction, membranes and the low speed pellet (inclusion body fraction). Initial experiments indicated that, unlike DmsABC, the majority of YnfEF and YnfG accumulated in inclusion bodies with only a small amount in the membrane and soluble fractions.

We carried out an extensive study to minimize inclusion body formation (see Appendix) including alteration of the *E. coli* host strain, growth media, IPTG concentration, and supplementation of the medium with molybdenum and iron. We examined the effect of co-expression of YnfI (DmsD) in case the chromosomal level of YnfI was limiting. We incubated the cells with chloramphenicol after allowing the cells to express YnfEFGH for 1 hour. Chloramphenicol inhibits protein synthesis and has been shown to allow improved folding of pre-synthesized proteins (34). None of these parameters significantly decreased the accumulation of inclusion bodies.

However, lowering the growth temperature from 37°C to 30°C improved the accumulation of YnfEFGH in the membrane. This suggested that expression from the *tac* promoter might be too rapid, resulting in misfolding and inclusion body formation. To test this we replaced the *tac* promoter with the *dms* promoter and expressed YnfFGH and YnfEFGH under anaerobic conditions at 30°C in BNN103 (*lon*⁻). BNN103 does not express DmsABC even though it has a chromosomal

copy of the *dmsABC* operon (unpublished results), making this a useful strain for expression studies. Figure 2.3 is an immunoblot of whole cells and subcellular fractions isolated from anaerobically-grown (on GF media) BNN103 harboring pSPL-d(FGH). The majority of the YnfFG accumulated in the membrane fraction and not in inclusion bodies (cf. lanes A, B and C). YnfF accumulated at the mature molecular weight whereas some premature YnfF was observed in the inclusion bodies (lane C). In a similar experiment, BNN103/pSPL-d(EFGH) showed the same result except that the YnfEF band was more intense (data not shown).

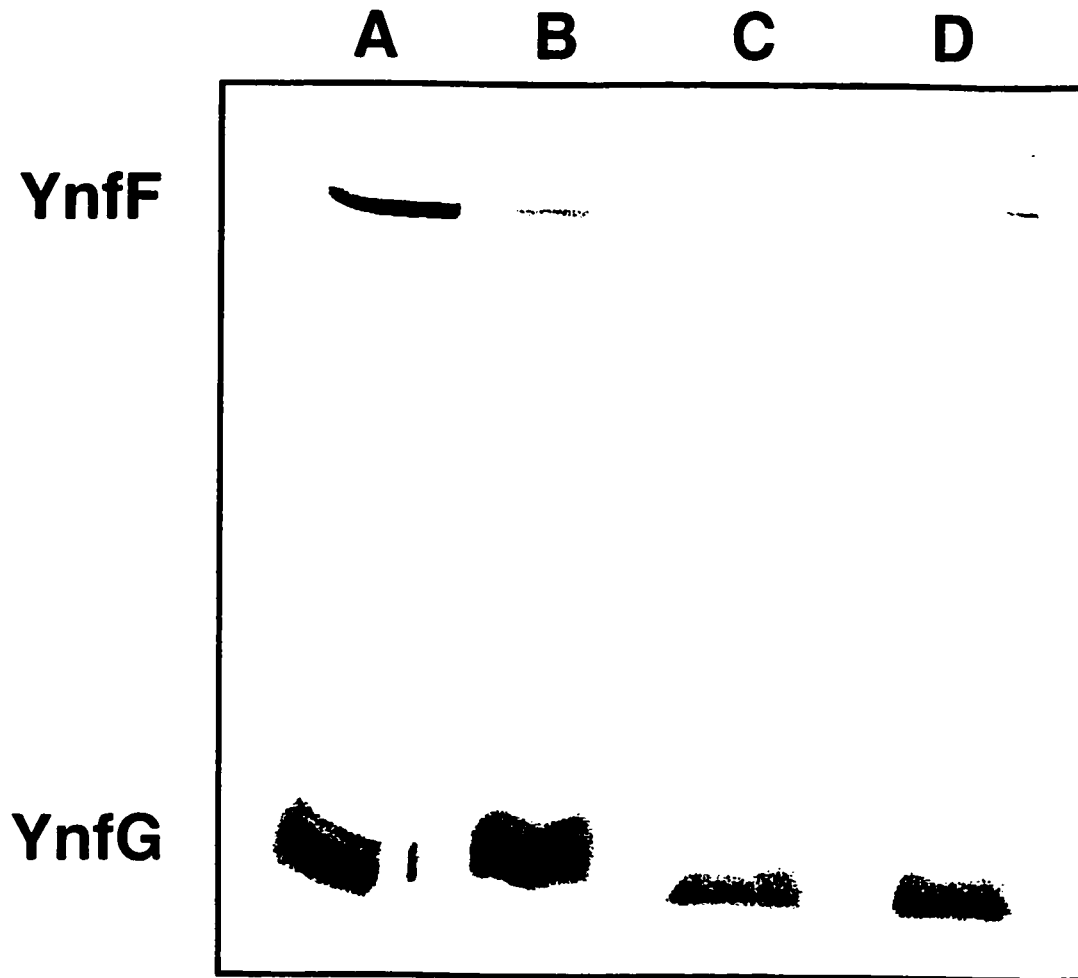


Figure 2.3. Expression of YnfFGH in *E. coli* BNN103 under *dms* promoter control. Cells were grown anaerobically for 24 hr at 30°C in GF medium, harvested and fractionated into subcellular fractions as detailed in Methods. 30 μ g of whole cells and low speed pellet fractions and 60 μ g of membrane and soluble fractions were subjected to electrophoresis and immunoblotting as previously described. Lane A, /pSPL-d(FGH) membranes; lane B, soluble fraction; lane C, low speed pellet; and lane D, whole cells.

2.3.4. Growth Complementation in DSS301

We tested whether overexpression of the Ynf proteins would complement DSS301 ($\Delta dmsABC$) for anaerobic growth on GD. At 30°C DSS301/pSPL-d(FGH) and DSS301/pSPL-d(EFGH) were able to support only very limited GD growth which was about one-third of the maximal cell density observed for pDMS160 expressing DmsABC (Figure 2.4).

In order to interchange subunits and examine the functional ability of the *ynf* ORFs by complementation in DSS301 we constructed a number of chimeric plasmids expressing combinations of the *ynf* and *dms* genes. DSS301 cells transformed with seven different Dms:Ynf chimeric constructs as well as various control plasmids (Table 2.1) were grown on GD at 30°C (Figure 2.5). DSS301/pSPL-dABC complemented growth indicating that the incorporation of restriction sites into the *dms* operon did not dramatically impair its function.

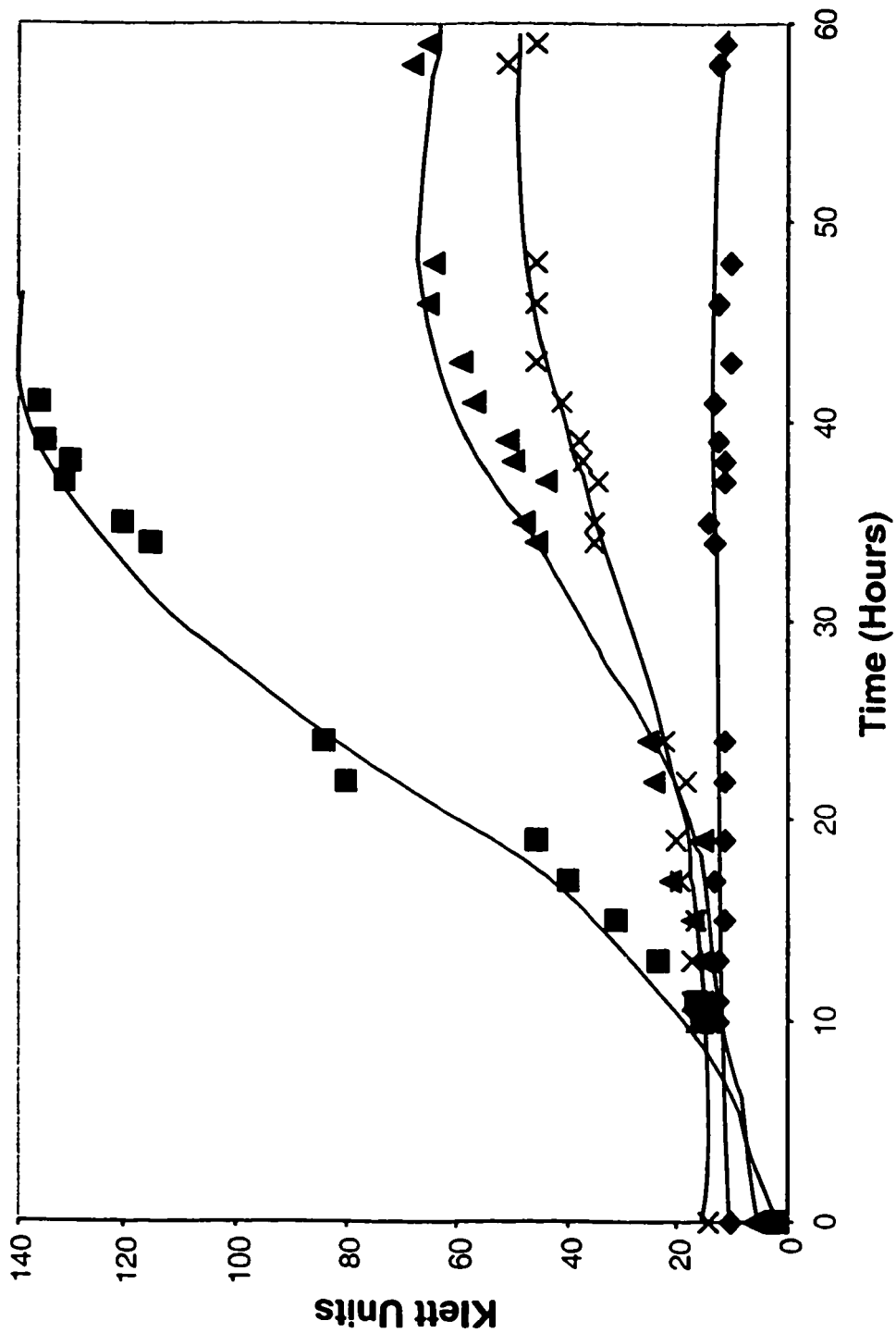


Figure 2.4. Anaerobic growth of *E. coli* DSS301 containing Ynf plasmids at 30°C on glycerol-DMSO medium. DSS301 ◆---◆; /pSPL-d(EFGH) X---X; /pSPL-d(FGH) ▲---▲; /pDMS160 ■---■. These data are representative of three individual experiments.

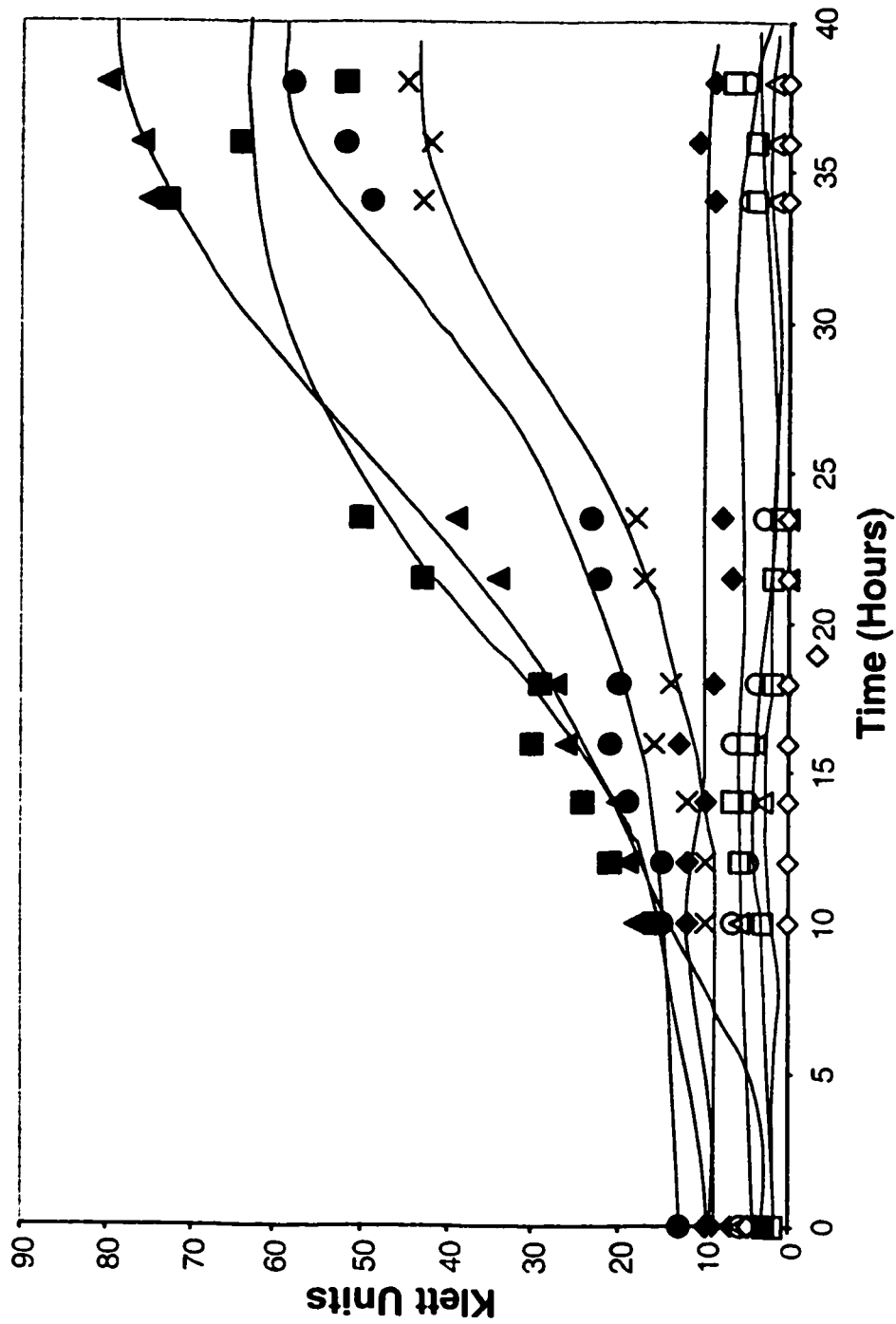


Figure 2.5. Anaerobic growth of *E. coli* DSS301 containing chimeric plasmids at 30°C on glycerol-DMSO medium.
 /pSPL-dABC▲---▲; DSS301/pPL-dAGH■---■; /pSPL-dABH ●---●; /pSPL-dFBC X---X;
 DSS301◇---◇; /pSPL-dEBCO○---○; /pSPL-dEFGC□---□; /pSPL-dFBCΔ---Δ; /pSPL-dEGH ◇---◇
 These data are representative of three separate experiments.

Exchange of the anchor subunit DmsC, in *dmsABC*, by YnfH (pSPL-dABH) resulted in 60% of the cell density of DSS301/pSPL-dABC. Thus, although YnfH is the most divergent subunit in the operon (60% identity with DmsC), it could serve as an anchor for DmsAB. YnfH could also interact with the menaquinol pool and pass reducing equivalents to DmsAB. We then exchanged both YnfG and YnfH for DmsBC (pSPL-dAGH). This plasmid could also support the growth of DSS301 indicating that YnfG is a functional electron transfer subunit and assembled the 4 [4Fe-4S] clusters necessary for electron transfer.

We next attempted to replace the DmsA subunit with YnfE (pSPL-dEBC). This plasmid could not support growth. Similarly, pSPL-dEGH could not support growth suggesting that YnfE did not have DMSO reductase activity or enzyme expression was insufficient to support growth. We replaced DmsA with YnfF and this plasmid (pSPL-dFBC) was also unable to support growth. However, when we examined pSPL-dFGC we found that it could support GD growth of DSS301. Similarly, pSPL-d(FGH) could also support similar levels of growth (Figure 2.4). Thus YnfF has some DMSO reductase catalytic activity and appears to interact better with YnfG than DmsB. When we combined both YnfE and YnfF (pSPL-dEFGC) no growth was observed.

2.3.5. Expression and Localization of the Chimeric Enzymes

The distribution of the chimeric Ynf:Dms enzymes was examined by immunoblotting subcellular fractions. As expected the background strain, DSS301 showed no immunoreactive bands (Figure 2.6A). The control, DSS301/pSPL-dABC showed good expression (Figure 2.6B) with enzyme in both the

membrane and soluble fractions. Both DSS301/ pSPL-dAGH (Figure 2.6C) and DSS301/ pSPL-dABH (Figure 2.6D) looked very much like DSS301/ pSPL-dABC, with more protein in the membrane fraction (by observation, band intensity is greater in the membrane fraction). This agrees with the growth experiments and indicates that YnfG and YnfH can interact with DmsA to form a functional holoenzyme.

Chimeric plasmids encoding YnfF in lanes E and F (DSS301/ pSPL-dFBC and DSS301/ pSPL-dFGC) in combination with the Ynf or Dms subunits generally resulted in poor expression of the large subunit. Figure 6F (DSS301/ pSPL-dFGC) shows that the small amount of YnfF expressed was localized to the membrane. This indicates that YnfFG were able to interact with DmsC for anchoring to the membrane. This was somewhat unexpected as DSS301/ pSPL-dFGC (and DSS301/ pSPL-(FGH)) could support anaerobic growth of DSS301 on glycerol-DMSO, whereas DSS301/ pSPL-dFBC could not, and we know that both DmsBC are functional. This could indicate a poor interaction between YnfF and DmsBC. Plasmids encoding a YnfE subunit (Figure 2.6G, H and I) generally had poor expression showing that these chimeras did not assemble well which accounts for the inability of these constructs to support growth.

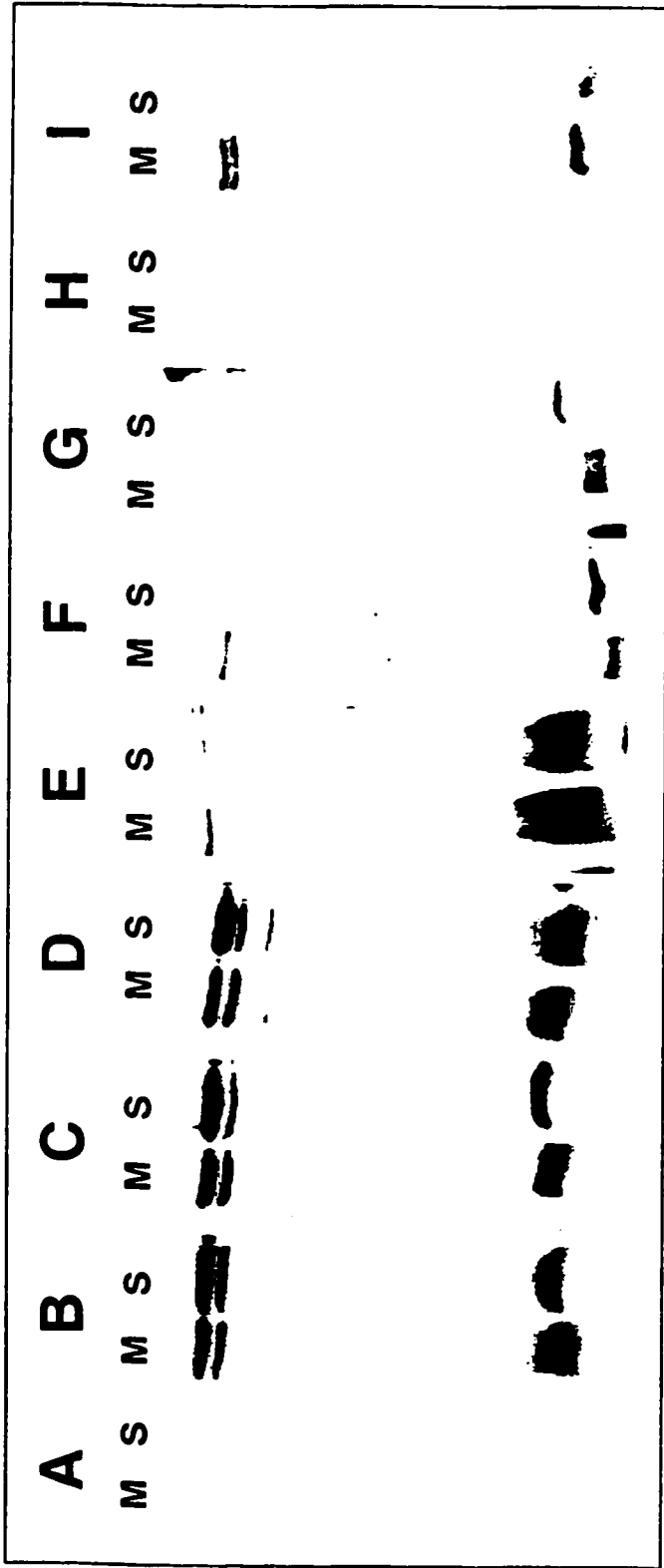


Figure 2.6. Immunoblots of membrane and soluble fractions from *E. coli* DSS301 complemented with chimeric plasmids. A. DSS301; B. /psPL-dABC; C. /psPL-dAGH; D. /psPL-dABH; E. /psPL-dFBC; F. /psPL-dFGC; G. /psPL-dEFGC; H. /psPL-dEBC; and I. /psPL-dEGH.

2.2.6. HOQNO Binding

Binding of the quinol analogue HOQNO to DmsC quenches its endogenous fluorescence and this provides a means of monitoring the interaction of DmsC with quinols and quantitating the amount of enzyme in the membrane (118). This is an additional method of examining the functionality of YnfH. HOQNO binding also provides a rough estimate of concentration of enzyme in the membrane, as it is known that there is one quinol binding site in DmsC (144, 220). Figure 2.7 shows the results of quenching of HOQNO fluorescence with membranes expressing proteins encoded by a series of chimeric plasmids. DSS301 membranes do not quench HOQNO fluorescence while membranes over-expressing DmsABC (DSS301/pDMS160) gave a concentration of DmsC of 0.49 nmoles DmsC/mg protein with a K_d of about 6 nM, in good agreement with previous studies (220). Membranes of DSS301/pSPL-dAGH and DSS301/pSPL-dABH had a specific concentration of 0.42 and 0.37 nmoles anchor subunit/mg, with K_d 's of 4 nM and 9 nM, respectively. Membranes isolated from cells expressing pSPL-dFGC, pSPL-d(FGH) and pSPL-d(EFGH) did not have measurable HOQNO binding due to the relatively low level of expression. For clarity each curve was raised, with the lowest curve (DSS301/pDMS160) raised 0.1 and each curve thereafter raised an additional multiple of 0.3.

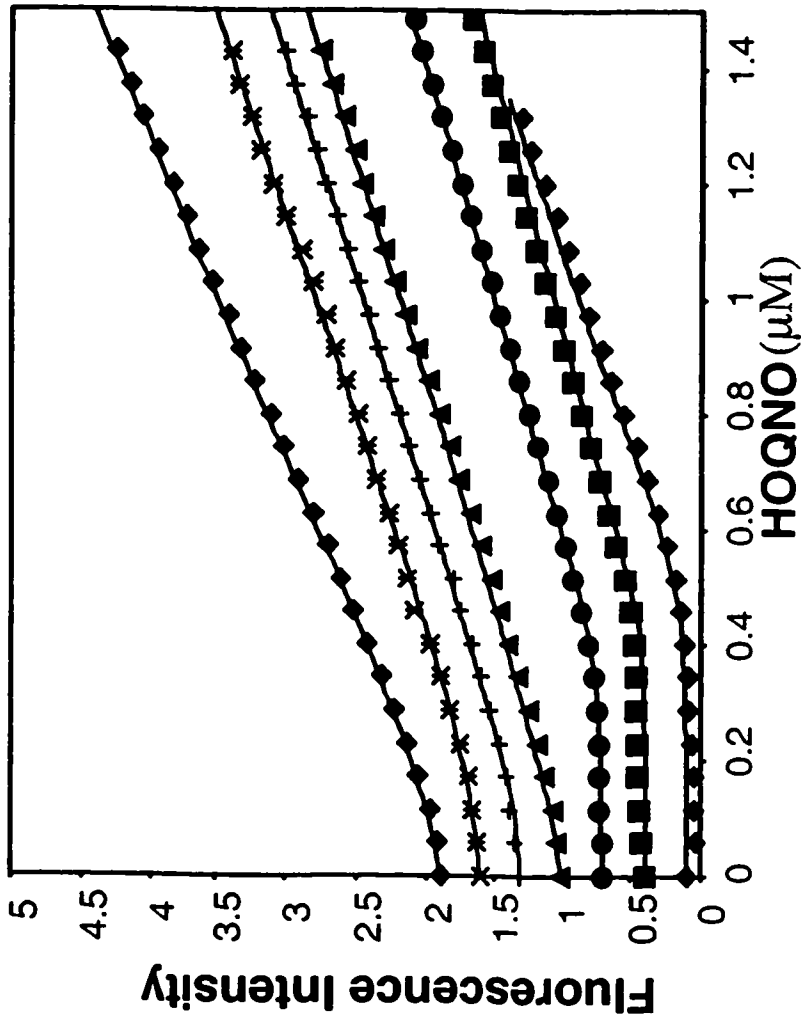


Figure 2.7. Quenching of HOQNO fluorescence. A range of concentrations of HOQNO in 50 mM MOPS pH 7.0

were mixed rapidly with the same buffer or with 1 mg/ml protein from DSS301 membranes containing

various chimeric proteins in the same buffer. At a given concentration of HOQNO, fluorescence quenching

was observed from the decrease in initial fluorescence intensity to the final fluorescence intensity.

DSS301 ◆---◆; /pDMS160 □---□; /pSPL-dAGH ■---■; /pSPL-dABH O---O; /pSPL-d(FGH) ▲---▲;

/pSPL-dFGC +---+; and /pSPL-d(EFGH) ●---●. These data are representative of three individual experiments.

2.3.7. Enzymatic Assays

Reduced benzyl viologen can be used as an electron donor to measure the enzymatic activity of the DMSO reductase catalytic dimer, DmsAB. We measured the activity of membranes isolated from DSS301 expressing proteins encoded by selected chimeric plasmids with TMAO as the acceptor (Table 2.3). TMAO is the best acceptor for DmsABC (47). DSS301/pSPL-dAGH and DSS301/pSPL-dABH expressed about 41% and 27% of the activity of DSS301/pDMS160 (DmsABC), respectively. Turnover number is calculated as the moles of substrate metabolized (or turned over) per second per mole of enzyme. The moles of enzyme were determined from the specific HOQNO binding (assuming a 1:1:1 molar ratio) calculated from HOQNO binding assays (Table 2.3). We were unable to determine turnover numbers of DSS301/pSPL-dFGC and DSS301/pSPL-d(FGH) due to their low expression. When YnfF replaced DmsA (DSS301/pSPL-dFGC) the activity was only 0.7% of that seen with DmsABC. No activity was seen when YnfE was present (data not shown).

We have previously shown that reduced lapachol can be used to monitor Quinol:TMAO oxidoreductase activity of DmsABC, providing a spectrophotometric assay for the function of the holoenzyme (140). The lapachol activity of DSS301/pSPL-dAGH and DSS301/pSPL-dABH reflected the benzyl viologen activity (Table 2.3), as did the lapachol activity of DSS301/pSPL-dFGC, which was very low.

Table 2.3. Enzymatic Activity of Chimeric Enzymes Expressed from Selected Chimeric Plasmids

Strain	Specific Activity Lapachol (μmoles/mg/min)	Specific Activity Benzyl Viologen (μmoles/mg/min)	Turnover Benzyl Viologen (/sec)
DSS301/pDMS160	1.945	59.07	1015
DSS301/pSPL-dAGH	1.050	22.33	441
DSS301/pSPL-dABH	0.799	13.38	298
DSS301/pSPL-dFGC	0.101	0.49	ND
DSS301/pSPL-dFGH	ND	0.73	ND
DSS301	<0.04	0.23	ND

Activity was measured as described in Methods with lapachol or benzyl viologen as the donor and TMAO as the acceptor. Turnover numbers were calculated from the specific enzyme concentration determined by HOQNO binding. ND = not determined.

2.3.8. Substrate Specificity of YnfF

We have previously examined the substrate specificity of DmsABC (154, 174, 204) and it was possible that YnfF has a different substrate preference. We tested the activity of membranes isolated from DSS301/pSPL-dFGC and DSS301/pSPL-d(FGH) with DMSO and a variety of N-oxides. With the DmsABC enzyme, TMAO is a much better substrate than DMSO (154). However, for YnfF containing enzymes, the TMAO activity was low and equivalent to DMSO activity (Table 2.4). The best activity in YnfFGH was observed with hydroxypyridine N-oxide, which was 7.9 fold better than TMAO. We did not measure the activity of YnfE chimeras due to the very poor expression.

Table 2.4. Benzyl Viologen Enzyme Assays of Membrane Fractions

Substrate	Specific Activity (μmoles/mg/min)		
	DSS301	DSS301/ pSPL-dFGC	DSS301/ pSPL-d(FGH)
TMAO	0.23	0.49	0.73
DMSO	0.13	0.66	0.82
ISNO	0.08	1.42	2.30
HPNO	0.08	2.23	3.32
CPNO	0.12	0.73	1.14
PNO	0.14	1.53	2.11

Activity is expressed as μ moles BV oxidized per mg membrane protein per minute. The concentration of each substrate is given in Methods. TMAO trimethylamine N-oxide; DMSO dimethyl sulfoxide; ISNO isonicotinic acid N-oxide; HPNO hydroxypyridine N-oxide; CPNO 2-chloropyridine N-oxide hydrochloride; PNO pyridine N-oxide.

2.3.9. Form A Fluorescence

An additional method of determining the functionality of the catalytic subunit is measuring the amount of molybdenum cofactor, as it is required for the reduction of substrate. The amount of molybdenum cofactor can be determined by quantitating the fluorescence of one of the pterin oxidation products, Form A. Figure 2.8 shows the fluorescence spectra of DSS301, DSS301/pDMS160 and the three constructs that grew anaerobically on DMSO. DSS301/pSPL-dAGH demonstrated the highest fluorescence of the chimeric enzymes and DSS301/pSPL-dABH shows intermediate fluorescence in agreement with the activity measurements. The presence of molybdenum cofactor was not unexpected due to the presence of the DmsA subunit in these chimeric enzymes. DSS301/pSPL-dFGC showed a low, but measurable level of Form A fluorescence as expected from the growth and expression studies whereas DSS301/pSPL-d(FGH) did not have any fluorescence (data not shown) suggesting that assembly and stability of FGC was better than FGH. It should be noted that protein level affects the amount of molybdenum cofactor, so constructs with poor fluorescence may be the result of poor expression.

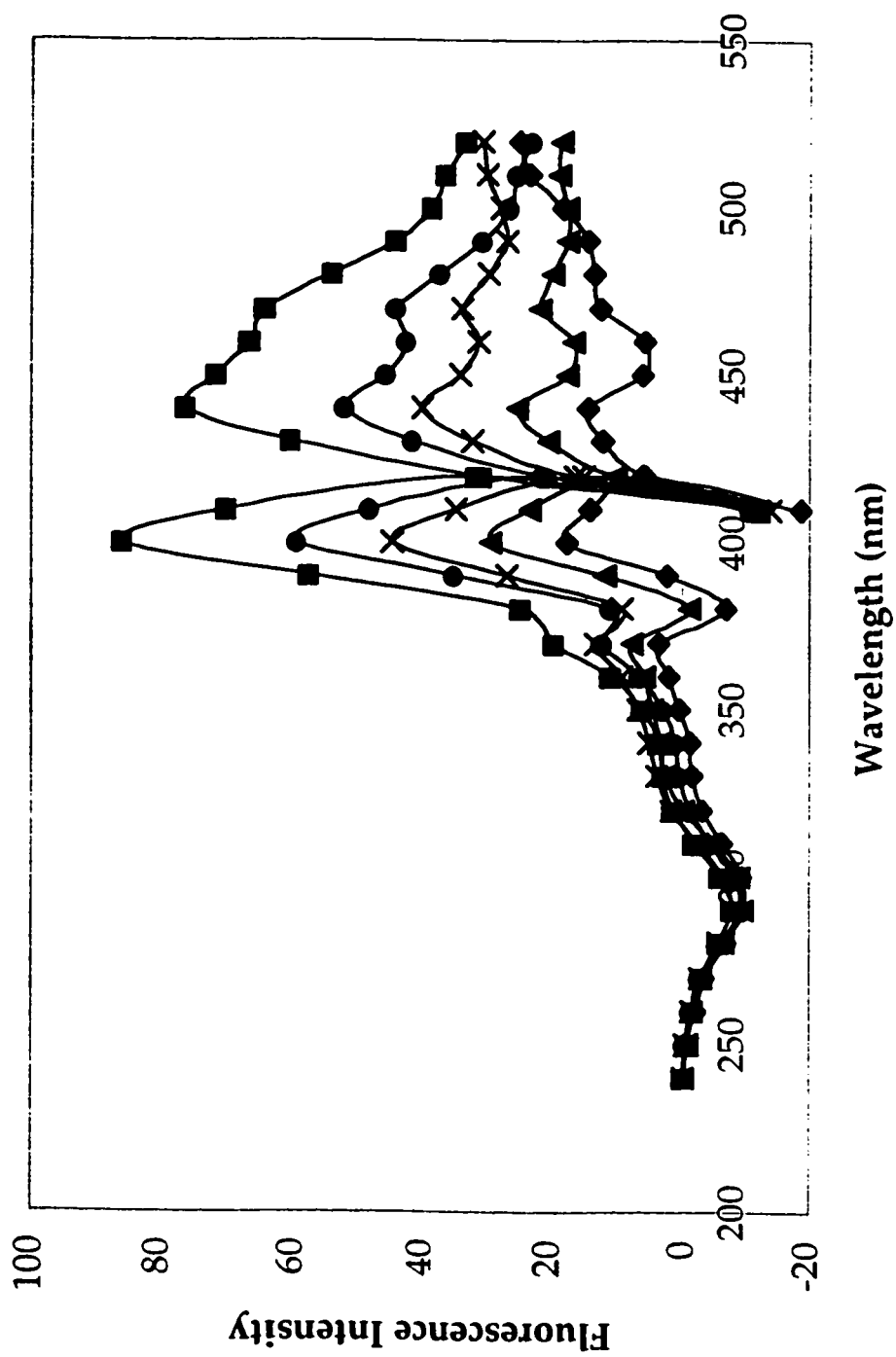


Figure 2.8. Form A fluorescence of DSS301 membranes expressing various chimeric enzymes. Samples were prepared as described in Methods. /pDMS160 ■---■; /pSPL-dABH ●---●; /pSPL-dABH X---X; /pSPL-dFGC ▲---▲; and DSS301 ◆---◆. These data are representative of two separate experiments.

2.3.10. Electron Paramagnetic Resonance of the Fe-S Clusters

To assay the functionality of the electron transfer subunit, the presence of iron-sulfur centres and their levels can be determined. DmsB has 4 [4Fe-4S] clusters coordinated by four Cys motifs, which can be observed by EPR spectroscopy at 4K (31). These clusters give characteristic g-values for iron-sulfur centres in EPR experiments. YnfG has the four Cys motifs and in order to determine whether there were iron-sulfur clusters present in the chimeric enzymes, EPR spectra were recorded for DSS301/pSPL-dAGH, DSS301/pSPL-dABH, DSS301/pSPL-dFGC, DSS301/pSPL-d(FGH) and DSS301/pSPL-d(EFGH). Figure 2.9A illustrates that DSS301/pSPL-dAGH and DSS301/pSPL-dABH exhibit EPR spectra similar to DSS301/pDMS160, and DSS301/pSPL-dFGC had a low but measurable spectrum. DSS301/pSPL-d(FGH) and DSS301/pSPL-d(EFGH) closely resemble the spectra of the DSS301. Figure 2.9B is the same spectra corrected DSS301 background to minimize the contribution of the FrdABCD [2Fe-2S] and [4Fe-4S] cluster signals.

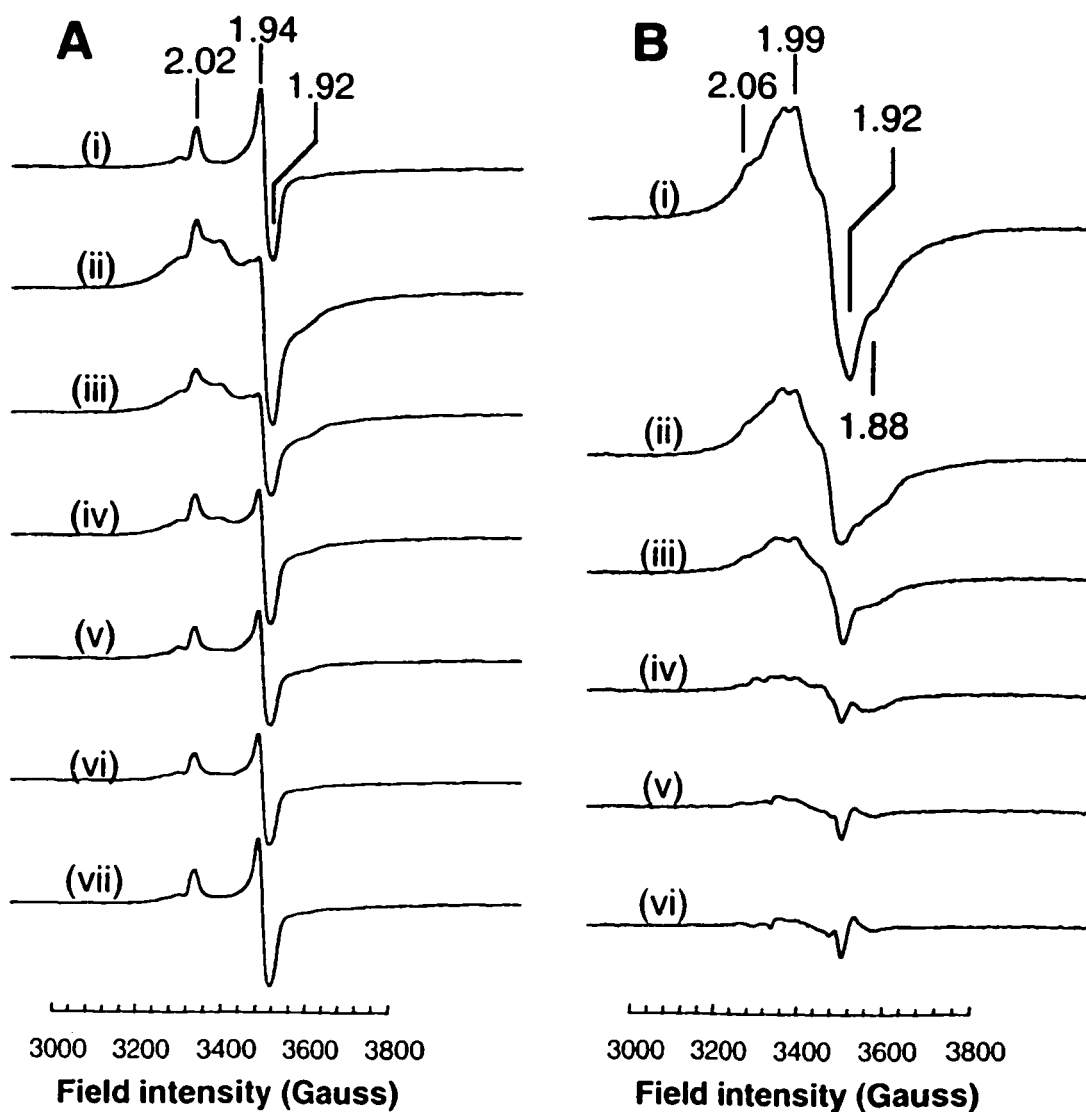


Figure 2.9. EPR spectra of dithionite-reduced membranes from DSS301 cells expressing chimeric Dms:Ynf proteins. **A.** EPR spectra of membranes from (i) DSS301; (ii) /pDMS160; (iii) /pSPL-dAGH; (iv) /pSPL-dABH; (v) /pSPL-dFGC; (vi) /pSPL-d(FGH); and (vii) /pSPL-d(EFGH). **B.** EPR difference spectra of DSS301 membranes transformed with plasmids expressing the Dms/Ynf proteins. (i) /pDMS160; (ii) /pSPL-dAGH; (iii) /pSPL-dABH; (iv) /pSPL-dFGC; (v) /pSPL-d(FGH); and (vi) /pSPL-d(EFGH).

2.4. Discussion

DMSO reductase is a heterotrimeric molybdoenzyme that functions as an electron transfer enzyme in the anaerobic respiratory chain. Since the discovery of a paralogue, the *ynfEFGHI* operon, which resulted from the *E. coli* genome sequencing project, we have been interested in its function. The striking similarity of YnfEFGH to DmsABC suggested a role as an alternate DMSO reductase with similar cell localization, reminiscent of the alternate nitrate reductases (19). Despite the success of cloning *ynfEFGH* behind the *tac* and *dms* promoters, which was necessitated by the lack of understanding of the native *ynf* promoter(s), we concluded that YnfEFGH is not an alternate DMSO reductase.

Two major differences distinguish YnfEFGH from DmsABC. The first is the tandem duplication of the putative catalytic subunits YnfE and YnfF and the second is the presence of a fifth open reading frame, *ynfI* (*dmsD*). Turner and colleagues have recently shown that YnfI is essential for the assembly and targeting of DmsABC to the membrane via the Tat/Mtt system and that it serves as a twin-arginine leader binding protein (119).

Two potential promoters have been identified by bioinformatic analysis preceding *ynfE* and *ynfF*. YnfI lacks its own promoter so must be expressed as the downstream gene in a polycistronic message composed of at least YnfFGHI, suggesting that YnfFGH should be expressed. However, our investigations over many years of a *dmsABC* deletion strain, DSS301, did not indicate that an alternate DMSO reductase was expressed or functional. This suggested that there

was either a translation problem for YnfEFGH or the proteins were made but were rapidly proteolyzed by *E. coli* even though they appeared so similar to DmsABC. To examine this conundrum, we expressed the YnfEFGH operon under *tac* promoter control from a multi-copy plasmid.

We were able to show that both YnfE/F cross-reacted with anti-DmsA antibody and that YnfG cross-reacted with anti-DmsB antibody. However, the expression of both YnfE and YnfF were poor compared to DmsA and YnfEFG tended to form inclusion bodies. A search for rare codons did not identify any obvious translational problems. It was also clear from this work that YnfG is expressed to higher levels than YnfEF. We were able to overcome the inclusion body problem by expressing YnfEFGH anaerobically using a *dms* promoter driven construct and growing at 30°C. Under these conditions YnfEFGH assembled in the membrane and YnfE and YnfF migrated as the mature form suggesting that they had been correctly handled by the Tat/Mtt protein translocation and targeting system (119, 158, 159, 203). However, the expression was still much poorer than DmsABC.

We created a series of chimeric enzymes in which the *dms* genes were replaced by *ynf* genes. Using this approach we showed that YnfH could serve as an anchor for DmsAB, as it bound HOQNO with similar affinity as DmsC and could complement anaerobic growth even though it was the least similar gene in the operon. Similarly, the YnfG subunit assembled iron-sulfur clusters that were indistinguishable from DmsB by EPR spectroscopy and could relay electrons

from DmsC or YnfH to the catalytic DmsA subunit as evidenced by GD growth and enzyme activity.

The problem of expression appeared to reside in *ynfE* and *ynfF*. When expressed from the *tac* promoter both YnfE and YnfF were observed in immunoblots. However, YnfE did not accumulate under anaerobic growth conditions and it interfered with the accumulation of YnfFG, suggesting a dominant negative effect. This suggests that the YnfE and YnfF subunits were proteolytically degraded during slow anaerobic growth. The expression of YnfF was poor but enough YnfFGH and YnfFGC accumulated in the membrane to support limited anaerobic growth on DMSO, although these two constructs behaved like the other four catalytic subunit exchange chimera in all other experiments. Catalytic substitution constructs performed poorly in GD growth experiment and enzyme assays, indicating that they likely have a different substrate specificity, and minimal fluorescence over the background in fluorescence assays probably reflects their low expression levels. It is these subunits that are responsible for the poor *dms* complementation as the other two are functional replacements of their *dms* paralogues. When we examined the substrate specificity of the YnfF we found that it differed from DmsA, with hydroxypyridine N-oxide as the best substrate.

We still do not know the physiological function of *ynfEFGH* nor why the catalytic subunit is tandemly duplicated. If *ynfEFGH* is not functional it must have been duplicated fairly recently given the very high homology. One possibility is that

the operon has been maintained to provide the *ynfI* gene since it is known to be required for membrane targeting of DMSO reductase (119).

Future studies will include determination of the Ynf substrate specificity and assays to elucidate the natural conditions under which the *ynf* promoter(s) are activated. This will illustrate the natural function of the *ynf* operon as it is definitely not a functional Dms replacement and is unlikely present for the sole purpose of expressing YnfI.

References

1. **Adams, B., A. T. Smith, S. Bailey, A. G. McEwan, and R. C. Bray.** 1999. Reactions of dimethyl sulfoxide reductase from *Rhodobacter capsulatus* with dimethyl sulfide and with dimethyl sulfoxide: complexities revealed by conventional and stopped-flow spectrophotometry. *Biochemistry*. **38(26):8501-8511.**
2. **Alexander, M.** 1974. Microbial formation of environmental pollutants. *Adv. Appl. Microbiol.* **18:1-73.**
3. **Alexeeva, S., B. D. Kort, G. Sawers, K. J. Hellingwerf, and M. J. D. Mattos.** 2000. Effects of limited aeration and of the ArcAB system on intermediary pyruvate catabolism in *Escherichia coli*. *J. Bacteriol.* **182(17):4934-4940.**
4. **Andreae, M. O.** 1980. Dimethyl sulfoxide in marine and fresh waters. *Limnol. Oceanogr.* **25:1054-1063.**
5. **Ansaldo, M., C. Bordini, M. Lepelletier, and V. Mejean.** 1999. TorC apocytochrome negatively autoregulates the trimethylamine N-oxide (TMAO) reductase operon in *Escherichia coli*. *Mol. Microbiol.* **33(2):284-295.**
6. **Augier, V., M. Asso, B. Guigliarelli, C. More, P. Bertrand, C.-L. Santini, F. Blasco, M. Chippaux, and G. Giordano.** 1993. Removal of the high-potential [4Fe-4S] centre of the β -subunit from *Escherichia coli* nitrate reductase. Physiological, biochemical, and EPR characterization of site-directed mutated enzymes. *Biochemistry*. **32:5099-5108.**
7. **Bamford, V., P. S. Dobbin, D. J. Richardson, and A. M. Hemmings.** 1999. Open conformation of a flavocytochrome c_3 fumarate reductase. *Nature Struct. Biol.* **6(12):1104-1107.**
8. **Barrett, E. L., and H. S. Kwan.** 1985. Bacterial reduction of trimethylamine oxide. *Annu. Rev. Microbiol.* **39:131-149.**
9. **Bauer, C. E., S. Elsen, and T. H. Bird.** 1999. Mechanisms for redox control of gene expression. *Annu. Rev. Microbiol.* **53:495-523.**

10. **Berg, B. L., J. Li, J. Heider, and V. Stewart.** 1991. Nitrate-inducible formate dehydrogenase in *Escherichia coli* K-12. I. Nucleotide sequence of the *fdnGHI* operon and evidence that opal (UGA) encodes selenocysteine. *J. Biol. Chem.* **266**:22380-22385.
11. **Berg, B. L., and V. Stewart.** 1990. Structural genes for nitrate-inducible formate dehydrogenase in *Escherichia coli* K-12. *Genetics.* **125**(4):691-702.
12. **Berks, B. C.** 1996. A common export pathway for proteins binding complex redox cofactors. *Mol. Microbiol.* **22**:393-404.
13. **Bilous, P. T., S. T. Cole, W. F. Anderson, and J. H. Weiner.** 1988. Nucleotide sequence of the *dmsABC* operon encoding the anaerobic dimethyl sulphoxide reductase of *Escherichia coli*. *Mol. Microbiol.* **2**(6):785-795.
14. **Bilous, P. T., and J. H. Weiner.** 1985. Dimethyl sulfoxide reductase activity by anaerobically grown *Escherichia coli* HB101. *J. Bacteriol.* **162**(3):1151-1155.
15. **Bilous, P. T., and J. H. Weiner.** 1988. Molecular cloning and expression of the *Escherichia coli* dimethyl sulfoxide reductase operon. *J. Bacteriol.* **170**(4):1511-1518.
16. **Bilous, P. T., and J. H. Weiner.** 1985. Proton translocation coupled to dimethyl sulfoxide reduction in anaerobically grown *Escherichia coli* HB101. *J. Bacteriol.* **163**(1):369-375.
17. **Bishop, R. E., and J. H. Weiner.** 1993. Overproduction, solubilization, purification and DNA-binding properties of AmpR from *Citrobacter freundii*. *Eur. J. Biochem.* **213**:405-412.
18. **Blasco, F., C. Iobbi, G. Giordano, M. Chippaux, and V. Bonnefoy.** 1989. Nitrate reductase of *Escherichia coli*: completion of the nucleotide sequence of the *nar* operon and reassessment of the role of the α and β subunits in iron binding and electron transfer. *Mol. Gen. Genet.* **218**:249-256.
19. **Blasco, F., C. Iobbi, J. Ratouchniak, V. Bonnefoy, and M. Chippaux.** 1990. Nitrate reductases of *Escherichia coli*: Sequence of the second nitrate reductase and comparison with that encoded by the *narGHJI* operon. *Mol. Gen. Genet.* **222**:104-111.

20. **Blattner, F. R., G. Plunkett, C. A. Bloch, N. T. Perna, V. Burland, M. Riley, J. Collado-Vides, J. D. Glasner, C. K. Rode, G. F. Mayhew, J. Gregor, N. W. Davis, H. A. Kirkpatrick, M. A. Goeden, D. J. Rose, B. Mau, and Y. Shao.** 1997. The complete genome sequence of *Escherichia coli* K-12. *Science*. **227**(5331):1453-1462.
21. **Bogachev, A. V., R. A. Murtazine, A. I. Shestopalov, and V. P. Skulachev.** 1995. Induction of the *Escherichia coli* cytochrome *d* by low $\Delta\mu\text{H}^+$ and by sodium ions. *Eur. J. Biochem.* **232**(1):304-308.
22. **Bokranz, M., M. Guttman, C. Kortnor, F. Kojro, F. Fahrenholz, F. Lauterbach, and A. Kroger.** 1991. Cloning and nucleotide sequence of the structural genes encoding the formate dehydrogenase of *Wolinella succinogenes*. *Arch. Microbiol.* **156**(2):119-128.
23. **Bolhuis, A., E. G. Bogsch, and C. Robinson.** 2000. Subunit interactions in the twin-arginine translocase complex of *Escherichia coli*. *FEBS Lett.* **472**:88-92.
24. **Bonnefoy, V., J. F. Burini, G. Giordano, M. C. Pascal, and M. Chippaux.** 1987. Presence in the 'silent' terminus region of the *Escherichia coli* K12 chromosome of cryptic gene(s) encoding a new nitrate reductase. *Mol. Microbiol.* **1**(2):143-150.
25. **Bonnefoy-Orth, V., M. Lepelletier, C.-C. Pascal, and M. Chippaux.** 1981. Nitrate reductase and cytochrome *b* nitrate reductase structural genes as parts of the nitrate reductase operon. *Mol. Gen. Genet.* **181**:535-540.
26. **Brot, N., and H. Weissbach.** 2000. Peptide methionine sulfoxide reductase: biochemistry and physiological role. *Biopolymers.* **55**(4):288-296.
27. **Brot, N., L. Weissbach, J. Werth, and H. Weissbach.** 1981. Enzymatic reduction of protein-bound methionine sulfoxide. *Proc. Natl. Acad. Sci. USA.* **78**(4):2155-2158.
28. **Browning, D. F., J. A. Cole, and S. J. Busby.** 2000. Suppression of FNR-dependent transcription activation at the *Escherichia coli* *nir* promoter by Fis, IHF and H-NS: modulation of transcription initiation by a complex nucleo-protein assembly. *Mol. Microbiol.* **37**(5):1258-1269.

29. **Bruschi, M., and F. Guerlesquin.** 1988. Structure, function and evolution of bacterial ferredoxins. *FEMS Microbiol. Rev.* **54**:155-176.
30. **Buc, J., C.-L. Santini, G. Blasco, R. Giordani, M. L. Cardenas, M. Chippaux, A. Cornish-Bowden, and G. Giordano.** 1995. Kinetic studies of a soluble $\alpha\beta$ complex of nitrate reductases α from *Escherichia coli*. Use of various $\alpha\beta$ mutants with altered β subunits. *Eur. J. Biochem.* **234**:766-772.
31. **Cammack, R., and J. H. Weiner.** 1990. Electron paramagnetic resonance spectroscopic characterization of dimethyl sulfoxide reductase of *Escherichia coli*. *Biochemistry.* **29**:8410-8416.
32. **Campillo-Campbell, A. D., and A. Campbell.** 1996. Alternative gene for biotin sulfoxide reduction in *Escherichia coli* K-12. *J. Mol. Evol.* **42**:85-90.
33. **Campillo-Campbell, A. D., D. Dykhuizen, and P. P. Cleary.** 1979. Enzymatic reduction of *d*-biotin-*d*-sulfoxide to *d*-biotin. *Methods Enzymol.* **62**:379-385.
34. **Carrió, M. M., and A. Villaverde.** 2001. Protein aggregation as bacterial inclusion bodies is reversible. *FEBS Lett.* **489**(1):29-33.
35. **Cattaneo, C., O. E. Craig, N. T. James, and R. J. Sokol.** 1997. Comparison of three DNA extraction methods on bone and blood strains up to 43 years old and amplification of three different gene sequences. *J. Foren. Sci.* **42**(6):1126-1135.
36. **Chang, L., L. I. Wei, J. P. Audia, R. A. Morton, and H. E. Schellhorn.** 1999. Expression of the *Escherichia coli* NRZ nitrate reductase is highly growth phase dependent and is controlled by RpoS, the alternative vegetative sigma factor. *Mol. Microbiol.* **34**(4):756-766.
37. **Chang, Y. Y., and J. E. J. Cronan.** 2000. Conversion of *Escherichia coli* pyruvate oxidase to an ' α -ketobutyrate oxidase'. *Biochem. J.* **352**(3):717-724.
38. **Chaudhry, G. R., and C. H. MacGregor.** 1983. *Escherichia coli* nitrate reductase subunit A: its role as the catalytic site and evidence for its modification. *J. Bacteriol.* **154**:387-394.

39. **Cole, J.** 1996. Nitrate reduction to ammonia by enteric bacteria: redundancy, or a strategy for survival during oxygen starvation? *FEMS Microbiol. Lett.* **136**(1):1-11.
40. **Cole, J. A.** 1968. Cytochrome c_{552} and nitrite reduction in *Escherichia coli*. *Biochim. Biophys. Acta.* **162**:356-368.
41. **Cole, S. T., C. Condon, B. D. Lemire, and J. H. Weiner.** 1985. Molecular biology, biochemistry and bioenergetics of fumarate reductase, a complex membrane-bound iron-sulfur flavoenzyme of *Escherichia coli*. *Biochim. Biophys. Acta.* **811**:381-403.
42. **Condon, C., and J. H. Weiner.** 1988. Fumarate reductase of *Escherichia coli*: an investigation of function and assembly using *in vivo* complementation. *Mol. Microbiol.* **2**(1):43-52.
43. **Darwin, A., Hussain, L. Griffiths, J. Grove, Y. Sambongi, S. Busby, and J. Cole.** 1993. Regulation and sequence of the structural gene for cytochrome c_{552} from *Escherichia coli*: not a hexahaem but a 50 kDa tetrahaem nitrite reductase. *Mol. Microbiol.* **9**:1255-1265.
44. **Dickie, P., and J. H. Weiner.** 1979. Purification and characterization of membrane-bound fumarate reductase from anaerobically grown *Escherichia coli*. *Can. J. Biochem.* **57**(6):813-821.
45. **Doherty, M. K., S. L. Pealing, C. S. Miles, R. Moysey, P. Taylor, M. D. Walkinshaw, G. A. Reid, and S. K. Chapman.** 2000. Identification of the active site acid/base catalyst in a bacterial fumarate reductase: a kinetic and crystallographic study. *Biochemistry.* **39**(35):10695-10701.
46. **Dueweke, T. J., and R. B. Gennis.** 1990. Epitopes of monoclonal antibodies which inhibit ubiquinol oxidase activity of *Escherichia coli* cytochrome *d* complex localize a functional domain. *J. Biol. Chem.* **265**:4273-4277.
47. **Dueweke, T. J., and R. B. Gennis.** 1991. Proteolysis of the cytochrome *d* complex with trypsin and chymotrypsin localizes a quinol oxidase domain. *Biochemistry.* **30**:3401-3406.

48. **Eaves, D. J., T. Palmer, and D. H. Boxer.** 1997. The product of the molybdenum cofactor gene *mobB* of *Escherichia coli* is a GTP binding protein. *Eur. J. Biochem.* **246**:690-697.
49. **Egan, S. M., and V. Stewart.** 1990. Nitrate regulation of anaerobic respiratory gene expression in *narX* deletion mutants of *Escherichia coli* K-12. *J. Bacteriol.* **172**:5020-5029.
50. **Eiglmeier, K., N. Honoré, S. Iuchi, E. C. C. Lin, and S. T. Cole.** 1989. Molecular genetic analysis of FNR-dependent promoters. *Mol. Microbiol.* **3**(7):869-878.
51. **Frey, B., G. Janel, U. Michelson, and H. Kerstein.** 1989. Mutations in the *Escherichia coli* *fnr* and *tgt* genes: control of molybdate reductase activity and the cytochrome *d* complex by *fnr*. *J. Bacteriol.* **171**(3):1524-1530.
52. **Garcia-Horsman, J. A., A. Pustinen, R. B. Gennis, and M. Wilstron.** 1995. Proton transfer in cytochrome *bo3* ubiquinol oxidase of *Escherichia coli*: Second-site mutations in subunit I that restore proton pumping in the mutant Asp135-Asn. *Biochemistry.* **34**:4428-4433.
53. **Gennis, R., and V. Stewart.** 1996. Respiration, p. 217-261. *In* F. C. Neidhardt (ed.), *Escherichia coli* and *Salmonella* cellular and molecular biology, vol. I. ASM Press, Washington.
54. **Gennis, R. B.** 1987. The cytochromes of *Escherichia coli*. *FEMS Microbiol. Rev.* **46**:387-399.
55. **Gennis, R. B.** 1998. How does cytochrome oxidase pump protons? *PNAS.* **95**(22):12747-12749.
56. **Georgiou, C. D., H. Fang, and R. B. Gennis.** 1987. Identification of the *cydC* locus required for the expression of the functional form of the cytochrome *d* terminal oxidase complex in *Escherichia coli*. *J. Bacteriol.* **169**:2107-2112.
57. **Grabau, C., and J. E. Cronan.** 1986. *In vivo* function of *Escherichia coli* pyruvate oxidase specifically requires a functional lipid binding site. *Biochemistry.* **25**:3748-3751.
58. **Guigliarelli, B., M. Asso, C. More, V. Augier, F. Blasco, J. Pommier, G. Giordano, and P. Bertrand.** 1992. EPR and redox characterization of iron-

- sulfur centres in nitrate reductases A and Z from *Escherichia coli*. Evidence for a high-potential and a low-potential class and their relevance in the electron-transfer mechanism. *Eur. J. Biochem.* **207**:61-68.
59. **Guigliarelli, B., A. Magalon, M. Asso, P. Bertrand, C. Frixon, G. Giordano, and F. Blasco.** 1996. Complete coordination of the four Fe-S centres of the β subunit from *Escherichia coli* nitrate reductase. Physiological, biochemical and EPR characterization of site-directed mutants lacking the highest or lowest potential [4Fe-4S] clusters. *Biochemistry.* **35**:4828-4836.
 60. **Hägerhäll, C.** 1997. Succinate:quinone oxidoreductases. Variations on a conserved theme. *Biochim. Biophys. Acta.* **1320**:107-141.
 61. **Hastings, S. F., T. M. Kaysser, F. Jiang, J. C. Salerno, R. B. Gennis, and W. J. Ingledew.** 1998. Identification of a stable semiquinone intermediate in the purified and membrane bound ubiquinol oxidase-cytochrome *bd* from *Escherichia coli*. *Eur. J. Biochem.* **255**(1):317-323.
 62. **Hata-Tanaka, A., K. Matsuura, S. Itoh, and Y. Anraku.** 1987. Electron flow and heme-heme interaction between cytochromes *b₅₅₈*, *b₅₉₅* and *d* in a terminal oxidase of *Escherichia coli*. *Biochim. Biophys. Acta.* **893**:289-295.
 63. **Hederstedt, L., and T. Ohnishi.** 1992. Progress in succinate:quinone oxidoreductase research, p. 163-198. *In* L. Ernster (ed.), *Molecular Mechanisms in Bioenergetics*. Elsevier Science Publishing, New York.
 64. **Hill, J. J., J. O. Alben, and R. B. Gennis.** 1993. Spectroscopic evidence for heme-heme binuclear centre in cytochrome *bd* ubiquinol oxidase from *Escherichia coli*. *Proc. Natl. Acad. Sci. USA.* **90**:5863-5867.
 65. **Hill, S., S. Viollet, A. T. Smith, and C. Anthony.** 1990. Roles for enteric *d*-type cytochrome oxidase in N₂ fixation and microaerobiosis. *J. Bacteriol.* **172**:2071-2078.
 66. **Hoshi, T., and S. Heinemann.** 2001. Regulation of cell function by methionine oxidation and reduction. *J. Physiol.* **531**(1):1-11.
 67. **Iobbi-Nivol, C., C. L. Santini, F. Blasco, and G. Giordano.** 1990. Purification and further characterization of the second nitrate reductase of *Escherichia coli* K12. *Eur. J. Biochem.* **188**(3):679-687.

68. **Iuchi, S.** 1993. Phosphorylation/dephosphorylation of the receiver module at the conserved aspartate residue controls transphosphorylation activity of histidine kinase in sensor protein ArcB of *Escherichia coli*. *J. Biol. Chem.* **268**:23972-23980.
69. **Iuchi, S., S. T. Cole, and E. C. C. Lin.** 1990. Multiple regulatory elements for the *glpA* operon encoding anaerobic glycerol-3-phosphate dehydrogenase and the *glpD* operon encoding aerobic glycerol-3-phosphate dehydrogenase in *Escherichia coli*: further characterization of respiratory control. *J. Bacteriol.* **172**:179-184.
70. **Iuchi, S., and E. C. Lin.** 1988. *arcA* (dye), a global regulatory gene in *Escherichia coli* mediating repression of enzymes in aerobic pathways. *Proc. Natl. Acad. Sci. USA.* **85**(6):1888-1892.
71. **Iuchi, S., and E. C. C. Lin.** 1992. Mutational analysis of signal transduction by ArcB, a membrane sensor protein responsible for anaerobic repression of operons involved in the central aerobic pathways in *Escherichia coli*. *J. Bacteriol.* **174**:3972-3980.
72. **Iuchi, S., and E. C. C. Lin.** 1987. The *narL* gene product activates the nitrate reductase operon and represses the fumarate reductase and trimethylamine N-oxide reductase operons in *Escherichia coli*. *Proc. Natl. Acad. Sci. USA.* **84**(11):3901-3905.
73. **Iuchi, S., and E. C. C. Lin.** 1992. Purification and phosphorylation of the Arc regulatory components of *Escherichia coli*. *J. Bacteriol.* **174**:5617-5623.
74. **Iuchi, S., Z. Matsuda, T. Fujiwara, and E. C. Lin.** 1990. The *arcB* gene of *Escherichia coli* encodes a sensor-regulator protein for anaerobic repression of the arc modulon. *Mol. Microbiol.* **4**(5):715-727.
75. **Iuchi, S., and L. Weiner.** 1996. Cellular and molecular physiology of *Escherichia coli* in the adaptation to aerobic environments. *J. Biol. (Tokyo).* **120**:1055-1063.
76. **Iverson, T. M., C. Luna-Chavez, G. Cecchini, and D. C. Rees.** 1999. Structure of the *Escherichia coli* fumarate reductase respiratory complex. *Science.* **284**(5422):1961-1966.
77. **Jawarowski, A., G. Mayo, D. C. Shaw, and H. D. Campbell.** 1981. Characterization of the respiratory NADH dehydrogenase of *Escherichia*

- coli* and reconstitution of NADH oxidase in *ndh* mutant membrane vesicles. *Biochemistry*. **20**:3621-3628.
78. **Johnson, J. L., L. W. Indermaur, and K. V. Rajagopalan.** 1991. Molybdenum cofactor biosynthesis in *Escherichia coli*. Requirement of the *chlB* gene product for the formation of molybdopterin guanine dinucleotide. *J. Biol. Chem.* **266**:12140-12145.
79. **Jones, R. W.** 1980. Proton translocation by the membrane-bound formate dehydrogenase of *Escherichia coli*. *FEMS Microbiol. Lett.* **8**:167-172.
80. **Jones, R. W., and P. B. Garland.** 1977. Sites and specificity of the reaction of bipyridylum compounds with anaerobic respiratory enzymes of *Escherichia coli*. *Biochem. J.* **164**:199-211.
81. **Jones, R. W., A. Lamont, and P. B. Garland.** 1980. The mechanism of proton translocation driven by the respiratory nitrate reductase complex of *Escherichia coli*. *Biochem. J.* **190**:79-94.
82. **Jourlin, C., A. Bengrine, M. Chippaux, and V. Mejean.** 1996. An unorthodox sensor protein (TorS) mediates the induction of the *tor* structural genes in response to trimethylamine N-oxide in *Escherichia coli*. *Mol. Microbiol.* **20**(6):1297-1306.
83. **Jourlin, C., G. Simon, J. Pommier, M. Chippaux, and V. Mejean.** 1996. The periplasmic TorT protein is required for trimethylamine N-oxide reductase gene induction in *Escherichia coli*. *J. Bacteriol.* **178**(4):1219-1223.
84. **Kalman, L. V., and R. P. Gunsalus.** 1990. Nitrate- and molybdenum-independent signal transduction mutations in *narX* that alter regulation of anaerobic respiratory genes in *Escherichia coli*. *J. Bacteriol.* **172**(12):7049-7056.
85. **Kellogg, N. W., R. D. Cadle, E. R. Allen, A. L. Laxrus, and E. A. Martell.** 1972. The sulfur cycle. *Science.* **175**(22):587-596.
86. **Khoroshilova, N., H. Beinert, and P. J. Kiley.** 1995. Association of a polynucleic iron-sulfur centre with a mutant FNR protein enhances DNA binding. *Proc. Natl. Acad. Sci. USA.* **92**:2499-2503.
87. **Kiene, R. P., and T. S. Bates.** 1990. Biological removal of dimethyl sulphide from sea water. *Nature (London).* **345**:702-704.

88. **Kita, K., C. R. T. Vibat, S. Meinhardt, J. R. Guest, and R. B. Gennis.** 1989. One step purification from *Escherichia coli* of complex II (succinate:ubiquinone oxidoreductase) associated with succinate reducible cytochrome *b₅₅₆*. *J. Biol. Chem.* **264**:2672-2677.
89. **Krafft, T., M. Bokranz, O. Klimmek, I. Schröder, F. Fahrenholz, E. Kojro, and A. Kröger.** 1992. Cloning and nucleotide sequence of the *psrA* gene of *Wolinella succinogenes* polysulfide reductase. *Eur. J. Biochem.* **206**:503-510.
90. **Kuritzkes, D. R., X.-Y. Zhang, and E. C. C. Lin.** 1985. Use of $\phi(glp-lac)$ in studies of respiratory regulation of the *Escherichia coli* anaerobic sn-glycerol-3-phosphate dehydrogenase genes (*glpAB*). *J. Bacteriol.* **157**:591-598.
91. **Kwon, O., K. Georgellis, and E. C. C. Lin.** 2000. Phosphorelay as the sole physiological route of signal transmission by the Arc two-component system of *Escherichia coli*. *J. Bacteriol.* **182**(13):3858-3862.
92. **Laemmli, U. K.** 1970. Cleavage of structural proteins during the assembly of the head of bacteriophage T4. *Nature (London)*. **227**:680-685.
93. **Lancaster, C. R., R. Gross, A. Haas, M. Ritter, W. Mäntele, J. Simon, and A. Kröger.** 2000. Essential role of Glu-C66 for menaquinol oxidation indicates transmembrane electrochemical potential generation by *Wolinella succinogenes* fumarate reductase. *Proc. Natl. Acad. Sci. USA.* **97**(24):13051-13056.
94. **Lancaster, C. R., R. Gross, and J. Simon.** 2001. A third crystal form of *Wolinella succinogenes* quinol:fumarate reductase reveals domain closure at the site of fumarate reduction. *Eur. J. Biochem.* **268**(6):1820-1827.
95. **Lancaster, C. R. D., A. Kröger, M. Auer, and H. Michel.** 1999. Structure of fumarate reductase from *Wolinella succinogenes* at 2.2 Å resolution. *Nature.* **402**:377-385.
96. **Leake, C. D., E. E. Rosenbaum, and S. W. Jacob.** 1967. Summary of the New York Academy of Sciences symposium on the "biological actions of dimethyl sulfoxide". *AIM J.* **141**(1):670-671.
97. **Leif, H., U. Weidner, A. Berger, V. Spher, M. Braun, P. v. Heek, T. Friedrich, T. Ohnishi, and H. Weiss.** 1993. *Escherichia coli* NADH

- dehydrogenase I, a minimal form of the mitochondrial complex I. *J. Biochem. Soc. Trans.* **21**:998-1001.
98. **Lester, R. L., and J. A. DeMoss.** 1971. Effects of molybdate and selenite on formate and nitrate metabolism in *Escherichia coli*. *J. Bacteriol.* **105**:1006-1014.
99. **Leys, D., A. S. Tsapin, K. H. Nealson, T. E. Meyer, M. A. Cusanovich, and J. J. V. Beeumen.** 1999. Structure and mechanism of the flavocytochrome *c* fumarate reductase of *Shewanella putrefaciens* MR-1. *Nature Struct. Biol.* **6**(12):1113-1117.
100. **Li, B., H. Wing, D. Lee, H. C. Wu, and S. Busby.** 1998. Transcription activation by *Escherichia coli* FNR protein: similarities to, and differences from, the CRP paradigm. *Nucleic Acids Res.* **26**(9):2075-2081.
101. **Lorence, R. M., J. G. Korland, and R. B. Gennis.** 1986. Coulometric and spectroscopic analysis of the purified cytochrome *d* complex of *Escherichia coli*: evidence for the identification of "cytochrome *a1*" as cytochrome *b595*. *Biochemistry.* **25**:2314-2321.
102. **Lovelock, J. E., R. J. Maggs, and R. A. Ramussen.** 1972. Atmospheric dimethyl sulphide and the natural sulphur cycle. *Nature (London).* **237**:452-453.
103. **Ma, J., A. Katsonouri, and R. B. Gennis.** 1997. Subunit II of the cytochrome *b₀₃* ubiquinol oxidase from *Escherichia coli* is a lipoprotein. *Biochemistry.* **36**(38):11298-11303.
104. **Macy, J., H. Kulla, and G. Gottschalk.** 1976. Hydrogen-dependent growth of *Escherichia coli* on L-malate:succinate formation. *J. Bacteriol.* **125**:423-428.
105. **Markwell, M. A., K. S. M. Haas, L. L. Beiber, and N. E. Tolbert.** 1978. A modification of the Lowry procedure to simplify protein determination in membrane and lipoprotein samples. *Anal. Biochem.* **87**:206-210.
106. **McAlpine, A. S., A. G. McEwan, A. L. Shaw, and S. Bailey.** 1997. Molybdenum active centre of DMSO reductase from *Rhodobacter capsulatus*: crystal structure of the oxidised enzyme at 1.82 Å resolution and the dithionite-reduced enzyme at 2.8 Å resolution. *J. Biol. Inorg. Chem.* **2**(6):690-701.

107. **Melville, S. B., and R. P. Gunsalus.** 1990. Mutations in *fnr* that alter anaerobic regulation of electron transport-associated genes in *Escherichia coli*. *J. Biochem.* **265**(31):18733-18736.
108. **Menon, N. K., C. Y. Chatelus, M. Dervartanian, J. C. Wendt, K. T. Shanmugam, J. H. D. Peck, and A. E. Przybyla.** 1994. Cloning, sequencing and mutational analysis of the *hyb* operon encoding *Escherichia coli* hydrogenase 2. *J. Bacteriol.* **176**:4416-4423.
109. **Menon, N. K., J. Robins, J. H. D. Peck, C. Y. Chatelus, E.-S. Choi, and A. E. Przybyla.** 1990. Cloning and sequencing of a putative *Escherichia coli* [NiFe] hydrogenase operon containing six open reading frames. *J. Bacteriol.* **172**:1969-1977.
110. **Miller, M. J., and R. B. Gennis.** 1985. The cytochrome *d* complex is a coupling site in the aerobic respiratory chain of *Escherichia coli*. *J. Biol. Chem.* **260**:14003-14008.
111. **Mitchell, P.** 1967. Proton-translocation phosphorylation in mitochondria, chloroplasts and bacteria: natural fuel cells and solar cells. *Fed. Proc. Natl. Acad. Sci. USA.* **26**:1370-1379.
112. **Moore, J. T., A. Uppal, F. Maley, and G. F. Maley.** 1993. Overcoming inclusion body formation in a high-level expression system. *Prot. Exp. Purif.* **4**:160-163.
113. **Morpeth, F. F., and D. H. Boxer.** 1985. Kinetic analysis of respiratory nitrate reductase from *Escherichia coli* K-12. *Biochemistry.* **24**:40-46.
114. **Moskovitz, J., J. M. Poston, B. S. Berlett, N. J. Nosworthy, R. Szczepanowski, and E. R. Stadtman.** 2000. Identification and characterization of a putative active site for peptide methionine sulfoxide reductase (MsrA) and its substrate stereospecificity. *J. Biol. Chem.* **275**(19):14167-14172.
115. **Motteram, P. A. S., J. E. G. McCarthy, S. J. Ferguson, J. B. Jackson, and J. A. Cole.** 1981. Energy conservation during the formate-dependent reduction of nitrite by *Escherichia coli*. *FEMS Microbiol. Lett.* **12**:317-320.
116. **Mowat, C. G., R. Moysey, C. S. Miles, D. Leys, M. K. Doherty, P. Taylor, M. D. Walkinshaw, G. A. Reid, and S. K. Chapman.** 2001. Kinetic and

- crystallographic analysis of the key active site acid/base arginine in a soluble fumarate reductase. *Biochemistry*. **40**(41):12292-12298.
117. **Newton, G., C.-H. Yun, and R. B. Gennis.** 1991. Analysis of the topology of the cytochrome *d* terminal oxidase complex of *Escherichia coli* by alkaline phosphatase fusions. *Mol. Microbiol.* **5**:2511-2518.
 118. **Okun, J. G., P. Lümmer, and U. Brandt.** 1999. Three classes of inhibitors share a common binding domain in mitochondrial complex I (NADH:ubiquinone oxidoreductase). *J. Biol.Chem.* **274**(5):2625-2630.
 119. **Oresnik, I. J., C. L. Ladner, and R. J. Turner.** 2001. Identification of a twin-arginine leader-binding protein. *Mol. Microbiol.* **40**:323-331.
 120. **Page, L., L. Griffiths, and J. A. Cole.** 1990. Different physiological roles of two independent pathways for nitrite reduction to ammonia by enteric bacteria. *Arch. Microbiol.* **154**:349-354.
 121. **Peakman, T., J. Crouzet, J. F. Mayaux, S. Busby, S. Mohan, N. Harborne, J. Wootton, R. Nicolson, and J. Cole.** 1990. Nucleotide sequence, organization and structural analysis of the products of genes in the *nirB-cysG* region of the *Escherichia coli* K-12 chromosome. *Eur. J. Biochem.* **191**:315-323.
 122. **Pierson, D. E., and A. Campbell.** 1990. Cloning and nucleotide sequence of *bisC*, the structural gene for biotin sulphoxide reductase in *Escherichia coli*. *J. Bacteriol.* **172**:2194-2198.
 123. **Pinsent, J.** 1954. The need for selenite and molybdate in the formation of formic dehydrogenases by members of the *coli-aerogenes* group of bacteria. *Biochem. J.* **57**:10-16.
 124. **Plunkett, G., V. Burland, D. L. Daniels, and F. R. Blattner.** 1993. Analysis of the *Escherichia coli* genome. III. DNA sequence of the region from 87.2 to 89.2 minutes. *Nucleic Acids Res.* **21**:3391-3398.
 125. **Pommier, J., M. A. Mandrand, S. E. Holt, D. H. Boxer, and G. Giordano.** 1992. A second phenazine methosulphate-linked formate dehydrogenase isoenzyme in *Escherichia coli*. *Biochim. Biophys. Acta.* **1107**:305-313.
 126. **Pommier, J., V. Méjean, G. Giordano, and C. Iobbi-Nivol.** 1998. TorD, a cytoplasmic chaperone that interacts with the unfolded trimethylamine N-

- oxide reductase enzyme (TorA) in *Escherichia coli*. J. Biol. Chem. **273**(26):16615-16620.
127. **Poole, R. K., L. Hatch, M. W. J. Cleeter, F. Gibson, G. B. Cox, and G. Wu.** 1993. Cytochrome *bd* biosynthesis in *Escherichia coli*: the sequences of the *cydC* and *cydD* genes suggest that they encode the components of an ABC membrane transporter. Mol. Microbiol. **10**:421-430.
128. **Poole, R. K., I. Salmon, and B. Chance.** 1994. The high-spin cytochrome *o'* component of the cytochrome *bo*-type quinol oxidase in membranes from *Escherichia coli*: formation of the primary oxygenated species at low temperatures is characterized by a slow "on" rate and low dissociation constant. Microbiol. **140**:1027-1034.
129. **Pope, N. R., and J. A. Cole.** 1982. Generation of a membrane potential by one of two independent pathways for nitrite reduction by *Escherichia coli*. J. Gen. Microbiol. **128**:219-222.
130. **Potter, L., P. Millington, L. Griffiths, and J. Cole.** 2000. Survival of bacteria during oxygen limitation. Int. J. Food Microbiol. **55**(1-3):11-18.
131. **Potter, L. C., and J. A. Cole.** 1999. Essential roles for the products of the *napABCD* genes, but not *napFGH*, in periplasmic nitrate reduction by *Escherichia coli* K-12. Biochem. J. **344**(1):69-76.
132. **Potter, L. C., P. Millington, L. Griffiths, G. H. Thomas, and J. A. Cole.** 1999. Competition between *Escherichia coli* strains expressing either a periplasmic or a membrane-bound nitrate reductase: does Nap confer a selective advantage during nitrate-limited growth? Biochem. J. **344**(1):77-84.
133. **Rabin, R. S., and V. Stewart.** 1993. Dual response regulators (NarL and NarP) interact with dual sensors (NarX and NarQ) to control nitrate- and nitrite-regulated gene expression in *Escherichia coli* K-12. J. Bacteriol. **175**:3259-3268.
134. **Rabin, R. S., and V. Stewart.** 1992. Either of two functionally redundant sensor proteins, NarX and NarQ, is sufficient for nitrate regulation in *Escherichia coli* K-12. Proc. Natl. Acad. Sci. USA. **89**:8419-8423.

135. **Rajagopalan, K. V.** 1996. Biosynthesis of the molybdenum cofactor, p. 674-679. In F. C. Neidhardt (ed.), *Escherichia coli* and *Salmonella* cellular and molecular biology, vol. 1. ASM Press, Washington.
136. **Reams, S. G., and D. P. Clark.** 1988. Glucose repression of anaerobic genes of *Escherichia coli* is independent of cyclic AMP. *FEMS Microbiol. Lett.* **56**:231-236.
137. **Reid, G. A., C. S. Miles, R. K. Moysey, K. L. Pankhurst, and S. K. Chapman.** 2000. Catalysis in fumarate reductase. *Biochim. Biophys. Acta.* **1459**(2-3):310-315.
138. **Richardson, D. J., B. C. Berks, D. A. Russell, S. Spiro, and C. J. Taylor.** 2001. Functional, biochemical and genetic diversity of prokaryotic nitrate reductases. *Cell. Mol. Life Sci.* **58**(2):165-178.
139. **Rothery, R. A., F. Blasco, and J. H. Weiner.** 2001. Electron transfer from heme b_L to the [3Fe-4S] cluster of *Escherichia coli* nitrate reductase A (NarGHI). *Biochemistry.* **40**:5260-5268.
140. **Rothery, R. A., I. Chatterjee, G. Kiema, M. T. McDermott, and J. H. Weiner.** 1998. Hydroxylated naphthoquinones as substrates for *Escherichia coli* anaerobic reductases. *Biochem. J.* **332**(1):35-41.
141. **Rothery, R. A., J. L. S. Grant, J. L. Johnson, K. V. Rajagopalan, and J. H. Weiner.** 1995. Association of molybdopterin guanine dinucleotide with *Escherichia coli* dimethyl sulfoxide reductase: effect of tungstate and a *mob* mutation. *J. Bacteriol.* **177**(8):2057-2063.
142. **Rothery, R. A., C. A. Trieber, and J. H. Weiner.** 1999. Interactions between the molybdenum cofactor and iron-sulfur clusters of *Escherichia coli* dimethyl sulfoxide reductase. *J. Biol. Chem.* **274**(19):13002-13009.
143. **Rothery, R. A., and J. H. Weiner.** 1991. Alteration of the iron-sulfur cluster composition of *Escherichia coli* dimethyl sulfoxide reductase by site-directed mutagenesis. *Biochemistry.* **30**:8296-8305.
144. **Rothery, R. A., and J. H. Weiner.** 1996. Interaction of an engineered [3Fe-4S] cluster with a menaquinol binding site of *Escherichia coli* DMSO reductase. *Biochemistry.* **35**:3247-3257.

145. **Rothery, R. A., and J. H. Weiner.** 1993. Topological characterization of *Escherichia coli* DMSO reductase by electron paramagnetic spectroscopy of an engineered [3Fe-4S] cluster. *Biochemistry*. **32**:5855-5861.
146. **Rowe, J. J., J. M. Yarbrough, J. B. Rake, and R. G. Eagon.** 1979. Nitrite inhibition of aerobic bacteria. *Curr. Microbiol.* **2**:51-54.
147. **Roy, C., and D. Lancaster.** 2001. Succinate:quinone oxidoreductases - what can we learn from *Wolinella succinogenes* quinol:fumarate reductase? *FEBS Lett.* **504**:133-141.
148. **Russell, P., H. L. Schrock, and R. B. Gennis.** 1977. Lipid activation and protease activation of pyruvate oxidase: evidence suggesting a common site of interaction on the protein. *J Biol. Chem.* **252**:7883-7887.
149. **Ruzicka, F. J., H. Beinert, K. L. Schepler, W. R. Dunham, and R. H. Sands.** 1975. Interaction of ubisemiquinone with a paramagnetic component in heart tissue. *Proc. Natl. Acad. Sci. USA.* **72**(8):2886-2890.
150. **Sagai, M., and M. Ishimoto.** 1973. An enzyme reducing adenosine N-oxide in *Escherichia coli*, amine N-oxide reductase. *J. Biochem.* **73**:843-859.
151. **Salerno, J. C., and T. Ohnishi.** 1980. Studies on the stabilized ubisemiquinone species in the succinate-cytochrome *c* reductase segment of the intact mitochondrial membrane system. *Biochem J.* **192**(3):769-781.
152. **Salgado, H., A. Santos-Zavaleta, S. Gama-Castro, D. Millan-Zarate, E. Diaz-Peredo, F. Sanchez-Solano, E. Perez-Rueda, C. Bonavides-Martinez, and J. Collado-Vides.** 2001. RegulonDB (version 3.2): transcriptional regulation and operon organization in *Escherichia coli* K-12. *Nucleic Acids Res.* **29**(1):72-74.
153. **Sambasivarao, D., D. G. Scraba, C. Trieber, and J. H. Weiner.** 1990. Organization of dimethyl sulfoxide reductase in the plasma membrane of *Escherichia coli*. *J. Bacteriol.* **172**(10):5938-5948.
154. **Sambasivarao, D., and J. H. Weiner.** 1991. Differentiation of the multiple S- and N-oxide-reducing activities of *Escherichia coli*. *Curr. Microbiol.* **23**:105-110.
155. **Sambasivarao, D., and J. H. Weiner.** 1991. Dimethyl sulfoxide reductase of *Escherichia coli*: an investigation of function and assembly by use of *in vivo* complementation. *J. Bacteriol.* **173**(19):5935-5943.

156. **Sambasivarao, D., and J. H. Weiner.** 1991. Dimethyl sulfoxide reductase of *Escherichia coli*: an investigation of function and assembly by use of *in vivo* complementation. *J. Bacteriol.* **173**(19):5935-5943.
157. **Sambrook, J., E. F. Fritsch, and T. Maniatis (ed.).** 1989. *Molecular cloning: A laboratory manual*, 2nd ed. Cold Spring Harbor Laboratory Press, Cold Spring Harbor, NY.
158. **Santini, C.-L., B. Ize, A. Chanal, M. Müller, G. Giordano, and L.-F. Wu.** 1998. A novel Sec-independent periplasmic protein translocation pathway in *Escherichia coli*. *EMBO J.* **17**(1):101-112.
159. **Sargent, F., E. G. Bogsch, N. R. Stanley, M. Wexler, C. Robinson, B. C. Berks, and T. Palmer.** 1998. Overlapping functions of components of a bacterial Sec-independent protein export pathway. *EMBO J.* **17**(13):3640-3650.
160. **Sauter, M., R. Böhm, and A. Böck.** 1992. Presence in the 'silent' terminus region of the *Escherichia coli* K12 chromosome of cryptic gene(s) encoding a new nitrate reductase. *Mol. Microbiol.* **6**(11):1523-1532.
161. **Sawers, R. G., S. P. Ballantine, and D. H. Boxer.** 1985. Differential expression of hydrogenase isoenzymes in *Escherichia coli* K-12: evidence for a third isoenzyme. *J. Bacteriol.* **164**:1324-1331.
162. **Sawers, R. G., D. J. Jamieson, C. F. Higgins, and D. H. Boxer.** 1986. Characterization and physiological roles of membrane-bound hydrogenase isoenzymes from *Salmonella typhimurium*. *J. Bacteriol.* **168**:398-404.
163. **Schindelin, H., C. Kisker, J. Hilton, K. V. Rajagopalan, and D. C. Rees.** 1996. Crystal structure of DMSO reductase: redox-linked changes in molybdopterin coordination. *Science.* **272**:1615-1621.
164. **Schneider, F., J. Löwe, R. Huber, H. Schindelin, C. Kisker, and J. Knäblein.** 1996. Crystal structure of dimethyl sulfoxide reductase from *Rhodobacter capsulatus* at 1.88 Å resolution. *J. Mol. Biol.* **263**:53-69.
165. **Schröder, I., R. P. Gunsalus, B. A. Ackrell, B. Cochran, and G. Cecchini.** 1991. Identification of active site residues of *Escherichia coli* fumarate reductase by site-directed mutagenesis. *J. Biol. Chem.* **266**(21):13572-13579.

166. Schryvers, A., E. Lohmeier, and J. H. Weiner. 1978. Chemical and functional properties of the native and reconstituted forms of the membrane-bound, aerobic glycerol-3-phosphate dehydrogenase of *Escherichia coli*. *J. Biol. Chem.* **253**:783-788.
167. Self, W. T., and K. T. Shanmugam. 2000. Isolation and characterization of mutated Fh1A proteins which activate transcription of the *hyc* operon (formate hydrogenlyase) of *Escherichia coli* in the absence of molybdate(1). *FEMS Microbiol. Lett.* **184**(1):47-52.
168. Settles, A. M., A. Yonetani, A. Baron, D. R. Bush, K. Cline, and R. Martienssen. 1997. Sec-independent protein translocation by the maize Hcf106 protein. *Science.* **278**(5342):1467-1470.
169. Shaw, D. J., and J. R. Guest. 1982. Amplification and product identification of the *fnr* gene of *Escherichia coli*. *J. Gen. Microbiol.* **128**(10):2221-2228.
170. Shaw, D. J., D. W. Rice, and J. R. Guest. 1983. Homology between CAP and Fnr, a regulator of anaerobic respiration in *Escherichia coli*. *J. Mol. Biol.* **166**(2):241-247.
171. Shimokawa, O., and M. Ishimoto. 1979. Purification and some properties of inducible tertiary amine N-oxide reductase from *Escherichia coli*. *J. Biochem.* **86**(6):1709-1717.
172. Shuber, A. P., E. C. Orr, M. A. Recny, P. F. Schendel, H. D. May, N. L. Schauer, and J. F. Ferry. 1986. Cloning, expression, and nucleotide sequence of the formate dehydrogenase genes from *Methanobacterium formicicum*. *J. Biol. Chem.* **261**(28):12942-12947.
173. Silvestro, A., J. Pommier, M. C. Pascal, and G. Giordano. 1989. The inducible trimethylamine N-oxide reductase of *Escherichia coli* K12: its localization and inducers. *Biochim. Biophys. Acta.* **999**:208-216.
174. Simala-Grant, J. L., and J. H. Weiner. 1996. Kinetic analysis and substrate specificity of *Escherichia coli* dimethyl sulfoxide reductase. *Microbiol.* **142**:3231-3239.
175. Simala-Grant, J. L., and J. H. Weiner. 1998. Modulation of the substrate specificity of *Escherichia coli* dimethyl sulfoxide reductase. *Eur.J. Biochem.* **251**:510-515.

176. **Simon, G., V. Mejean, C. Jourlin, M. Chippaux, and M. C. Pascal.** 1994. The *torR* gene of *Escherichia coli* encodes a response regulator protein involved in the expression of the trimethylamine N-oxide reductase genes. *J. Bacteriol.* **176**(18):5601-5606.
177. **Simon, J., R. Gross, O. Einsle, P. M. Kroneck, A. Kröger, and O. Klimmek.** 2000. A NapC/NirT-type cytochrome *c* (NrfH) is the mediator between the quinone pool and the cytochrome *c* nitrite reductase of *Wolinella succinogenes*. *Mol. Microbiol.* **35**(3):686-696.
178. **Sodergren, E. J., and J. A. DeMoss.** 1988. *narI* region of the *Escherichia coli* nitrate reductase (*nar*) operon contains two genes. *J. Bacteriol.* **170**:1721-1729.
179. **Solomon, P. S., A. L. Shaw, I. Lane, G. R. Hanson, T. Palmer, and A. G. McEwan.** 1999. Characterization of a molybdenum cofactor biosynthetic gene cluster in *Rhodobacter capsulatus* which is specific for the biogenesis of dimethyl sulfoxide reductase. *Microbiol.* **145**(6):1421-1429.
180. **Spiro, S., and J. R. Guest.** 1991. Adaptive responses to oxygen limitation in *Escherichia coli*. *TIBS.* **16**:310-314.
181. **Spiro, S., and J. R. Guest.** 1990. FNR and its role in oxygen-regulated gene expression in *Escherichia coli*. *FEMS Microbiol. Rev.* **75**:399-428.
182. **Spiro, S., R. E. Roberts, and J. R. Guest.** 1989. FNR-dependent repression of the *ndh* gene of *Escherichia coli* and metal ion requirement for FNR-regulated gene expression. *Mol. Microbiol.* **3**:601-608.
183. **Stewart, V.** 1988. Nitrate respiration in relation to facultative metabolism in enterobacteria. *Microbiol. Rev.* **52**:190-232.
184. **Stewart, V.** 1982. Requirement of Fnr and NarL functions for nitrate reductase expression in *Escherichia coli* K-12. *J. Bacteriol.* **151**:1320-1325.
185. **Stewart, V., and C. H. MacGregor.** 1982. Nitrate reductase in *Escherichia coli*: involvement of *chlC*, *chlE* and *chlG* loci. *J. Bacteriol.* **151**:788-799.
186. **Strack, B., M. Lessl, R. Calendar, and E. Lanka.** 1992. Sequence motif, -E-G-Y-A-T-A-, identified within the primase domains of plasmid-encoded I- and P-type primases and the alpha protein of the *Escherichia coli* satellite phage P4. *J. Biol. Chem.* **267**:13062-13072.

187. **Strom, A. R., J. A. Olafsen, and H. Larsen.** 1979. Trimethylamine oxide: a terminal electron acceptor in anaerobic respiration of bacteria. *J. Gen. Microbiol.* **112(2):**315-320.
188. **Takagi, M., T. Tsuchiya, and M. Ishimoto.** 1981. Proton translocation coupled to trimethylamine N-oxide reduction in anaerobically grown *Escherichia coli*. *J. Bacteriol.* **148(3):**762-768.
189. **Taylor, P., S. L. Pealing, G. A. Reid, S. K. Chapman, and M. D. Walkinshaw.** 1999. Structural and mechanistic mapping of a unique fumarate reductase. *Nat. Struct. Biol.* **6(12):**1108-1112.
190. **Trageser, M., S. Spiro, A. Duchene, E. Kojro, F. Fahrenholz, J. R. Guest, and G. Uden.** 1990. Isolation of intact FNR protein (Mr 30,000) of *Escherichia coli*. *Mol. Microbiol.* **4(1):**21-27.
191. **Trageser, M., and G. Uden.** 1989. Role of cysteine residues and of metal ions in the regulatory functioning of FNR, the transcriptional regulator of anaerobic respiration in *Escherichia coli*. *Mol. Microbiol.* **3:593-600.**
192. **Trieber, C. A., R. A. Rothery, and J. H. Weiner.** 1996. Consequences of removal of a molybdenum ligand (DmsA-Ser-176) of *Escherichia coli* dimethyl sulfoxide reductase. *J. Biol. Chem.* **271(44):**27339-27345.
193. **Trieber, C. A., R. A. Rothery, and J. H. Weiner.** 1994. Multiple pathways of electron transfer in dimethyl sulfoxide reductase of *Escherichia coli*. *J. Biol. Chem.* **269(10):**7103-7109.
194. **Turner, R. J., J. L. Busaan, J. H. Lee, M. Michalak, and J. H. Weiner.** 1997. Expression and epitope tagging of the membrane anchor subunit (DmsC) of *Escherichia coli* dimethyl sulfoxide reductase. *Prot. Eng.* **10(3):**285-290.
195. **Tyson, K. L., J. A. Cole, and S. J. W. Busby.** 1994. Nitrite and nitrate regulation at the promoters of two *Escherichia coli* operons encoding nitrite reductase: identification of common target heptamers for both NarP- and NarL-dependent regulation. *Mol. Microbiol.* **13:1045-1055.**
196. **Uden, G., and J. Bongaerts.** 1997. Alternative respiratory pathways of *Escherichia coli*: energetics and transcriptional regulation in response to electron acceptors. *Biochim. Biophys. Acta.* **1320:217-234.**

197. **Unden, G., and A. Duchene.** 1987. On the role of cyclic AMP and the Fnr protein in *Escherichia coli* growing anaerobically. *Arch. Microbiol.* **147(2):195-200.**
198. **Unden, G., and J. Schirawski.** 1997. The oxygen-responsive transcriptional regulator FNR of *Escherichia coli*: the search for signals and reactions. *Mol. Microbiol.* **25(2):205-210.**
199. **Walker, W. H., and T. P. Singer.** 1970. Identification of the covalently bound flavin of succinate dehydrogenase as 8- α -(histidyl) flavin adenine dinucleotide. *J. Biol. Chem.* **245(16):4224-4225.**
200. **Wallace, B. J., and I. G. Young.** 1977. Role of quinones in electron transport to oxygen and nitrate in *Escherichia coli*. Studies with a *ubiAmenA* double quinone mutant. *Biochim. Biophys. Acta.* **461:84-100.**
201. **Weidner, U., S. Geier, A. Ptock, T. Friedrich, H. Leif, and H. Weiss.** 1993. The gene locus of the proton-translocating NADH: ubiquinone oxidoreductase in *Escherichia coli*. *J. Mol. Biol.* **233:109-122.**
202. **Weiner, J. H.** 1992. The fumarate and dimethyl sulphoxide reductases of anaerobic electron transport in *Escherichia coli*: current status and future perspectives. *World J. Microbiol. Biotech.* **8(1):102-106.**
203. **Weiner, J. H., P. T. Bilous, G. M. Shaw, S. P. Lubitz, L. Frost, G. H. Thomas, J. A. Cole, and R. J. Turner.** 1998. A novel and ubiquitous system for membrane targeting and secretion of cofactor-containing proteins. *Cell.* **93:93-101.**
204. **Weiner, J. H., D. P. MacIsaac, R. E. Bishop, and P. T. Bilous.** 1988. Purification and properties of *Escherichia coli* dimethyl sulfoxide reductase, an iron-sulfur molybdoenzyme with broad substrate specificity. *J. Bacteriol.* **170(4):1505-1510.**
205. **Weiner, J. H., R. A. Rothery, D. Sambasivarao, and C. A. Trieber.** 1992. Molecular analysis of dimethyl sulfoxide reductase: a complex iron-sulfur molybdoenzyme of *Escherichia coli*. *Biochim. Biophys. Acta.* **1102:1-18.**
206. **Weiner, J. H., G. Shaw, R. J. Turner, and C. A. Trieber.** 1993. The topology of the anchor subunit of dimethyl sulfoxide reductase of *Escherichia coli*. *J. Biol. Chem.* **268:3238-3244.**

207. **Westenberg, D. J., R. P. Gunsalus, B. A. Ackrell, H. Sices, and G. Cecchini.** 1993. *Escherichia coli* fumarate reductase *frdC* and *frdD* mutants. Identification of amino acid residues involved in catalytic activity with quinones. *J. Biol. Chem.* **268**(2):815-822.
208. **White, W. B., and J. G. Ferry.** 1992. Identification of formate dehydrogenase-specific mRNA species and nucleotide sequence of the *fdhC* gene of *Methanobacterium formicicum*. *J. Bacteriol.* **174**:4997-5004.
209. **Williams, S. M., N. J. Savery, S. J. Busby, and H. J. Wing.** 1997. Transcription activation at class I FNR-dependent promoters: identification of the activating surface of FNR and the corresponding contact site in the C-terminal domain of the RNA polymerase α subunit. *Nucleic Acids Res.* **25**(20):4028-4034.
210. **Wing, H. J., S. M. Williams, and S. J. Busby.** 1995. Spacing requirements for transcription activation by *Escherichia coli* FNR protein. *J. Bacteriol.* **177**(23):6704-6710.
211. **Wissenbach, U., A. Kroger, and G. Uden.** 1990. The specific functions of menaquinone and demethylmenaquinone in anaerobic respiration with fumarate, dimethyl sulfoxide, trimethylamine N-oxide and nitrate by *Escherichia coli*. *Arch. Microbiol.* **154**:60-66.
212. **Wissenbach, U., D. Ternes, and G. Uden.** 1992. An *Escherichia coli* mutant containing only demethylmenaquinone, but no menaquinone: effects on fumarate, dimethyl sulfoxide, trimethylamine N-oxide and nitrate respiration. *Arch. Microbiol.* **158**:68-73.
213. **Yamamoto, I., M. Hinakura, S. Seki, Y. Seki, and H. Kondo.** 1989. Reduction of N-oxide and S-oxide compounds of *Escherichia coli*. *J. Gen. Appl. Microbiol.* **35**:253-259.
214. **Yamamoto, I., and M. Ishimoto.** 1978. Hydrogen-dependent growth of *Escherichia coli* in anaerobic respiration and the presence of hydrogenases with different functions. *J. Biochem. (Tokyo)*. **84**:673-679.
215. **Yamamoto, I., N. Okubo, and M. Ishimoto.** 1986. Further characterization of trimethylamine N-oxide reductase from *Escherichia coli*, a molybdoprotein. *J. Biochem.* **99**(6):1773-1779.

216. **Ye, S., and T. J. Larson.** 1988. Structures of the promoter and operator of the *glpD* gene encoding aerobic *sn*-glycerol-3-phosphate dehydrogenase of *Escherichia coli* K-12. *J. Bacteriol.* **170**:4209-4215.
217. **Young, R. A., and R. W. Davis.** 1983. Efficient isolation of genes by using antibody probes. *Proc. Natl. Acad. Sci. USA.* **80**:1194-1198.
218. **Zeyer, J., P. Eicher, S. G. Wakeham, and R. P. Schwoerzenbach.** 1987. Oxidation of dimethyl sulfide to dimethyl sulfoxide by phototrophic purple bacteria. *Appl. Env. Microbiol.* **53**:2026-2032.
219. **Zhang, G., and J. H. Weiner.** 2000. CTAB-mediated purification of PCR products. *BioTechniques.* **29**(5):982-986.
220. **Zhao, Z., and J. H. Weiner.** 1998. Interaction of 2-n-heptyl-4-hydroxyquinoline-N-oxide with dimethyl sulfoxide reductase of *Escherichia coli*. *J. Biol. Chem.* **273**(33):20758-20763.
221. **Zinder, S. H., and T. D. Brock.** 1978. Dimethyl sulphoxide reduction by micro-organisms. *J. Gen. Microbiol.* **105**(2):335-342.
222. **Zinoni, F., A. Birkmann, T. C. Stadtman, and A. Bock.** 1986. Nucleotide sequence and expression of the selenocysteine-containing polypeptide of formate dehydrogenase (formate-hydrogen-lyase-linked) from *Escherichia coli*. *Proc. Natl. Acad. Sci. USA.* **83**(13):4650-4654.

Appendix: Inclusion Body Reduction

It became apparent early on during fractionation of *ynf* construct-containing cells that the majority of Ynf protein was being directed into inclusion bodies. The very first experiment showed nearly all Ynf protein was localized in the low speed pellet fraction. This made localization of the Ynf enzyme impossible so we set out to reduce or prevent this formation.

The first attempt consisted of three experiments. We tried reducing the growth temperature to room temperature (22°C), addition of excess molybdenum and metal mix to ensure that these components were not limiting during protein synthesis, and tried growing on a less rich, peptone-fumarate, in the hopes of slowing down cell growth and thus the rate of protein expression. None of these variations resulted in decreased inclusion body formation.

We then hypothesized that improper folding may be the result of overexpression of YnfEFGH without the concomitant overexpression of YnfI, the fifth gene of the operon. We cotransformed Ynf plasmid-containing strains with a YnfI-expressing plasmid in the same *tac* promoter background. These cells were grown at room temperature and induced with a lower amount of IPTG (0.1 mM instead of 1 mM). We found that the addition of YnfI actually decreased band intensity overall and the only obvious bands were still in the low speed pellet fraction.

Another attempt to slow down protein synthesis was to further decrease IPTG induction level by inducing with 0.01 mM instead of 0.1 mM and growing at room temperature. Although this was the best condition thus far, the majority of protein was still localized in inclusion bodies. It also was apparent that 0.01 mM IPTG is insufficient for optimal protein synthesis.

A new minimal media, tryptone phosphate (TP), suggested by an inclusion body paper (110) was then tested as was DSS301 anaerobic growth with 0.01 mM IPTG. Neither growth in TP media nor anaerobic growth decreased in inclusion body formation and again we found that 0.01 mM IPTG was insufficient for full protein induction. The DSS301 anaerobic growth experiment also illustrated a very strange phenomenon. Although both DSS301 strains (containing YnfFGH and YnfEFGH) were grown identically, the cell density of DSS301/pSPL-(EFGH) was visibly less than its DSS301/pSPL-(FGH) counterpart, suggestive of a dominant negative effect of YnfE on the rest of the proteins (or genes). Immunoblot analysis showed almost no reactive bands in DSS301/pSPL-(EFGH) whereas in DSS301/pSPL-(FGH), although most protein remained in the low speed pellet fraction, there were still obvious bands in all fractions. We proposed that something had gone wrong with the DSS301/pSPL-(EFGH) strain on transformation since YnfEFGH shows protein bands when expressed in TG1, but on repeating the transformation and blotting the fractions there was no improvement. This may indicate that the dominant negative effect is more pronounced (or only occurs) in the deletion strain.

A different *E. coli* strain, BNN103, a Lon⁻ protease strain, was transformed with the Ynf plasmids. We proposed that the absence of the Lon protease would decrease the amount of protein degradation and therefore decrease inclusion body formation. We found that despite the fact that the majority of protein was still in the low speed pellet fraction, there was a significant improvement in protein observed in the membrane and soluble fractions.

We next tried replacing the *tac* promoter with the native *dms* promoter and transformed these plasmids into DSS301 as it is the only true *dms* deletion strain. The cells were grown anaerobically for 48 hours and fractionated. Although the expression of DSS301/pSPL-d(EFGH) is improved over its *tac* promoter counterpart the expression was still not as good as observed in BNN103.

We examined the growth period for DSS301/*dmsP* strains, proposing that 48 hours was not optimal. Both DSS301/pSPL-d(FGH) and /pSPL-d(EFGH) were grown anaerobically for 24, 48 and 72 hours on GF and whole cells immunoblotted and examined for maximal protein expression. We found that both strains showed optimal expression at 24 hours.

Since the best expression was observed in BNN103 cells we tested *dms* promoter plasmids to determine the optimal growth period. Cells were grown in the same manner as described above (with DSS301 cells) and separated into fractions. We noticed that at 48 hours there was a significant amount of Dms protein observed in the BNN103 parent strain, enough to make interpretation of plasmid-

containing strains difficult. We tried the same experiment, growing for only 18 hours but this proved to be insufficient protein expression.

Because all attempts resulted in the majority of protein in inclusion bodies we took a new approach. We grew BNN103 strains with *dms* promoter constructs anaerobically on GF at 37°C. After 24 hours 100 or 200µg/ml chloramphenicol was added to stop chromosomal protein expression and cell growth (34). This results in all cell materials being diverted to plasmid protein synthesis. Following chloramphenicol incorporation cells were either sedimented by centrifugation and processed immediately or grown an additional 24 or 48 hours. Immunoblots showed there was no reduction in inclusion body formation.

The final attempt at inclusion body prevention proved successful. BNN103/*dmsP* strains were grown anaerobically at 30°C for 24, 30, 48 and 54 hours. The cells were split into fractions and immunoblotted. The parent strain BNN103 showed no evidence of background DmsAB expression even up to 54 hours of growth. At all time points in both strains there was more protein in the soluble and membrane fractions than in low speed pellet fractions and as the growth period increased more protein moved from the soluble fraction into the membrane fraction. This was the condition we decided to adopt throughout the remainder of the thesis project.